ESA CONTRACT REPORT

Contract Report to the European Space Agency

Measurement of Seasonal CO_2 Fluctuations from Space

May 2004

Authors: P.D. Watts, A.P. McNally, J-N. Thépaut, M. Matricardi, R.J. Engelen and N. Bormann

Final report for ESA contract 14644/00/NL/JSC

ESA Study Manager: J. Pedro V. Poiares Baptista

ECMWF
Shinfield Park
Reading
RG2 9AX
United Kingdom

For additional copies please contact: library@ecmwf.int

Series: ECMWF - ESA Contract Report

A full list of ECMWF Publications can be found on our web site under:
http://www.ecmwf.int/publications/

Contract Report to the European Space Agency

Measurement of Seasonal CO_2 Fluctuations from Space

Authors: P.D. Watts, A.P. McNally, J-N. Thépaut, M. Matricardi, R.J. Engelen and N. Bormann

Final report for ESA contract 14644/00/NL/JSC

ESA Study Manager: J. Pedro V. Poiares Baptista

European Centre for Medium-Range Weather Forecasts

Shinfield Park, Reading, Berkshire, UK

May 2004

Table of Contents

Executive Summary

This is the fourth and final report for the contract study on measurement of seasonal CO_2 fluctuations from space. Although most of the work is not necessary specific to any particular satellite instrument, observations of the AIRS instrument (Aumann, 2003) were used to perform the study. This report summarizes the main points of the first 3 reports (1QR, 2QR and 3QR), describes work done in the final quarter and presents some overall conclusions and recommendations. It is suggested that this report should only be read in conjunction with the 3 reports already submitted.

The contract statement of work identifies four distinct work-packages (radiative transfer, data sampling, use of real AIRS data, and system implementation)

In WP1 (radiative transfer) much experience has been gained from the operational monitoring of the AIRS radiance data to characterize radiative transfer errors. In many cases the source of the errors are understood and supported by other studies. The largest problems appear in the water vapour region. Errors in the 4.5 micron band are enhanced in part by poor specification of N_2O and in part by (during sunlight) non-Local Thermodynamic Equilibrium effects.

In WP2 (data sampling) the implications of various data reduction strategies have been considered. While the spectral compression using principal components is very efficient with some impressive noise reduction qualities, the lower risk option of channel selection is adopted (also in view of this being the only product available in real time). The high prevalence of cloud cover means great care must be taken with any spatial sampling of the data.

In WP3 (science study) the development and enhancements to the cloud detection scheme for AIRS are documented and it is shown that the algorithm has now reached a reasonable state of maturity. Issues related to bias correction have been studied and a robust strategy for data monitoring has been installed.

In WP4 (system implementation) work has resulted in a day-one system for the assimilation of AIRS radiances. Experiments have shown that the AIRS radiance data have a small, but consistent positive impact upon the quality of NWP analyses and forecasts. Testing has shown that the impact is sufficiently robust that the AIRS radiances are now used operationally at ECMWF. In addition, the simultaneous production of CO_2 estimates from AIRS is shown to have great potential. Monthly mean column amounts for both troposphere and stratosphere have been produced and show some interesting details. The error characteristics are promising, but careful validation has to be carried out to confidently use these column estimates in for instance flux inversion studies.

1. WP 1 Validation of a fast radiative transfer model (RTM) for AIRS

The fast radiative transfer model (RTTOV) has been extended to include variable CO_2 profile concentrations; both the forward (radiance calculation) and Jacobian (radiance gradient calculation) models are complete. The Jacobians of the new model with respect to the CO_2 profile were tested by comparison to values obtained by perturbation of the forward model and exact agreement is found. The validation of the forward model consisted of two aspects: accuracy with respect to the LBL model and the underlying accuracy of the LBL model itself. The addition of the variable CO_2 profile to RTTOV (on the models 43 levels) was achieved with no discernable degradation of the accuracy with respect to the LBL as outlined below.

Fast model validation against the training LBL model is relatively straightforward and has been done for the AIRS RTTOV under separate contract, Matricardi et al, 2001. In CO_2 sounding bands the fast model bias against the LBL is generally less than 0.03 K and the standard deviation less than 0.05 K. There are a number of channels, particularly within the 15 μm band, where both bias and standard deviation can be up to 0.2 K. This is within AIRS instrument noise levels (Figure 1) but there could be justification for omitting these channels from the CO_2 estimation process. Channels in water vapour and ozone sensing bands have higher fast model errors but even these have been reduced by careful choice of fast model predictors to rms values of less than 0.3 K. In summary, the fast model is not expected to contribute significant errors in the majority of channels and the minority that do can be eliminated as these errors are very well characterised.

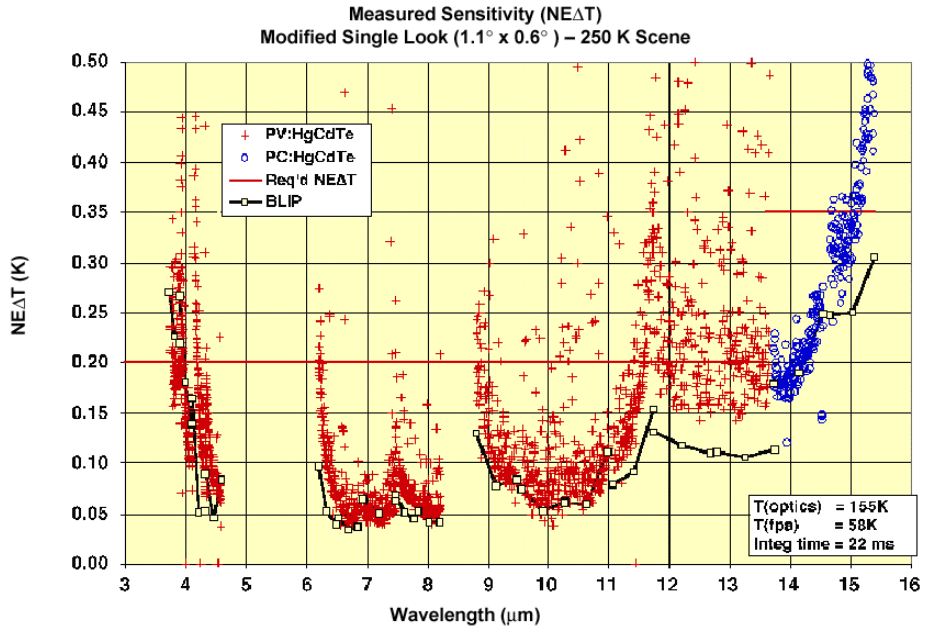

Figure 1 AIRS flight model measured NEdT (from http://www-airs.jpl.nasa.gov)

Validation of the LBL model underlying the fast model is a more complicated task. It can be tackled indirectly by intercomparisons of different LBL models or directly by comparisons to measured spectra. Rizzi et al. 2001 compared measured spectra obtained from the High resolution Interferometer Sounder (HIS) (on board the ER-2 at 20 Km) during the first Convection and Moisture Experiment (CAMEX) with two LBL codes (GENLN2 and HARTCODE). They showed spectroscopic uncertainties could lead to errors in RTM forward calculations for AIRS of up to 1 K. With over one year's AIRS data monitored against the ECMWF forecast model we are now in a position to comment on how these spectroscopic errors appear with real AIRS data. Such monitoring potentially leads to an ambiguity between NWP model error and spectroscopic error. However, the CAMEX experiment provides one important source of independent information and the high vertical resolution of the AIRS data itself can be exploited as another.

The AIRS instrument has proved to be extremely stable in radiance and spectral calibration. Bias estimates made six months apart are usually very similar except where an obvious forecast model seasonal bias is apparent. The biases (mean observation minus forecast model first guess) for our current best cloud detection methodology are shown in Figure 2 as red dots. The small black dots are the differences found between the High resolution Interferometer Sounder (HIS) instrument down looking from an aircraft at 20 Km, and calculations made using GENLN2 from the in situ atmospheric data (temperature, humidity, ozone etc). (GENLN2 is the base line by line model used to train the RTTOV fast model used at ECMWF.) Noise in the HIS instrument data makes the comparison somewhat meaningless in the regions < 650 cm^{-1}, 1050 - 1150 cm^{-1}, 1450 - 1800 cm^{-1} and 2200 - 2400 cm^{-1}. Elsewhere, it can be seen that AIRS biases are generally consistent in size with that expected from CAMEX. More specific details can be seen.

650-750 cm^{-1}; CO_2 sounding band. In the upper part of the band AIRS biases are systematically greater than zero and less scattered than the HIS. The positive bias is probably attributable to ECMWF forecast model bias in the stratosphere. The higher scatter in the HIS biases may be due to instrument noise, or perhaps because of its higher spectral resolution: some averaging of on/off line spectroscopic modelling error may be taking place in the AIRS measurements. In the lower part of the band the AIRS biases drop below zero and

this may be due to neglect of P/R branch mixing in GENLN2 (Strow, personal communication, 2003) although residual cloud errors may be contributing.

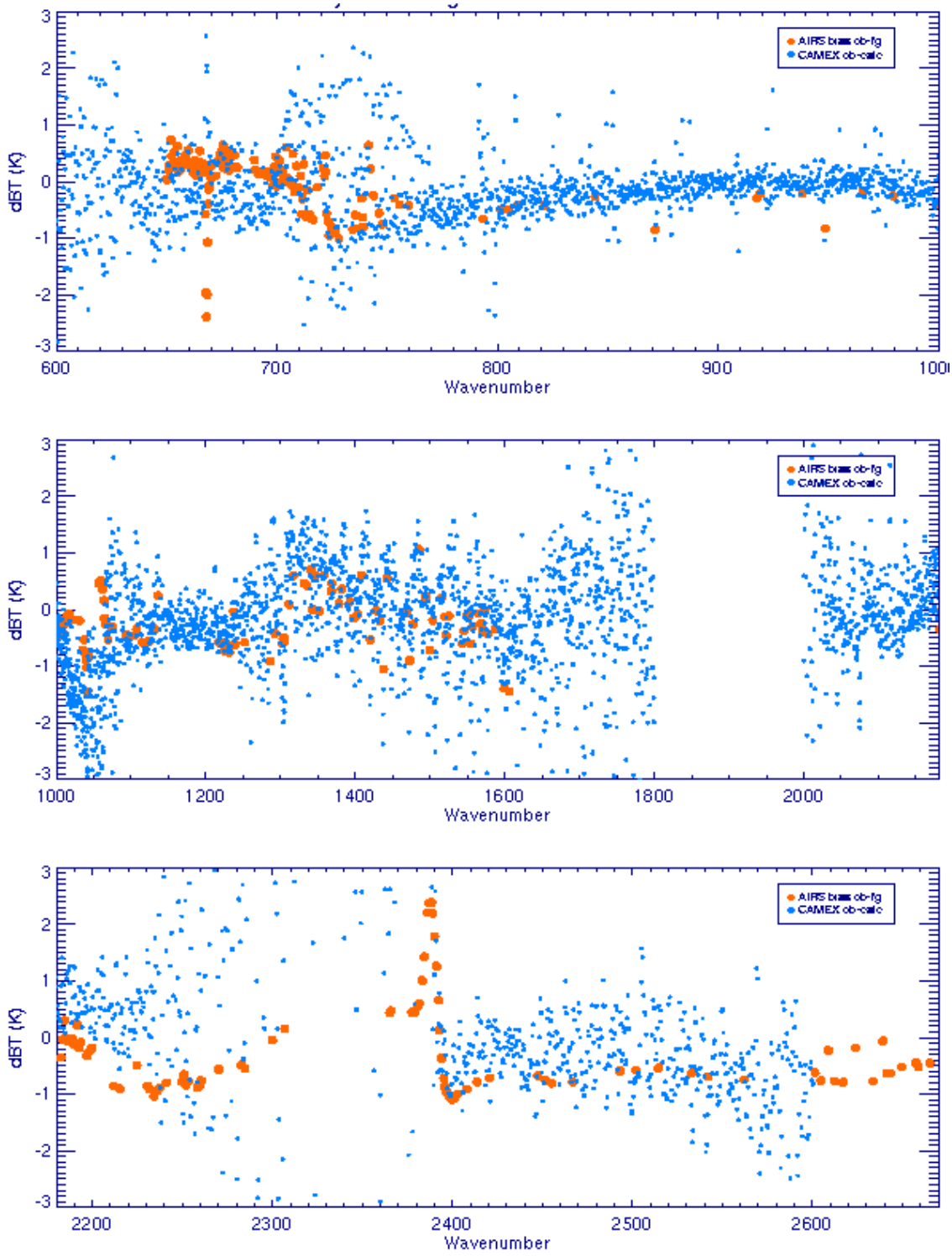

Figure 2 Bias vector found with current 'best current' algorithms (red) plotted with CAMEX GENLN2 / HIS interferometer differences. Data: June 1-5 2003.

750 - 1000 cm^{-1}; Window region. Most AIRS channels in this region have biases that are very consistent with the HIS departures. The two AIRS channels that clearly stand out from the main cluster also stand out in the

HIS, clearly demonstrating that these are spectroscopic in origin. (Improved water continuum modelling (Matricardi, 2003) in GENLN2 since has improved the fit of these channels and that of the other anomalous channels in this region).

Little can be made of the CAMEX results in the 1000-1100 cm^{-1} ozone region since ozone was poorly measured in the campaign. However, the 'dipole' error structure seen in the AIRS biases has the characteristics of poor modelling of the ozone absorption. It is also seen in the AIRS science team RTM kCARTA (Strow, 2003).

1200-1600 cm^{-1}; Water vapour band. The large scatter and overall shape of the biases here are consistent between HIS and AIRS suggesting these arise from spectroscopic errors. The sensitivity of the CAMEX results to specification of humidity, and uncertainty of the size of ECMWF forecast model biases both suggest that this conclusion should be speculative, but that CAMEX and ECMWF should have the same humidity bias structure would seem unlikely.

2180-2300 cm^{-1}; (4.5 micron) CO_2 sounding band. This region is potentially an important sounding band for CO2, however the AIRS biases are currently rather large; up to 1K. It is probable that two effects are involved here. Figure 3 shows the AIRS biases in this region with the spectral signature in N_2O (scaled to be of the same magnitude).

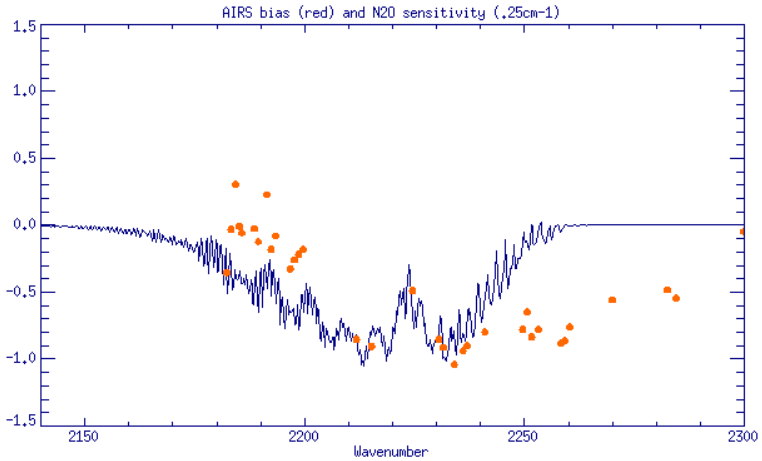

Figure 3 AIRS biases and scaled effect of incorrect N_2O concentration.

In particular the signature around 2210-2240 cm^{-1} appears to be that of N_2O. Beyond 2240 cm^{-1} the CO_2 absorption becomes strong and biases here may become more a result of poor CO_2 line shape modelling (Strow, personal communication, 2003). In addition to the spectral signature for N_2O, maps of bias in the 2230 cm^{-1} and at 1303 cm^{-1} (where there is almost pure N_2O absorption) contain very similar patterns (not shown).

This region also shows non-LTE effects which are currently not modeled in the RTM. Figure 4 shows dramatically the difference in departures (difference between the observed brightness temperatures and the model forecasted brightness temperatures) observed in daylight and night-time data at 4.381 micron (2282.6 cm^{-1}). The non-LTE contribution appears to have a strong limb effect but only a weak dependence on solar elevation (shown by little change along track).

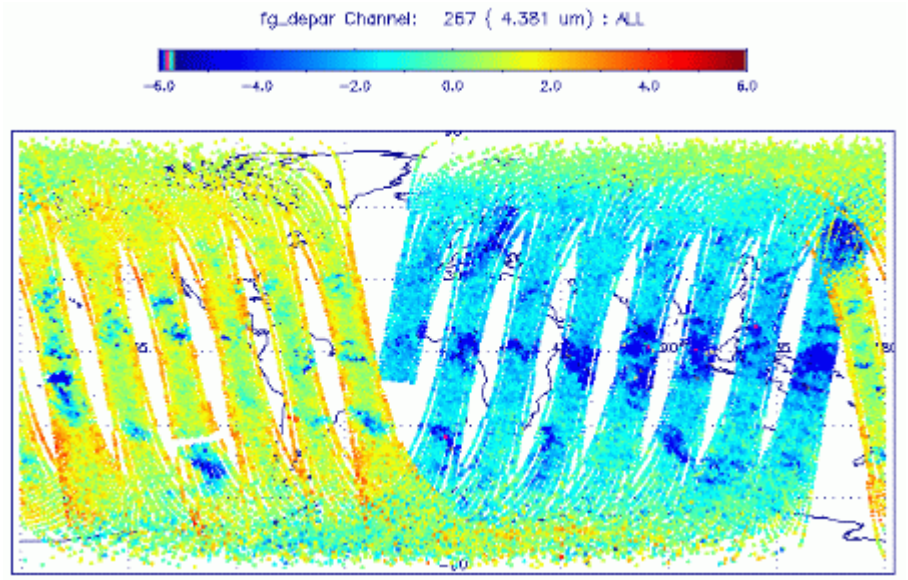

Figure 4 Departures in 4.381 micron channel showing daytime (left) and night-time orbits.

Differences in monitored biases (mean observed minus model first guess departures) between daylight and night-time data show clearly the spectral region that is affected. Figure 5 shows the observed effect and the non-LTE effect estimated using the Oxford MIPAS LBL model (for three scenarios, all with solar elevation 60° (Dudhia et al., 2001)). The agreement is good enough to firmly attribute the effect to non-LTE but not to model it sufficiently accurately beyond about 2250 cm^{-1}). Note that the estimate non-LTE effect during night-time is negligible (not shown).

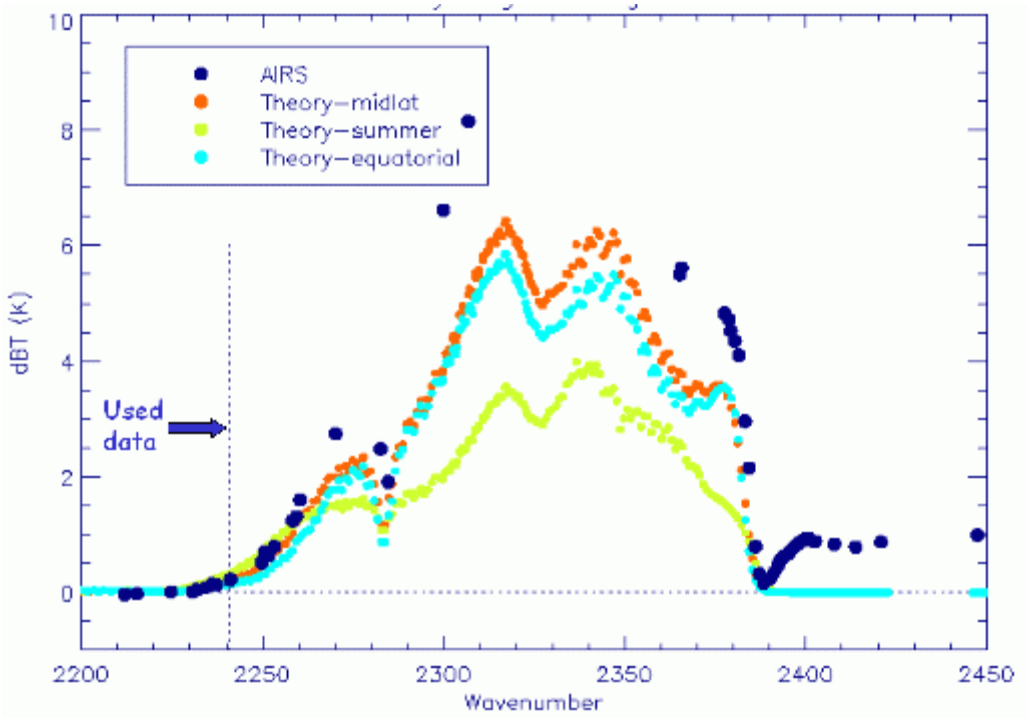

Figure 5 Daylight minus night-time AIRS biases (black dots) compared to non-LTE calculations in the 2200 - 2450 cm^{-1} region.

2380-2660 cm^{-1}; (4.2 micron) CO_2 sounding band. Another potentially important sounding band for CO_2 and again there are significant biases present. The HIS comparison also shows the strong positive bias through the sounding region (2385-2405 cm^{-1}) although the HIS noise is quite high here. The rest of the region, with relatively small and stable biases is a window region and of little interest to the CO_2 estimation.

The biases described above are typically of order 0.5 K, which, given the size of seasonal cycle CO_2 signals (~0.3-0.4 K), is rather large. A global bias can be corrected, however, and this is done in the current operational AIRS NWP assimilation. What is perhaps more important is the variation in the corrected bias. A first attempt to correct the airmass variation in bias has been made. The method estimates a global correction factor for the absorption coefficients in each channel. The result is an airmass dependent bias correction, because the absorption coefficients are temperature dependent. A full description of the method and some first results can be found in Watts and McNally (2004), which is attached.

2. WP 2 Science study to optimise AIRS data usage for NWP applications and for CO_2 work

In principle it would be best to have access to all AIRS measured radiances in near-real-time (NRT) for use in NWP applications and the estimation of CO_2. However, such a volume of data cannot feasibly be disseminated by the satellite agency or efficiently assimilated by the NWP centres and some data reduction steps are required. This section considers various options.

2.1 Spectral data reduction

The AIRS instrument has 2378 channels, but obviously these do not provide 2378 independent pieces of information. Two approaches to reducing the spectral information have been studied, channel selection and spectral compression.

2.1.1 Channel selection

This is a very simple approach and involves selecting a more manageable number of channels from the AIRS spectrum and discarding the rest. The aim is obviously to select the most useful channels for the particular application. Several bands within the AIRS spectrum have been identified as useful for NWP and CO_2 estimation purposes. As the CO_2 absorption bands are very important for temperature sounding, the two requirements are by no means mutually exclusive. Although somewhat arbitrary, the following bands have been defined to aid description and are treated independently in the prototype cloud screening method (see section 3).

LW	('Longwave' 15 µm CO2)	15.4 to 11.1 µm
O3	('Ozone' 9 µm O3)	9.99 to 8.09 µm
6M	('6 micron' 6 µm H_2O)	8.07 to 6.23 µm
SW1	('Shortwave^{-1}' 4.5 µm CO_2)	4.58 to 4.44 µm
SW2	('Shortwave-2' 4.2 µm CO_2)	4.20 to 3.75 µm

As a first step in defining the utility of an AIRS channel measurement, the response of the channel to a standard perturbation in each principle atmospheric quantity was determined using the line-by-line model (GENLN2). The atmospheric quantities and the standard perturbation considered were air temperature (T, dT = model error), skin temperature (Ts, dTs = model error), CO_2 (dCO_2 = seasonal climatological), water

vapour (q, dq = model error), N_2O (dN_2O = Seasonal climatological) and Ozone (O3, dO3 = model error). 'Model error' indicates a perturbation equivalent to current estimates of the ECMWF NWP 6h short-range forecast error. Radiance perturbations from the LBL model were convolved with the Flight Model specification of the AIRS channel response functions. The O3 and 6M bands are not directly relevant to the CO_2 estimation problem and are not discussed here. They will of course contribute to the estimation through improved temperature, moisture and ozone analyses.

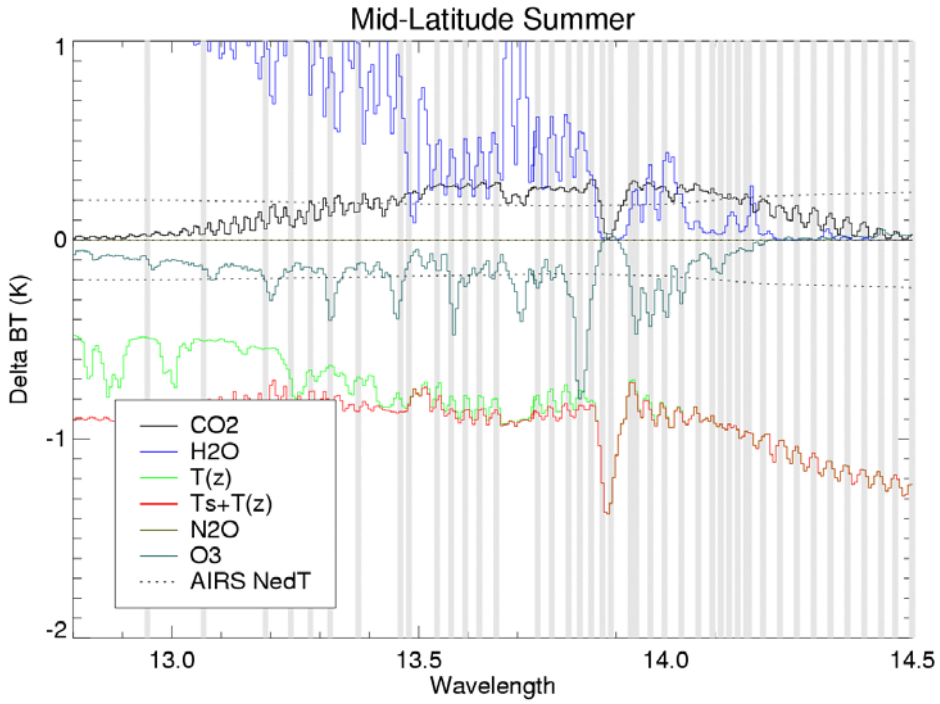

Figure 6 Response of LW band AIRS channels to standard perturbations in atmospheric and surface quantities. See text for details. Grey vertical bars indicate channels targeted by NESDIS for transmission immediately post-launch. Dotted line indicates the approximate Flight Model channel radiometric noise.

Results for the portion of the LW band sensitive to CO_2 are shown in Figure 6. The response to CO_2 is seen to be at or around the basic instrument noise level, indicating that a moderate amount of data averaging will deliver a reasonably high signal-to-noise level. However, there are several other significant responses in this band that will complicate interpretation. Naturally, a strong response is seen with respect to atmospheric temperature. This signal however, can probably be well determined either directly, or, more likely, through the assimilation system, by the AMSU-A instrument measurements made coincidently with the AIRS measurements. Less tractable problems will arise from the signals from ozone and water vapour. Assimilation of the O3 and 6M bands AIRS data will significantly reduce model uncertainties in these quantities but their presence will undoubtedly, in the context of CO_2 estimation, lead to signal aliasing unless great care is taken.

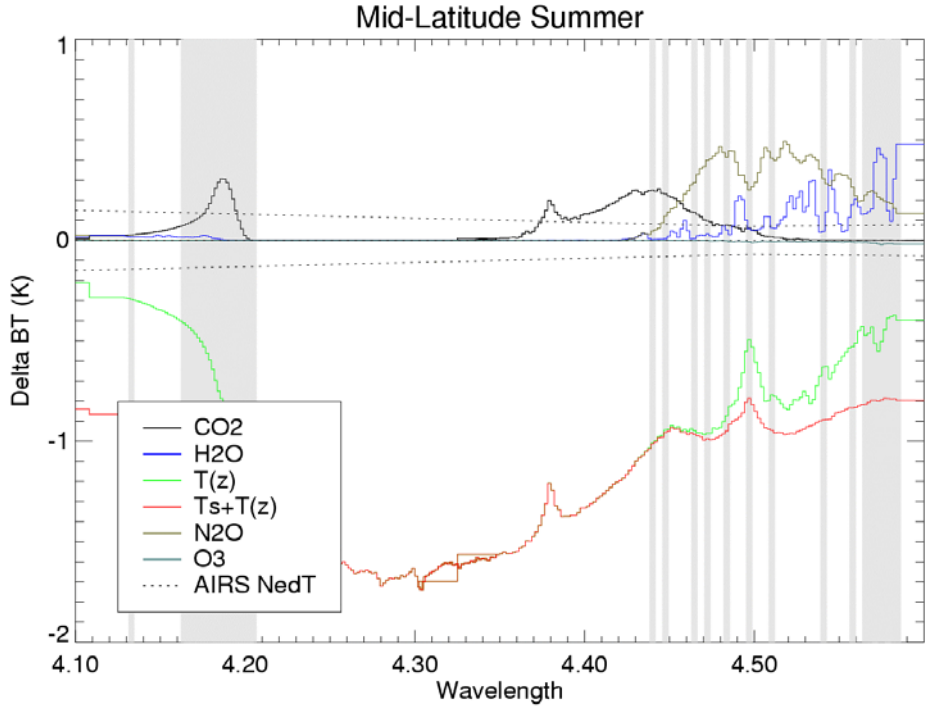

Figure 7 As Figure 6 but for the shortwave bands of AIRS

The responses in the SW bands are shown in Figure 7. The SW-2 (4.2 μm) band appears extremely promising as it is a) very clean - no ozone and only traces of water vapour sensitivity, and b) subject to low instrument noise levels (< 0.2 K). Some problems have been revealed by detailed study related to cloud detection (see WP 3) and levels of solar contamination during daylight need to be established before being sure that this is a high priority band for temperature and CO_2 sounding.

Thus taking into account issues of noise and information content, a reasonably robust channel selection can be made that conveys much of the required information. The grey bars on Figure 6 and Figure 7 show the 324 channels that NESDIS currently disseminate as part of the NRT BUFR AIRS data. The channels chosen appear qualitatively reasonable, with selections either aiming for low water and ozone contributions or the opposite, and avoiding channels with significant multiple contributions. They were selected by using an original selection of 281 channels plus an extra set of 43 channels specifically chosen for CO2 estimation as described in Crevoisier et al (2003). Indeed a more objective channel selection obtained by implementing the method described in Rodgers (2000) (which determines the relative information content of each channel compared to the information already held by an assimilation system) lends considerable support to the channels chosen by NESDIS.

While the selection of channels is a robust approach to reducing the data volume, discarding the remaining channels is not without cost. The discarded channels may well only provide redundant information, but this redundancy can be used to effectively reduce the noise in the assimilation system. This point is illustrated in Figure 8 where the analysis error is simulated from a system that uses the original 281 NESDIS channels, the now operationally disseminated 324 channels, and the full 2378 channels. While this is a simulation (and it assumes that all components are perfectly known and modeled) it clearly shows the value of redundant channels. Thus there is some incentive to access this information lost by channel selection.

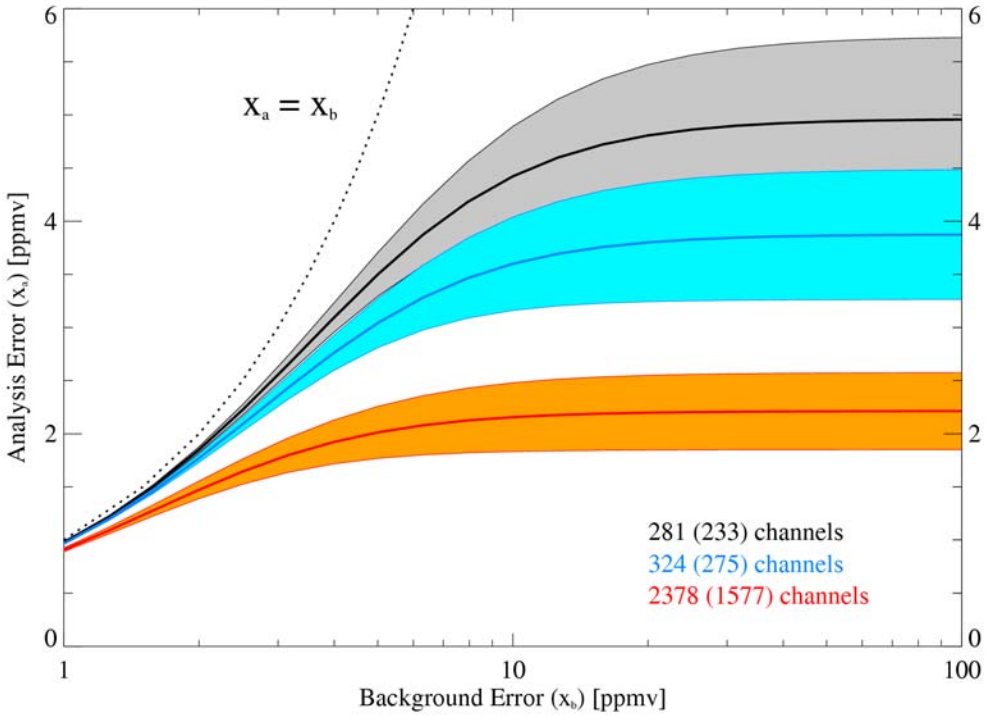

Figure 8 Estimated CO2 analysis error as a function of background error for three different sets of channels: all AIRS channels (red), 324 channels used at ECMWF (blue), and original 281 NESDIS channels (black). The shaded areas show the variability for various atmospheric profiles.

2.1.2 Spectral compression

A number of techniques exist to compress the measured spectra into a much smaller volume and thus allow a much more efficient transmission of data. Arguably the most mature of these is the use of principal components (or eigenvectors). Compression of the AIRS data by this method is detailed in an earlier report. Essentially a measured spectrum is projected onto the eigenvectors of a prepared training sample and a (limited) number, M, of the resulting projection coefficients are transmitted to the user. The data compression obtained arises from the use of an incomplete set of eigenvectors, the premise being that much of the information content of the complete spectra may be retained; the discarded coefficients are assumed to describe mainly measurement noise. A further enhancement is for the data provider to compress and send the spectra as a truncated set of principal components, but to additionally evaluate the residual (or reconstruction error) in each channel and disseminate these in a highly packed form (the idea being that the residuals should be small, of order tenths of a Kelvin).

Such compression combined with residual transmission allows the user to receive a much smaller amount of data from which the full spectra (i.e. all channels) can be reconstructed exactly. While this effectively solves the problem of transmitting the data, it is still probably not feasible for the user to assimilate all 2378 AIRS channels. However, the truncated eigenvectors are effectively an efficient encapsulation of the whole measured spectrum that can be used in two ways. Firstly, the radiances that are reconstructed are de-noised by the truncation (as seen in Figure 9).

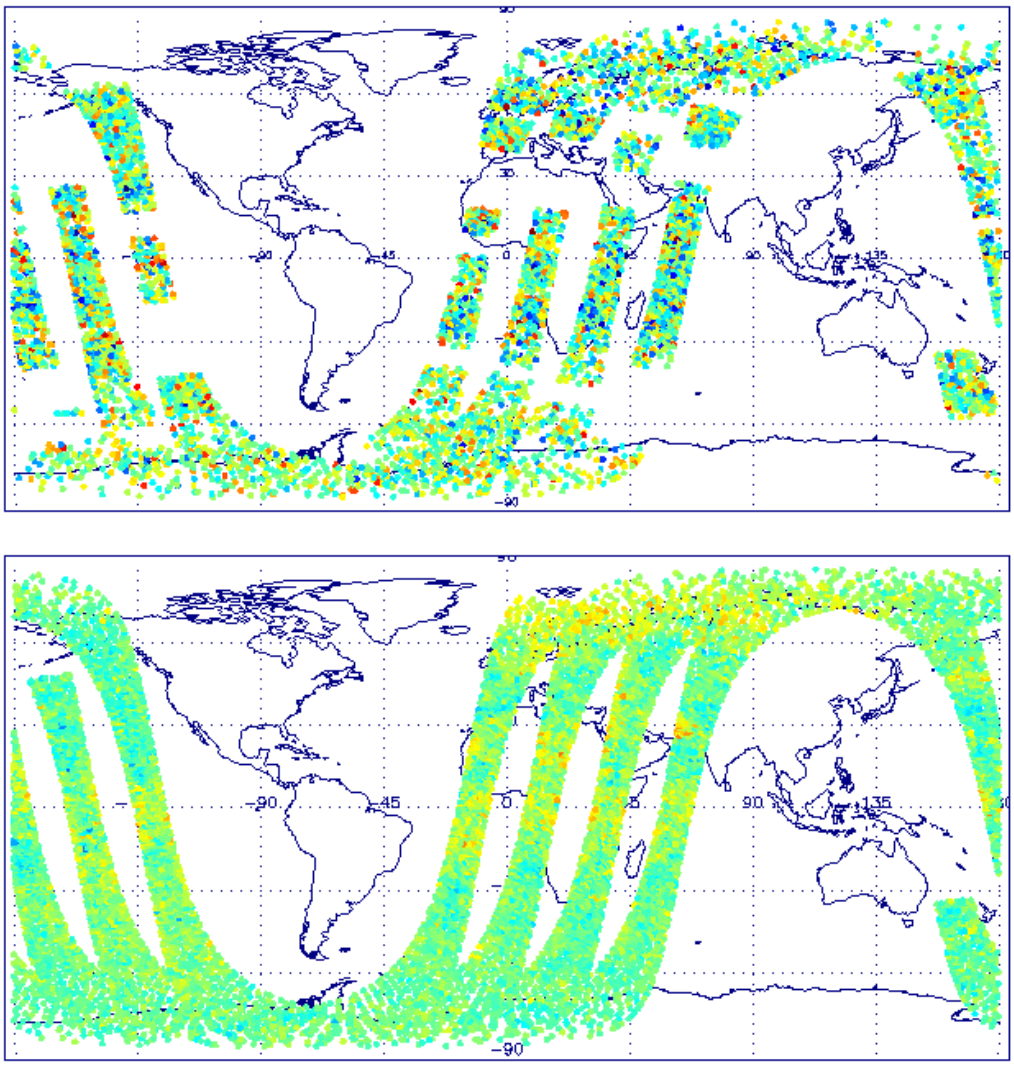

Figure 9 Observed minus computed radiance departures for AIRS channel 123 before (top) and after (bottom) de-noising using a spectral eigenvector method.

Assimilation of, for example, 324 de-noised channels will give a better analysis than the equivalent use of 324 real radiances (assuming the de-noised error characteristics are modeled correctly, including inter-channel correlations). Secondly, a truncated set of eigenvectors (or principal components) could actually be assimilated directly. This would require the development of an appropriate forward operator (in eigenvector space), but could, in principle, be a very efficient way of conveying the information from all channels to the analysis.

The primary problem with this approach is that, as yet, our understanding of issues related to the training of spectral eigenvectors and their use in NWP is not very mature, and the safer option of channel selection seems most appropriate.

2.2 Spatial data reduction

The AIRS instrument measures spectra on 90 pixels across each scan line, sampling the atmosphere approximately every 15-20Km. This sampling is currently much finer than the resolution of the ECMWF analysis (in which the data are to be used) and thus spatial thinning is an obvious way to reduce the AIRS

data volume. Currently NESDIS disseminate 1 AIRS pixel in 9 which still exceeds the analysis resolution. However, the thinning is fixed to select the centre pixel from the AIRS 3x3 array that aligns with the larger AQUA AMSUA instrument footprint. While this has a number of advantages, mainly allowing a regular sampling of any scan dependent bias patterns (and was at the request of the NWP community), it is not necessarily optimal for the avoidance of cloud contamination. For the estimation of CO_2 and NWP applications we are primarily concerned with clear radiance data (at least until methods for dealing with cloud contamination are more mature) and a more selective thinning could result in a similar volume of data being transmitted with a far higher proportion of clear scenes. The complication is that the data producer would need to implement a robust technique for identifying clear scenes. This is a non-trivial task and care would have to be taken to ensure that the disseminated data population was not skewed towards a particular cloud detection method (possibly inconsistent with tests that would subsequently be applied by the NWP centres to identify cloud).

While the operational AIRS data assimilation uses an extra thinning to minimize horizontal error correlations, the CO_2 data assimilation currently uses all data disseminated by NESDIS as described above. This is done to collect as many CO_2 estimates as possible to increase data averaging possibilities. The individual CO_2 estimates are very noisy, because the signal-to-noise ratio for CO_2 is low. There is also no constraint from the forecast model in space and time as there is for all other variables. As described in section 4, we currently use monthly averaged data on a 1° x 1° degree longitude-latitude grid with a further moving average with a 15° x 15° degree box. This provides smooth fields with relatively low errors (on the order of 2 ppmv). Some first results indicate that is probably feasible to calculate weekly averages, but any shorter time period used for the averaging increases the noise significantly.

3. WP 3 Science study with real AIRS data

The technical data flow of AIRS data through the IFS has been established. The AIRS data arrive in BUFR format from NOAA/NESDIS and the ECMWF Observational Database (ODB) has been modified to recognize and make available the observed radiances to the assimilation system. The analysis modules (relating to quality control, observation errors, interfaces to the radiative transfer model and post analysis diagnosis) originally designed to handle raw radiance data from other platforms have been extended and adapted to deal with AIRS data. The key elements are described below.

3.1 Cloud screening

Cloud effects on infrared radiances are extremely strong and it is important to have a robust and effective strategy to deal with this. At present, although the modeling of cloud radiative transfer is developing rapidly and the promise of assimilation of cloud affected radiances becoming closer, the accuracy required (particularly for CO_2 estimation) implies that we must develop a strategy for screening observations affected by cloud rather than explicitly modeling cloud effects. Previous cloud screening methods have the limited aim of determining whether the field of view (fov) contains cloud or not. Many 'cloud contaminated' fovs will nevertheless contain measurements in channels that are entirely responsive to the atmosphere above the cloud. In the context of CO2 estimation (i.e. low signal to noise) it makes sense to attempt to utilize these measurements.

The cloud detection scheme developed at ECMWF is described in McNally and Watts 2003 and the details of its operation will not be reproduced here. Briefly, it makes use of the fact that within the assimilation

system we have a good prior knowledge of the atmospheric state to predict the AIRS spectrum that would be measured in clear sky. The actual measured spectrum is compared and a digital filter used to search for the characteristic signature of cloud. There are tunable parameters which are currently set to very stringent values for the purpose of CO_2 and NWP. While this inevitably results in some data, which are in fact clear, being flagged as cloudy and rejected, it is considered the safest approach for these initial uses of AIRS data.

Since the publication of the method, further validation and testing has resulted in a number of refinements being adopted. One of these improves the detection of water vapour sensitive radiances. Larger uncertainties in the prior estimate of the atmospheric moisture profile (compared to temperature for example) led to an excessively stringent rejection of data. A technique has been incorporated to use information about the cloud conditions from the more reliable dry channel filtering to assist the filtering of the moisture sensitive channels. The result is a much higher yield of clear data with no loss of safety (i.e. no increase in missed cloud contamination) shown in Figure 10.

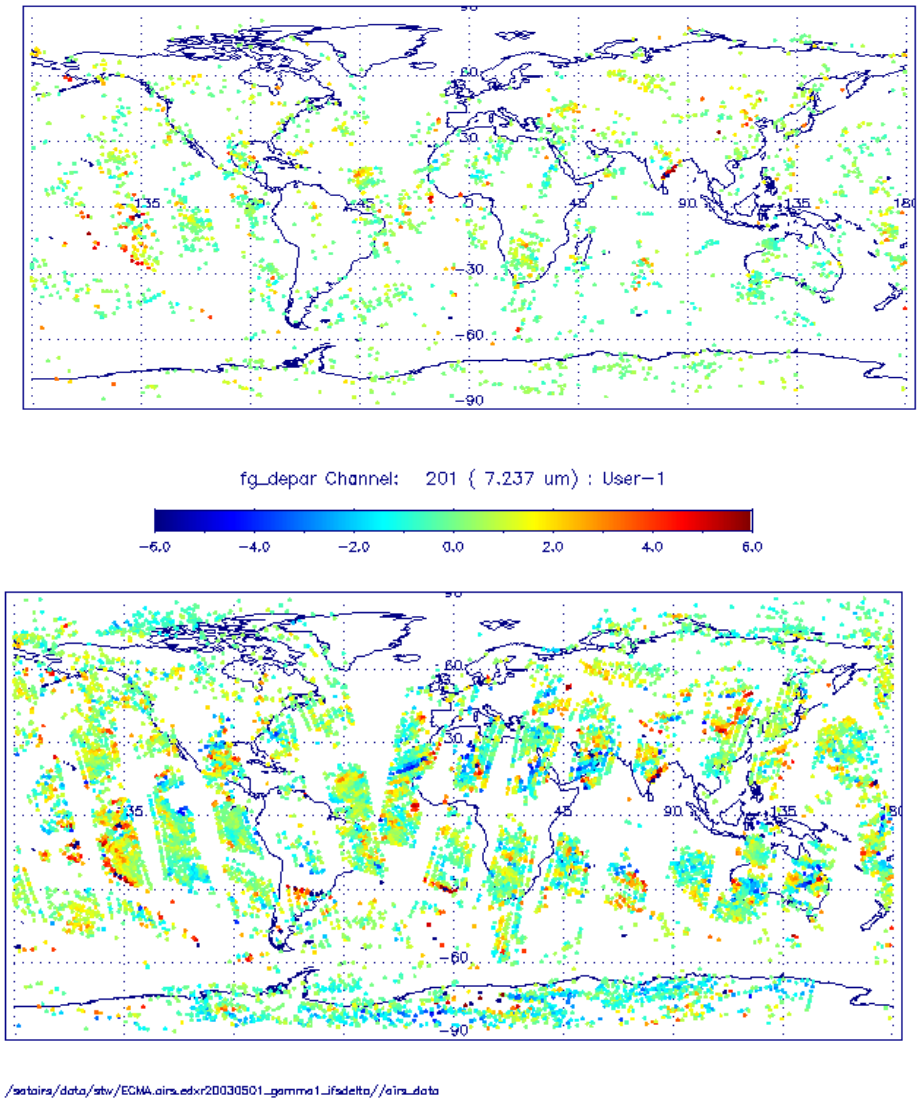

Figure 10 Output of the cloud screening algorithm without (top) and with (bottom) using the cross-band cloud detection.

3.2 Data monitoring

A central part of the assimilation of any data is a comprehensive monitoring of the input measurements. This is usually done by comparing the data against equivalent quantities computed from the NWP background (often called departures or innovations) not only because such information is readily available, but because these departures are what actually drive adjustments to the atmospheric quantities (e.g. temperature or CO_2) during the analysis.

The monitoring of radiance departures actually examines the quality of the entire assimilation system and provides information on random and systematic errors in: the measured data, the radiative transfer model used in the assimilation, the screening for atmospheric contamination (e.g. clouds / rain) and of course the underlying NWP background estimate of the atmospheric parameters.

While there is considerable heritage at ECMWF in this area, the monitoring of AIRS radiances (due to the shear number of channels) presented some new challenges. Previously for instruments such as the AMSUA (with only 15 channels) each channel could be monitored in some detail. However, even with the significantly spectrally sampled AIRS data set containing 324 channels this was not possible. Thus a staged approach has been adopted. A broad overview of the departures in all channels is provided by a time evolving Hovmoller diagram as shown in Figure 11. Statistics for each channel averaged over the globe (or other predefined geographical areas such as the tropics) are represented by a single pixel. Thus only significant changes in groups of channels (or bands) are readily visible in such a plot. In addition to this overview, a small group of key channels have channels have been selected for individual monitoring in that they have close analogue channels on other instruments. Time series and / or geographical maps of these are then monitored in detail and cross checked against the performance of independent channels on other instruments / satellites (see Figure 11). While it is still possible that individual channels can develop small problems that may go undetected, experience has shown that the adopted approach has worked well so far and is readily extendable to use with a much larger number of channels (e.g. the full 2378) if ever required.

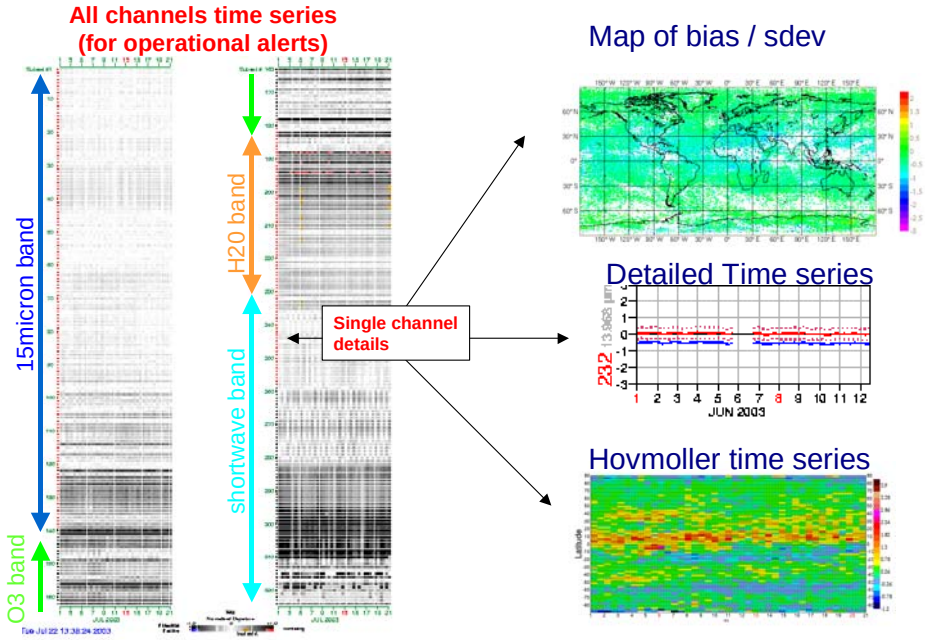

Figure 11 Examples of AIRS data monitoring as used operationally at ECMWF.

3.3 Bias correction

The investigations presented in WP1 and the routine monitoring activities confirm there are systematic errors in the AIRS data and / or radiative transfer model that must be corrected before any assimilation. Depending on the source of the problem, the biases can take the form of a simple global offset, or complicated air-mass / seasonally dependent errors. The primary difficulty is the absence of a globally available standard against which the biases can be evaluated. The best we have is the NWP background, but this of course can itself suffer from (sometimes significant) systematic errors.

The bias correction approach that has been adopted for the initial use of AIRS is a constant global offset applied to each channel. This is inconsistent with the more sophisticated air-mass dependent corrections applied to the use of other instruments in the ECMWF system, but was justified as follows. With AIRS being such a new and complex instrument, it was considered that a simple flat bias correction would aid the understanding of the response of the assimilation system to the AIRS radiances. In this way the possibility of a poorly trained air-mass varying correction could be eliminated from the diagnosis of any interesting or anomalous features found in the analyzed fields (particularly important for CO2 estimation where horizontal gradients are the key information we hope to extract from the system). In addition to these somewhat pragmatic considerations, it was found that bias structures for AIRS were generally flatter and more uniform than had been observed with previous instruments suggesting the instrument was very well calibrated and spectrally characterized.

At the time of writing this report a more sophisticated approach to bias correction is being considered that essentially produces an air-mass dependent correction from a fixed adjustment to the computed transmittance in a particular channel (see also WP1). This approach is described in Watts and McNally 2004. The method makes the assumption that the main source of variable bias comes from problems in the radiative transfer model and that, to first order, these are relatively constant systematic errors made in computing the absorption. This fixed absorption error translates into a variable (or air-mass dependent) adjustment via the atmospheric lapse rate. Initial experiments are very encouraging and such an approach has the additional benefit of providing information about radiative transfer modeling errors that may be (and in fact currently are) feeding back into improved absorption models.

3.4 Observation errors

Measurement noise is reasonably well defined from the instrument flight model characterization (see Figure 1) with values between 0.05 and 0.4 K NedT depending on channel. For the 4 and 15 μm CO_2 sounding channels, NedT values are generally close to 0.2 K. Forward model (radiative transfer) noise must also be accounted for in the specification of observation errors in the assimilation process. While this originates from fast model and line-by-line (or 'spectroscopic error') contributions, neither term is particularly well characterized. With this in mind, a rather simplified model has been assumed:

- 0.6 K in dry tropospheric channels with minimal surface sensitivity
- 1.0 K in stratospheric channels
- 2.0 K in window and water vapour channels

While this is certainly not optimal, the values may be considered reasonable and conservative, consistent with other aspects of the AIRS usage.

4. WP 4 Design/ development/ initial testing of an assimilation strategy for NWP and a production strategy for CO2.

On the basis of the studies described in WP3 the ECMWF 4DVAR assimilation system has been modified to use AIRS radiance data and allow the simultaneous estimation of CO_2. We have implemented CO_2 in the assimilation system as an independent column variable for both the troposphere and stratosphere meaning that CO_2 is not a tracer variable in the transport model and is only estimated at the observation locations. No background error correlations exist between CO_2 and all the other assimilation variables and there is also no vertical error correlation between the tropospheric column and the stratospheric column. In practice this means that, while the forecast model variables like temperature and water vapour appear in the control vector as 3-dimensional fields at initial time t0, CO_2 appears in this control vector as a vector of column variables at all observation locations. The link between the initial state and the states at observation locations and times does not exist for CO_2.

This procedure allowed for a relatively quick implementation of CO_2 in the data assimilation system allowing us to explore the capabilities of the system to estimate CO_2. Although this implementation makes full use of the accurate temperature and water vapour analysis fields constrained by all available observations, it also has some limitations. By assimilating column CO_2 values instead of full profiles a hard constraint is applied to the analysis in the form of a fixed profile shape. This removes some of the flexibility in the adjustments and can lead to errors if the used profile shape is far from the truth.

The two column estimates can vary independently and are separated by a variable tropopause estimated from the background temperature profile based on a lapse rate definition. This ensured that information from the stratosphere did not dominate the tropospheric analysis results. However, any potential useful correlations between stratospheric CO_2 and tropospheric CO_2 are disregarded. Another drawback is that the extend of the tropospheric column is quite variable. Depending on the tropopause height and the cloud top height, the column varies from shallow to deep allowing respectively less or more channels to be used in the tropospheric analysis.

While the operational data assimilation system uses several bands throughout the spectrum (see WP1), the CO_2 data assimilation system currently only uses the longwave CO_2 band. This was done to minimize the effect of other absorbers on the CO_2 estimates, while the AIRS observations were still be monitored and adjusted. On the longer term the CO_2 estimation will be part of the full operational system using all available AIRS observations.

4.1 Impact of AIRS on the NWP system

The baseline AIRS configuration described above has been tested at full resolution in 12hr 4DVAR using cycle 25R4 of the IFS between 10 Dec 2002 and 19 March 2003 (a total of 100 cases) and is subsequently referred to as “AIRS”. The control against which the AIRS impact is compared (subsequently referred to as “CTRL”) is generally the operational system. In summary, results with the ‘AIRS’ system show a small but consistent positive improvement over the ‘CTRL’ system. We show a couple of diagnostics to demonstrate this.

4.1.1 Changes to the analysis.

Figure 12 shows a difference map (AIRS minus CTRL) of RMS analysis temperature increments at 500hPa (averaged over a ten day period in December 2002). While the contour interval is extremely fine (shading starting at 0.1K) the map shows that there are slightly larger increments over the oceans (where most of the AIRS radiances are used) and a small (but fairly consistent) decrease in increments at radiosonde stations when the AIRS radiances are assimilated (the large increase over central Africa originates from the use of AIRS data over lake Chad that is treated as "sea" in the assimilation). The reduced increments at radiosonde stations is an encouraging diagnostic and shows that the extra work being done by the AIRS data in the analysis improves the agreement with radiosonde data through the assimilation cycle.

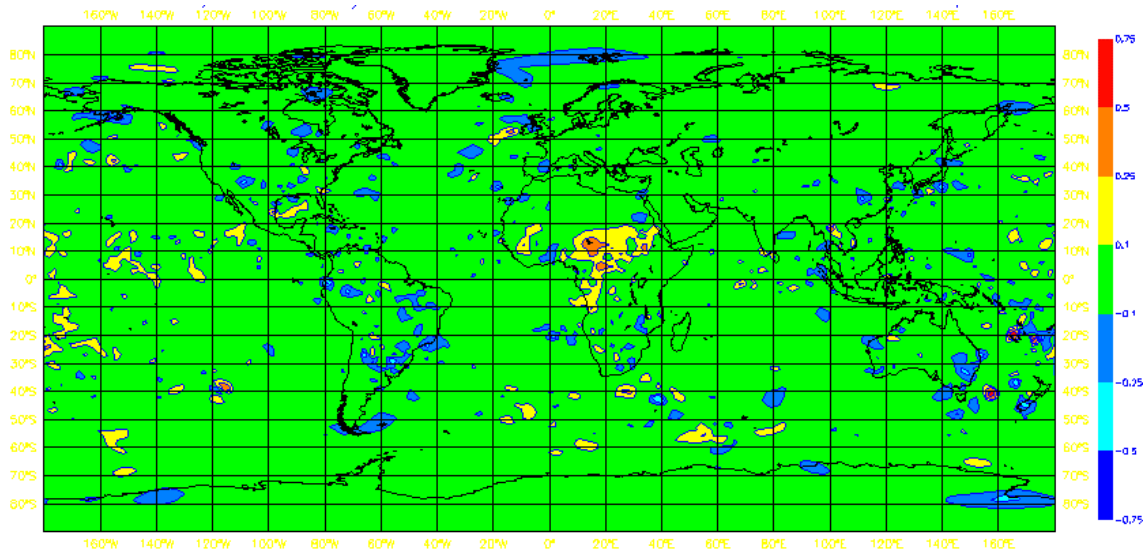

Figure 12 Difference map showing RMS analysis increments of the AIRS system minus those of the CTRL for temperature at 500hPa (averaged over 10 days). Shading starts at 0.1K.

4.1.2 Impact on forecast quality.

Averaged over 100 cases there is a very small, but very consistent improvement at all ranges in the Northern Hemisphere (the results of significance testing are contained in Table 1 and Table 2 show that the improvement is statistically significant at the 1% level for day-5). For the European area (embedded in the Northern Hemisphere statistics) the positive impact is marginally clearer, but less significant. In the Southern Hemisphere, only a slight improvement is seen at day-3 (significant at the 5% level) and beyond this no improvement is seen over the CTRL (the negative impact at day^{-1}0 was not found to be significant < 10%). The verification of temperature forecasts from the 2 systems is generally consistent with the height results in the mid-latitudes, but they additionally show a positive impact of the AIRS in the tropical temperatures at 200hPa. The same statistic for the southern hemisphere shows larger RMS errors when AIRS data are used, but a closer investigation indicates a large systematic difference between the AIRS and CTRL analyses, localized to the edge of the Antarctic continent and not evident at any other level than 200hPa.

In the statistical significance testing of the forecast impact (shown in Table 1 and Table 2) red indicates a positive impact due to AIRS and blue a negative impact. The percentage figure indicates the level at which a t-test found the results statistically significant. If no significance better than 10% is found the result is marked with an X.

The assimilation of AIRS radiances with the baseline system described here shows no adverse effects in the analysis (in terms of the fit to other observations) and slightly reduced analysis increments at radiosonde locations. Overall the forecast performance of the baseline AIRS assimilation scheme is encouraging, essentially showing a consistent positive impact in most areas and parameters.

Table 1 Significance testing of 1000 hPa (first figure) and 500 hPa (second figure) height forecast verification

Forecast Range	Northern Hemisphere	Southern Hemisphere	Europe
day-3	5% / 1%	5% / 10%	X / 2%
day-5	0.1% / 1%	10% / X	10% / 5%
day-7	X / X	X / X	X / X

Table 2Significance testing of 1000 hPa (first figure) and 500 hPa (second figure) wind forecast verifications

Forecast Range	Northern Hemisphere	Southern Hemisphere	Europe
day-3	X / 5%	0.1% / 0.1%	10% / 0.5%
day-5	0.1% / 0.1%	2% / 5%	5% / X
day-7	0.1 / 2%	X / X	X / 10%

4.2 Estimation of CO_2

Some first results of the CO_2 data assimilation scheme are presented here to illustrate the capabilities of the system. The background values used in the assimilation, shown in Figure 13, were zonal mean monthly averaged mixing ratios based on surface flask observations from the previous year (GlobalView, 2003). These averaged flask observations are based on maritime air samples and a constant value of 2 ppmv was added to compensate for the annual trend. The background error was set to 30 ppmv and was deliberately taken large to minimise the contribution of the background to the analysis in these preliminary experiments. Individual analysis values at the observation locations were gridded onto a 1° x 1° latitude longitude grid for a whole month. Within a grid box the data were averaged using a weighted average with the analysis errors as weights. This 1° x 1° grid was then smoothed with a 15° x 15° moving boxcar average. Each individual grid box needed to have more than 10 observations within a month to be included in the smoothing averaging. Therefore, some geographical areas have no data in the final monthly mean fields because of consistent high cloud cover.

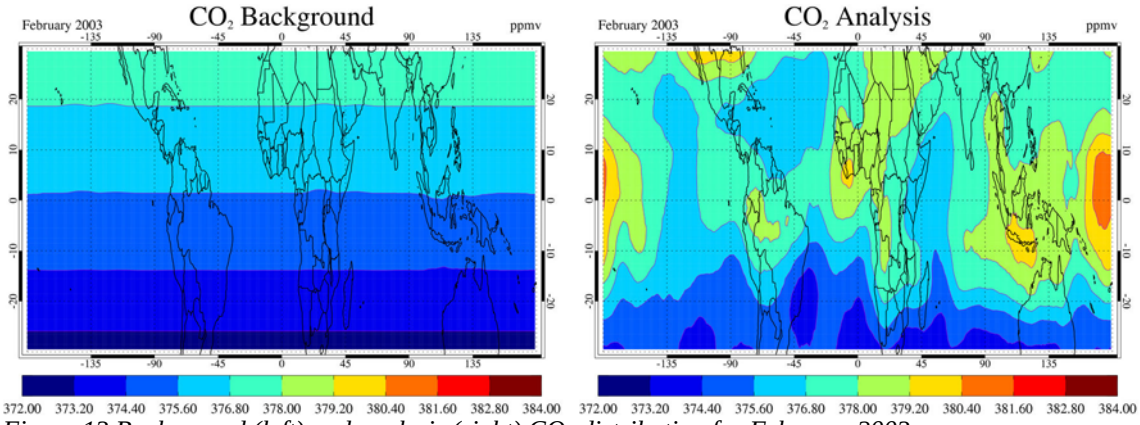

Figure 13 Background (left) and analysis (right) CO_2 distribution for February 2003.

Figure 13 shows the CO_2 analysis results for February 2003 and Figure 14 for August 2003. The left panels show the background values and the right panels show the actual analysis results. Both figures show that the analysis adds structure to the zonal background field. Although the main north-south gradient remains, meridional variability is produced by the analysis. In the equatorial region the analysis tends to have more CO_2 in the convective areas, especially in the West Pacific. Another feature can be observed over the southern part of North America. A careful analysis was done using AMSU-A data to see if these features were caused by biases in the temperature analysis. This seems indeed to be the case for the high values over southern North America in February, where a cold bias is observed in the temperature analysis field compared to AMSU-A measurements. This could cause a positive bias in the CO_2 field. However, for the other regions such a cold analysis bias is not present. Also, plots of AIRS first-guess departures (the difference between the observed brightness temperatures and the model simulated brightness temperatures from the 6-hour forecast) that drive the analysis show the same patterns as the CO_2 analysis field. These patterns are very dissimilar from the AMSU-A first-guess departures and can therefore not be explained completely by errors in the temperature forecast.

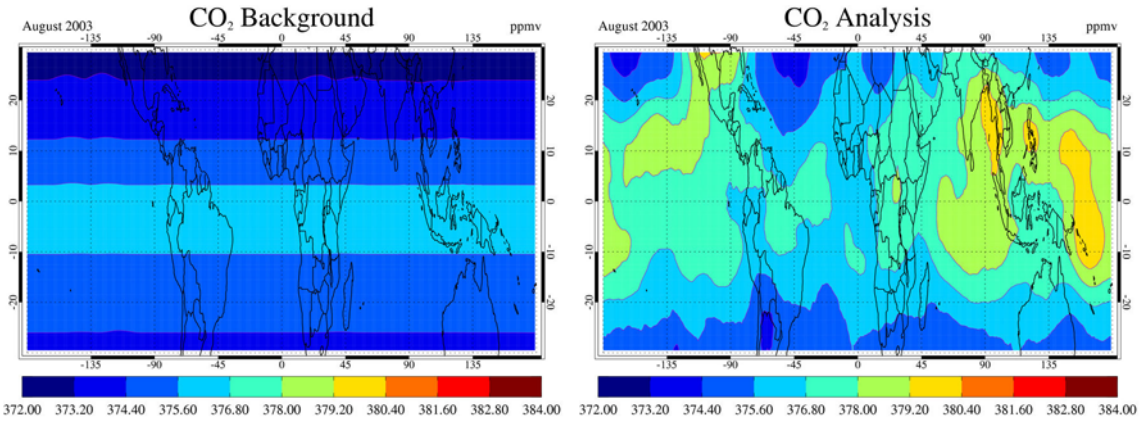

Figure 14 Background (left) and analysis (right) CO_2 distribution for August 2003.

The higher CO_2 values on the west side of Africa in February could be explained by biomass burning effects. Similar patterns in the MOPITT carbon monoxide observations can be observed over that area in February 2003 (see http://www.eos.ucar.edu/mopitt/data/index.html). The high values in the western Pacific are probably more surprising. One explanation could be that anthropogenic emissions from Southeast Asia are lifted up and transported to the western Pacific by the general circulation. During this part of the year there is

a circular wind pattern in the middle troposphere bringing air east from the Southeast Asian coast and then south to the middle of the Pacific. However, more careful analysis of the results should be carried out before drawing firm conclusions. For example, clouds are detected in our cloud detection scheme within a small error margin. Therefore, it is in principle possible to have a systematic error in the lower channels due to undetected clouds resulting in a CO_2 bias of a few ppmv. Also, air-mass dependent errors in the radiative transfer (e.g., the spectroscopy) could cause systematic errors in the CO_2 analysis results on regional scales.

5. Conclusions and Recommendations

Based on the experience gained during the project we can draw the following conclusions and make the following recommendations:

Advanced infrared sounders provide thousands of spectral channels. However, it is not feasible to use all these channels (e.g. bandwidth limits in the trans-Atlantic line for AIRS data). Data reduction or compression methods have to be used in order to transmit and process the satellite data in near real time. At present, ECMWF uses a careful selection of 324 channels from the AIRS instrument that represents all relevant atmospheric variables of interest. The amount of data is even further reduced by using only 1 out of every 9 footprints. Spectral data compression methods could be used as well to reduce the amount of data to be assimilated in the NWP system. These methods provide the whole observed spectrum after data transmission and have the potential to reduce the noise in the spectra as well. However, a careful analysis has to be made for the cut-off point to make sure that small signals are not treated as noise.

The instrument noise characteristics of the AIRS instrument are quite good, but the noise is still large compared to the actual CO_2 signal. This results in noisy CO_2 analysis results, especially in the stratosphere. Significant averaging is therefore needed to reduce the noise. Any instrument with better noise characteristics would improve the individual CO_2 results and therefore allow for shorter time averages than the currently used monthly means.

Improved radiative transfer modelling is also required to obtain better results. Because the CO_2 signal is so small, small errors in the spectroscopy will have an impact on the CO_2 results. Temperature dependent spectroscopy errors could even create regional biases that are difficult to correct in flux inversion calculations. A first attempt to correct these regional biases in the radiative transfer has been described in WP2, but more careful analysis is needed. Proper modelling of solar effects in the short-wave spectral range would allow the use of this spectral band. There are many CO_2 sensitive channels in this spectral region and including these in the data assimilation would improve the CO_2 results.

Based on the promising CO2 results ECMWF is now heading towards operational monitoring of CO_2. Within the proposed GEMS project, atmospheric CO_2 will be estimated from AIRS, IASI, and CrIS observations. At the same time, major efforts will be made to model the carbon fluxes at the surface using relevant satellite data. On the long-term this should lead to a full monitoring system using all relevant satellite data to constrain atmospheric CO_2 as well as the surface fluxes.

To improve this monitoring capability, instruments specially designed to observe CO_2 could be a very useful addition. Infrared sounder instruments are generally not sensitive in the lower troposphere and also have a low signal-to-noise ratio with respect to CO_2. Most of the signal in these observed radiances comes from the

atmospheric temperature variability and little from CO_2 itself. Furthermore, the required accuracy for CO_2 observations (on the order of 1%) makes the estimation of CO_2 from infrared radiances a daunting task. As an alternative approach, a satellite sounder with high spectral resolution in the near-infrared seems to be promising. Studies in the United States for the upcoming Orbiting Carbon Observatory (OCO) mission seem to suggest that this approach can achieve the required accuracy. These measurements are also sensitive to the lower troposphere, which is a real advantage. Main problems here are the low signal-to-noise ratio over the ocean (apart from sun glint areas) and the extensive radiative transfer modeling needed to accurately simulate the atmospheric scattering effects. A long-term approach would be the use of active instruments, such as near-infrared lidar, but this will need extensive scientific study and technical development, which is outside the scope of this study.

References

Aumann, H. H., M. T. Chahine, C. Gautier, M. D. Goldberg, E. Kalnay, L. M. McMillin, H. Revercomb, P. W. Rosenkranz, W. L. Smith, D. H. Staelin, L. L. Strow, and J. Susskind, AIRS/AMSU/HSB on the Aqua mission: design, science objectives, data products, and processing systems. *IEEE Trans. Geosci. Remote Sensing*, **41**, 253-264, 2003.

Crevoisier C., A. Chedin, and N. Scott, AIRS channel selection for CO2 and other trace-gas retrievals. *Quart. J. Roy. Meteor. Soc.*, **129**: 2719-2740, 2003.

Dudhia A., P. E. Morris, and R. J. Wells, Fast monochromatic radiative transfer calculations for limb sounding. *J. Quant. Spectroscopy*, **74**, 745-756, 2001.

Engelen, R. J., E. Andersson, F. Chevallier, A. Hollingsworth, M. Matricardi, A. P. McNally, J.-N. Thépaut, and P. D. Watts, Estimating atmospheric CO2 from advanced infrared satellite radiances within an operational 4D-Var data assimilation system: Methodology and first results. Submitted to *J. Geophys. Res*., 2004.

GLOBALVIEW-CO2, Cooperative Atmospheric Data Integration Project - Carbon Dioxide, CD-ROM, NOAA CMDL, Boulder, Colorado [Also available on Internet via anonymous FTP to ftp.cmdl.noaa.gov, Path: ccg/co2/GLOBALVIEW], 2003.

Matricardi, M.: RTIASI-4, a new version of the ECMWF fast radiative transfer model for the infrared atmospheric sounding interferometer. *ECMWF Tech. Memo*, **425**, 2003.

Rizzi R, M. Matricardi, and F. Miskolczi, On the simulation of up-looking and down-looking high-resolution radiance spectra using two different radiative transfer models. *ECMWF Tech. Memo*, **343**, 2001.

Rodgers, C. D., Inverse Methods for Atmospheric Sounding. Theory and Practice, World Scientific, 2000.

Watts, P. D., and A. P. McNally, Identification and correction of radiative transfer modeling errors for atmospheric sounders: AIRS and AMSU-A. In preparation, 2004.

Annex 1: First Interim Report to the European Space Agency

Measurement of Seasonal CO_2 Fluctuations from Space

February 2002

Authors: P.D.Watts, A.P.McNally, J-N. Thépaut and M. Matricardi

ESA contract No. 14644/00/NL/JSC

European Centre for Medium-Range Weather Forecasts

Table of Contents

Annex 1 - Executive Summary

This is the first quarterly report for the contract study on measurement of seasonal CO_2 fluctuations from space. The statement of work identifies four distinct workpackages (radiative transfer, data sampling, use of real AIRS data and system implementation) and schedules these to run in sequence. Whilst this structure is logical it has proved expedient to tackle areas in three of the four workpackages during this first period.

In **WP1** (radiative transfer) the fast radiative transfer model (RTTOV) has been incorporated within the ECMWF integrated forecast system and simulates AIRS and AMSU measurements. Validation aspects are awaiting adaptations to this code, namely the enhancement of the dependency on trace gases including CO_2 from fixed to variable quantities; these are expected to be complete early in 2002.

Several aspects of **WP2** (data sampling) have progressed significantly. Methods for achieving the necessary reduction in AIRS data volume prior to transmission have been studied. The options, channel selection or eigenvector compression of the entire AIRS spectrum, have been evaluated and preliminary conclusions favour the use of selection as the eigenvector technique is relatively immature in this application and could lead to poorly understood degradation of the data. The 4.2 and 4.5 μm bands have been identified as most useful for CO_2 estimation and within these, the 4.2 μm band is well sampled within the planned Near Real Time (NRT) dissemination system, the 4.5 μm band is not. Improved coverage of this band has been requested. The CO_2 signal is also significant within the 15 μm band but with ambiguous signals from ozone and water vapour; concurrent use of the particular ozone (9.6 μm) and water (6-7 μm) bands is therefore strongly recommended. A formal study on channel selection for information content is being undertaken and preliminary results support the NESDIS NRT selection; extension of this study to CO_2 sensitivity is planned.

Most progress has been made within **WP3** (science study). End to end flow of simulated AIRS and AMSU data through the ECMWF system has been established. Realistic (cloud affected) AIRS simulated radiances are being used for the development, testing and evaluation of a candidate cloud screening algorithm. The digital filter algorithm utilises estimates of the clear radiances from the NWP model, employs a novel channel ordering system and estimates the lowest peaking cloud-free channel in a particular sounding. Detection is based on the expected general behaviour of the cloud signal. Results of preliminary testing using simulated data show that the method is capable of efficient detection of cloud-free measurements. Residual contamination is within instrument noise levels for tropospheric sounding channels. A second cloud screening algorithm, which would be an extended application of a published method (English and Eyre 1999), is under preliminary investigation.

No progress has yet been made on **WP4** (system implementation).

A1-1. WP 1 Validation of a fast radiative transfer model (RTM) for AIRS

Validation of the fast radiative transfer model (RTTOV-AIRS) requires the validation of both the fast model against its training model (GENLN2 line by line output) and the validation of the training data. Fast models, which unavoidably add some error to RTM calculations compared to the most accurate LBL calculations, are required in any practical situation. However, the current situation for infrared RTM calculations is that errors tend to be dominated by inaccuracies in the basic spectroscopic data, i.e. in the LBL calculations.

A1-1.1 Validation of RTTOV against LBL data

Fast model validation against the training LBL model is relatively straightforward and has been done for the AIRS RTTOV under separate contract, Matricardi et al, 2001. In CO_2 sounding bands the fast model bias against the LBL is generally less than 0.03 K and the standard deviation less than 0.05 K. There are a number of channels, particularly within the 15 μm band, where both bias and standard deviation can be up to 0.2 K. This is within AIRS instrument noise levels (Figure 1) but there could be justification for omitting these channels from the CO_2 estimation process.

Channels in water vapour and ozone sensing bands have higher fast model errors but even these have been reduced by careful choice of fast model predictors to rms values of less than 0.3 K. In summary, the fast model is not expected to contribute significant errors in the majority of channels and the minority that do can be eliminated as these errors are very well characterised.

A1-1.2 Validation of GENLN2 LBL data

Validation of the LBL model underlying the fast model is a more complicated task. It can be tackled indirectly by intercomparisons of different LBL models or directly by comparisons to measured spectra. Intercomparisons do not reveal basic spectroscopic errors that are common between LBL models. At present this section draws entirely upon Rizzi et al. 2001 for a preliminary look at validation of GENLN2. Measured spectra were obtained from the High resolution Interferometer Sounder (HIS) (on board the ER-2 at 20 Km) during the first Convection and Moisture Experiment. Two LBL codes (GENLN2 and HARTCODE) were compared to the measured spectra. Results are somewhat compromised by errors from natural atmospheric variability and HIS noise but some interesting results are obtained.

Differences between HIS and the two LBL codes are similar indicating the two codes are in good agreement. In spectral regions where the HIS variability (along the flight track) is low, it is inferred that the differences are attributable to LBL (spectroscopic or algorithmic) errors. We can comment on two important regions for CO_2 estimation. Around 15 μm there appear to be problems with the LBL simulation of the high frequency branch of the band; rms errors up to 0.8 K are found. At 4.5 μm, HIS variability is increasing but there is evidence for LBL errors of at least 0.5 K. No reliable information is available at 4.2 μm. At 0.2 cm^{-1} resolution the errors in the 15 and 4.5 μm bands can be seen to be highly structured with positive-negative deviations of around 0.5-1K related to the individual absorption line positions. AIRS channels in these bands have a width of around 1 and 3 cm^{-1} respectively – in neither case wide enough to average the oscillations (as would a similarly placed HIRS channel for example).

These results, although preliminary, serve to demonstrate that validation of the LBL aspect of the RTM is extremely important. Errors of the magnitude reported in Rizzi et al. 2001 are very significant and a strategy to handle or remove them needs to be developed.

A1-2. WP 2 Science study to optimise AIRS data usage for NWP applications and for CO_2 work

The purpose of this workpackage is to establish strategies for handling and making best use of the large data volumes represented by the Aqua instrumentation at full spectral and spatial resolution. Tasks in this area are

therefore divided into spectral sampling, spatial sampling /averaging and use of other Aqua platform instrumentation.

A1-2.1 Spectral sampling

Two approaches to spectral sampling have been investigated; the sampling of channels and / or bands of the AIRS measurements and the compression of the full AIRS spectrum using eigenvector compression.

A1-2.1.1 Eigenvector compression

Compression of the AIRS data by this method is detailed in Appendix A. Essentially a measured spectrum is projected onto the eigenvectors of a prepared training sample and a (limited) number, *M*, of the resulting projection coefficients are transmitted to the user. The data compression obtained arises from the use of an incomplete set of eigenvectors, the premise being that much the information content of the complete spectra may be retained; the discarded coefficients are assumed to describe mainly measurement noise.

As a result of our initial studies we may conclude the following:

The rate at which the reconstruction error grows as the value of *M* decreases (i.e. with increasingly efficient compression) has been investigated in simulation by a number of studies (e.g. Huang and Antonelli 2001, Goldberg *pers.com.*). It has been found that using 200 leading eigenvectors allows each channel to be reproduced in the absence of clouds with a rms reconstruction error within the expected instrument noise limits for AIRS. To achieve the same reconstruction accuracy in cloudy-sky conditions it has been estimated that up to 500 eigenvectors would be required. However, some important points should be considered

1) The studies performed so far by Goldberg suggest the eigenvectors need to be updated regularly (i.e. recomputed every month or so) to maintain the same reconstruction accuracy. While the logistics of updating and transmitting the results to the NWP centres is not difficult, the drift is obviously a cause for some concern (suggesting an air-mass or seasonal variation). Such drifts would potentially create difficulties in the implementation of an effective bias correction scheme.

2) Reproducing the spectra to within the instrument noise (in an rms sense) may not be adequate for NWP or CO_2 estimation. The choice of metric to measure reconstruction error is very important as some aspects of the spectra (relating to different atmospheric features, possibly with low variance) are clearly more important in NWP than others. Also, and as a general rule, elements in the processing chain that introduce noise should be avoided unless they are absolutely necessary.

3) Many NWP centres will require access to cloudy radiances (if only to perform their own cloud detection) and thus a compression factor of less than 5 (2377/500) is not a huge saving (compared to the efficient “technical” compression tools such as BUFR that do not degrade the accuracy of the data).

With these points in mind the use of eigenvectors as a solution to the purely technical problem of excessive data transfer volumes may not be best (given the risk of degrading the data in a less than fully understood way) and a purely technical (non-loss) compression seems more appropriate.

A1-2.1.2 Band and channel selection

Several bands within the AIRS spectrum have been identified as useful for NWP and CO_2 estimation purposes. As the CO_2 absorption bands are very important for temperature sounding, the two requirements are by no means mutually exclusive. Although somewhat arbitrary, the following bands have been defined to aid description and are treated independently in the prototype cloud screening method (see WP 3).

LW	('Longwave' 15 μm CO_2)	15.4 to 11.1 μm
O3	('Ozone' 9 μm O_3)	9.99 to 8.09 μm
6M	('6 micron' 6 μm H_2O)	8.07 to 6.23 μm
SW1	('Shortwave-1' 4.5 μm CO_2)	4.58 to 4.44 μm
SW2	('Shortwave-2' 4.2 μm CO_2)	4.20 to 3.75 μm

As a first step in defining the utility of an AIRS channel measurement, the response of the channel to a standard perturbation in each principle atmospheric quantity was determined using the line by line model (GENLN2). The atmospheric quantities and the standard perturbation considered were air temperature (T, δT = model error), skin temperature (T_s, δT_s = model error), CO_2 (δCO_2 = seasonal climatological), water vapour (q, δq = model error), N_2O (δN_2O = Seasonal climatological) and Ozone (O3, δO3 = model error). 'model error' indicates a perturbation equivalent to current estimates of the ECMWF NWP 6h shortrange forecast error. Radiance perturbations from the LBL model were convolved with the Flight Model specification of the AIRS channel response functions. The O3 and 6M bands are not directly relevant to the CO_2 estimation problem and are not discussed here. They will of course contribute to the estimation through improved temperature, moisture and ozone analyses.

Results for the portion of the **LW** band sensitive to CO_2 are shown in Figure 2. The response to CO_2 is seen to be at or around the basic instrument noise level, indicating that a moderate amount of data averaging will deliver a reasonably high signal to noise level[1]. However, there are several other significant responses in this band which will complicate interpretation. Naturally, a strong response is seen with respect to atmospheric temperature. This signal however, can probably be well determined either directly, or, more likely, through the assimilation system, by the AMSU-A instrument measurements made coincidently with the AIRS measurements (see 2.3). Less tractable problems will arise from the signals from ozone and water vapour. Assimilation of the O3 and 6M bands AIRS data will significantly reduce model uncertainties in these quantities but their presence will undoubtedly, in the context of CO_2 estimation, lead to signal aliasing unless great care is taken.

The grey bars on Figure 2 show the channels that NESDIS currently plan to disseminate at launch. They appear qualitatively reasonable, with selections either aiming for low water and ozone contributions or the opposite, and avoiding channels with significant multiple contributions. Channel selection has been put on a more quantitative basis by implementing the method of Rodgers 1998 which determines the relative information content of each channel compared to the information already held by an assimilation system. Although initial tests using this method give an optimized channel set that includes around 40% of the NESDIS selection, the accuracy of temperature and humidity retrieval (evaluated using a one-dimensional variational analysis scheme) is very similar with both optimized and NESDIS channel sets, except in the

[1] This assumes of course that there are no significant bias errors present due to, for example, calibration and spectroscopic inaccuracies.

stratosphere. Studies with the Rodgers method will be extended to include a) larger numbers of channels and b) information content on trace gases and CO_2 in particular.

The responses in the SW bands are shown in Figure 3. The **SW-2 (4.2 μm)** band appears extremely promising as it is a) very clean – no ozone and only traces of water vapour sensitivity, and b) subject to low instrument noise levels (< 0.2 K). Some problems have been revealed by detailed study related to cloud detection (see WP 3) and levels of solar contamination during daylight need to be established before being sure that this is a high priority band for temperature and CO_2 sounding. The figure shows that NESDIS currently plan to transmit the whole of the CO_2 sensitive part of the SW-2 band.

The **SW-1 (4.5 μm)** band shown on the same figure reveals almost equally good characteristics at the shorter wavelength end of this band with instrument noise levels lower even than the SW-2 band. At longer wavelengths (>4.43 μm), water vapour, N_2O and CO (from 4.54 – 4.81 μm not shown) contributions become significant. What is apparent in this band is the lack of channels in the planned NRT stream; this is being addressed in consultation with NOAA-NESDIS.

A1-2.1.3 Summary

EOF compression, whilst a neat theoretical construct, has some characteristics that make it an undesirable strategy at this stage. The alternative route of preselected channels transmitted uncompressed appears preferable.

All bands of the AIRS instrument measurement are of utility to the CO_2 estimation problem, if not directly then through improved temperature, humidity and moisture analyses.

Within bands there is qualitative evidence that the selection of channels made to date by NOAA-NESDIS is appropriate apart from the lack of channels in the 4.5 μm band. This conclusion is supported by preliminary studies of information content although these have so far only been conducted within the context of information on temperature and humidity.

A1-2.2 Spatial sampling / averaging

No work has been undertaken yet on sampling or averaging strategies.

A1-2.3 Simultaneous use of other instrument data

AMSU-A data from AQUA will be available at full resolution to supplement the AIRS data. It is anticipated that information from the AMSU-A will be used via its incorporation within the assimilation (improving the quality of the temperature analysis) and not by direct mapping of the AMSU-A radiances to the AIRS footprint. However, there may be a case for explicit colocation of AMSU-A and AIRS prior to the assimilation to assist cloud detection in the latter. There are initiatives within the AIRS science team to fund the colocation of AQUA/MODIS data to the AIRS footprint which would be another valuable resource for cloud detection. It is not yet clear if this facility will be active on day-1.

A1-3. WP 3 Science study with real AIRS data

This workpackage is concerned with providing the infrastructure and pre-processing techniques required to handle AIRS data prior to assimilation into the NWP system. Whilst clearly we do not have access at present to real AIRS data, much can be achieved with the use of simulated measurements. Progress in this workpackage includes establishing the data flow for AIRS in the IFS (Integrated Forecast System) and a substantial study of the problem of cloud detection in the AIRS measurements.

Using the NESDIS supplied simulated AIRS data to supply location and viewing geometry, we have the facility to calculate simulated clear and cloudy AIRS observations using atmospheric fields from the ECMWF model (Chevallier et al, 2001). For testing purposes, a limited 6 hour data set consisting of 4633 soundings with global coverage has been generated (see Figure 11 for locations).

A1-3.1 Data Flow in the IFS

The technical data flow of AIRS data through the IFS has been established. The AIRS data will arrive in BUFR format from NOAA/NESDIS and the ECMWF Observational Database (ODB) has been modified to recognize and make available the observed radiances to the assimilation system. The analysis modules (relating to quality control, observation errors, interfaces to the radiative transfer model and post analysis diagnosis) originally designed to handle raw radiance data from other platforms have been extended and adapted to deal with AIRS data. End-to-end tests have been sucessfully performed with NESDIS simulated data.

A1-3.2 Cloud screening

Cloud effects on infrared radiances are extremely strong and it is very important to have a robust and effective strategy to deal with this. At present, although the modelling of cloud radiative transfer is developing rapidly and the promise of assimilation of cloud affected radiances becoming closer, the accuracy required (particularly for CO_2 estimation) implies that we must develop a strategy for screening observations with cloud rather than explicitly modelling cloud effects. Previous cloud screening methods have the limited aim of determining whether the field of view (fov) contains cloud or not. Many ‘cloud contaminated’ fovs will nevertheless contain measurements in channels that are entirely responsive to the atmosphere above the cloud. In the context of CO_2 estimation (i.e. low signal to noise) it makes sense to attempt to utilise these measurements.

In developing a cloud screening method we have aimed to:

i) Retain measurements wherever possible,

ii) Utilise the forecast model estimates of the cloud-free radiances

iii) Utilise the high number of AIRS channels and their extensive coverage in the vertical,

iv) Be conservative so that residual contamination is very low.

ii) gives us a background against which even small cloud effects can in principle be detected and iii) allows us to achieve i) by retaining measurements in channels that respond to the cloud-free atmosphere above the cloud.

The strategy has been to order the AIRS channels according to some criteria such that cloud effects are monotonically increasing and then apply a filter to the measured minus estimated brightness temperatures to identify at which channel (in the ordered space) the cloud effect becomes significant. Channels peaking higher in the atmosphere can then be considered clear of clouds and used in the subsequent assimilation; channels peaking lower can be rejected.

A1-3.2.1 Channel ordering

AIRS channels are ordered according to the pressure at which the ratio of radiance effect of an opaque black cloud to the total clear radiance ($\delta R/R$) exceeds a threshold of 0.01 (appendix B describes this process and the other options that were available in more detail). This method essentially corresponds to ordering according to the location of the tail of the weighting function. Ordering is done dynamically (i.e. for each sounding) to allow for the variations in channel weighting functions with atmosphere.

Figure 4 shows the distribution of assigned pressure levels for the 228 NRT channels obtained using the test data set. A clear progression of channels through the troposphere can be seen in the LW (channels 20-50) and SW2 (180-190) bands where variations in the channels' assigned pressures are of order 50mb. The upper parts of these bands show a wider spread of pressures related to the presence of the tropopause inversion. If a channel radiance ratio does not reach threshold value in a cold sense before the tropopause is reached, then a large pressure differential is required for the radiance ratio to reach threshold value in a warm sense as the cloud progresses through the warmer stratosphere. Channels with a delicate balance in this region can therefore flip between quite different levels because of changes in the atmospheric profiles. The 6M band (120-160) shows clearly the large range of pressures resulting from humidity changes. Also seen is that the long wavelength side (SW2) of the 4 μm CO_2 absorption band (175-182) is not well represented in the NRT set; all the upper sounding channels are missing. Finally, note that the O3 band (90-110) channel pressures are almost all very near the surface: although they have a strong response to O_3, they are all also partial window channels and with the low radiance ratio threshold used, they are assessed as low peaking. Channel 49 (13.8665 μm) has assigned pressures anywhere from 600 to 30 mb caused, we speculate, by ozone absorption obscuring low level sensitivity in high ozone profiles.

A1-3.2.2 Synthetic AIRS radiances

AIRS simulated measurements, expressed as brightness temperatures, from clear and cloudy atmospheric conditions have been calculated, these will be denoted by T_B^{clear} and T_B^{cloudy} respectively. To complete the simulation, a term to allow for errors in the NWP model must be added to T_B^{clear}, and a term to allow for noise in the measurements model must be added to T_B^{cloudy}. Estimates are available for each:

Measurement noise is obtained from the AIRS Flight Model data (see Figure 1: an envelope to the scatter is fitted for the purposes of this study). Noise is assumed to be uncorrelated and is respresented by the (diagonal) covariance matrix **O**.

Model noise is characterised by the model error covariance **B** which, in this case, is constructed from separate covariances for the temperature, humidity and ozone profile errors and terms representing surface parameters (skin temperature etc.) An implication of this is that temperature and humidity (and ozone) errors are not intercorrelated; this is unikely to be true but at present this is the best approximation available.

The jacobians of the RTM model, $\mathbf{H_T} = d\mathbf{T_B}/d\mathbf{T}$, $\mathbf{H_Q} = d\mathbf{T_B}/d\mathbf{Q}$ and $\mathbf{H_O} = d\mathbf{T_B}/d\mathbf{O_3}$ are used to map model errors into measurement space: $\mathbf{M} = \mathbf{H.B.H^T}$ where ^{T} represents the matrix transpose.

Random realisations of **M** are added to the simulated clear measurements, and random realisations of **O** are added to the cloudy simulations (which are the proxy AIRS measurements)[2]. This process, which of course allows for the re-ordering of channels, is illustrated in Figure 5 and Figure 6. The cloud screening problem is essentially one of extracting the cloud signal from the combined signal and noise, $\delta T_B = (T_B^{cloudy} + O) - (T_B^{clear} + M)$. Two methods have been explored and evaluated on the test data set as described in the following sections.

A1-3.2.3 Digital filter screening

The digital filter method is based on the assumption that, in channel ordered space, a cloud signal will monotonically increase (in the direction top of atmosphere downwards) from the first affected channel. Once a significant cloud signal is detected in a low peaking channel, the δT_B signal is analysed 'upwards' to establish the point at which the cloud signal ends and thus establish the first cloud-free channel. A low pass filter is required to smooth high frequency **M+O** noise and prevent the filter stopping prematurely. Appendix D gives full details of the filter implementation.

The digital filter method has potential advantages in that it:

is based on sound physical reasoning

detects equally well cold cloud over warm surfaces (normal) and warm cloud over cold surfaces.

does not make detailed prior assumptions about either the cloud signal or the model and observation statistics.

is tuneable: window width trades off cloud-free channel resolution against sensitivity

Its potential disadvantages are that:

it cannot use statistical information

it may be sensitive to the exact channel ordering

it is not capable of treating all bands (4 -15 μm) together[3].

A1-3.2.4 Quantitative evaluation of filter performance

Using synthetic data the performance of the detection system can be evaluated quantitatively. It is known whether a channel for a given sounding is cloud-free as both cloudy and cloud-free model derived brightness

[2] We actually add realisations of M+O to the difference δT_B since the cloud screening operates on these differences and not on the brightness temperatures.

[3] Over short wavelength ranges within bands the effect of cloud is relatively constant; between bands the effect changes significantly (mainly due to enhanced scattering for shorter wavelengths.

temperatures are available[4]. The error due to cloud for a channel incorrectly classified as clear can therefore be assessed. It would be simple of course to design a filter to be extremely stringent which obtained very few mis-classifications and accumulated very low errors; the cost would be severe loss of data. A measure of the detector efficiency is therefore included in our analysis. Channel / soundings are classified into one of four outcomes: Clear 'hit' (determined clear, actually clear), cloudy 'hit', cloudy 'miss' (determined clear, actually cloudy) and clear 'miss' (determined cloudy, actually clear). The 'hits' are obviously successful outcomes, a clear 'miss' does not introduce errors into the system but leads to loss of data and a cloudy 'miss' leads to errors.

The error analysis figures referred to in this section consist of four sections each. Figure 7 is an example for the digital filter detection on the LW band. Top left shows the counts of the four classifications. The abscissa (in all plots) is the ordered channel number from highest assigned pressure to lowest (since the channels are ordered dynamically a channel number cannot be assigned to a particular AIRS channel). The lower left plot shows the efficiency of channel use defined as the number of times an (ordered) channel was determined clear divided by the number of times it was actually clear. High efficiencies are desirable but of course must be traded with accuracy. The top right plot shows the mean (line) and standard deviations (bars) of the effect of cloud on the clear misses. Bottom right shows similar statistics but for all determined clear cases (the clear hits do not contribute any error). This latter plot and the efficiency are perhaps the most significant results although the statistics of the clear misses need to be monitored since even a low number of highly erroneous observations can have serious detrimental effect on the model analysis.

Figure 7 are the **LW band** results using our best estimates of the filter controlling parameters (only the first 60 channels are shown as, in the remainder, the surface response becomes very high). The hit rate plot shows that hits (solid and dot-dash) dominate the results but that a significant number of clear misses are found for channel numbers between 20 and 40 - the bulk of the tropospheric channels (see Figure 8 for the vertical location of a selection of LW channels). Cloudy misses are apparent in low numbers from channel 15 to the surface. The efficiency plot shows that a good proportion of upper level channels is utilised, and low peaking channel usage, e.g. channel 40, remains as high as 40%. Mean errors in the cloudy misses are quite small (absolute values < 0.05 K) for channels down to number 30 although some higher standard deviations are seen. Below this, mean errors increase steadily to about –0.1 K and standard deviations to about 0.4 K. Around the lowest tropospheric, non surface sensing, channel 40, the mean error is about –0.1K and the standard deviation around 0.15 K. The statistics for the all-clear cases lower right show the higher channel values reduced significantly because of domination by the clear hits. For lower channels the mean error asymptotes at around –0.06K with a standard deviation around 0.3K. At channel 40 the mean and standard deviation are respectively, –0.04 and 0.1K. This performance is quite favourable compared to an AIRS instrument noise of around 0.2K in this band. Note that the results described here are for an assumed noise in the surface skin temperature of 1 K, i.e. an ocean-type surface accuracy. However, results for an assumed error of 5 K, i.e. a land-type accuracy, are very similar.

Results for the **SW-2** band are shown in Figure 9 (only the first 16 channels of the 45 are shown (see Figure 10 for the vertical location of a selection of SW-2 channels). Results are comparable to Figure 7 with some significant differences. More cloudy misses are apparent and these occur at low numbered channels giving

[4] A threshold for the difference nevertheless has to be defined; a cloud effect of absolute value less than 0.01 K is assumed to indicate a cloud-free measurement.

rise to lower efficiencies than found for the LW band. This is mostly due to a residual sensitivity at high pressure (long tails in the weighting functions) found even in the channels peaking high in the atmosphere. This implies it is quite difficult to find a SW-2 band measurement that is completely cloud-free; the error plot for the cloudy misses shows however, that the contamination caused is at a very low level and channels in this band remain useful. Mean errors in the misses and all-clears are significantly lower than in the LW band. Care must be taken interpreting these figures since from the lower channels (> 10) it is apparent that warm cloud (cold surface) is a significant contributor. It is possible that in global statistics like these, warm and cold biases could cancel, however, standard deviations in channels 0-10 of < 0.03 K show this is not the case here. Below channel 10 biases and standard deviations are larger, but these are surface sensing channels.

A1-3.2.5 Summary

A cloud screening system has been designed coded and tested on simulated clear and cloudy AIRS measurements. It operates and relies on reordering of the AIRS channels within bands according to their sensitivity to cloud in order to screen for clear channels rather than clear fields of view. The benefits of this are illustrated in Figure 11 and Figure 12 showing respectively, a map of the lowest clear channel and some example channel sets that are made available. Efficiencies and error statistics of the scheme applied to the test data are very encouraging. A second, statistically based, filter is under preliminary investigation.

A1-4. WP 4 Design/ development/ initial testing of an assimilation strategy for NWP and a production strategy for CO_2.

No progress made to date on this workpackage.

References

Matricardi M, Chevallier F and Tjemkes S, An improved general fast radiative transfer model for the assimilation of radiance observations. *ECMWF Tech Memo* 345. 2001.

Rizzi R, Matricardi M, and Miskolczi F, On the simulation of up-looking and down-looking high-resolution radiance spectra using two different radiative transfer models. *ECMWF Tech Memo* 343. 2001.

Rodgers CD, Information content and optimisation of high spectral resolution remote measurements, *Remote sensing: inversion problems and natural hazards, advances in space research*, **21** (3) 361-367 1998

Huang HL, Antonelli P, Application of principal component analysis to high-resolution infrared measurement compression and retrieval, *Journal of Applied Meteorology*, **40** (3) 365-388, 2001

Chevallier F, Bauer P, Kelly G, Jakob C and McNally T. Model clouds over Oceans as seen from space: Comparison with HIRS/2 and MSU radiances. *Journal of Climate*, **14** 4216-4229, 2001

English SJ, Eyre JR, Smith JA, A cloud-detection scheme for use with satellite sounding radiances in the context of data assimilation for numerical weather prediction, Q*uarterly Journal of the Royal Meteorological Society*, **125** (559): 2359-2378, Part A Oct 1999

Appendix 1A: EOF compression

1A.1 Background

In the timeframe we expect AQUA to be launched (Spring 2002) it is unlikely that telecommunications links will allow the timely transfer of spectra containing all 2378 AIRS channels at the required spatial resolution. As a "day-1" solution NASA/NOAA/NESDIS plan to disseminate a reduced channel set (approximately 300) in near-real-time (NRT) to NWP users. However, the selected channels are essentially fixed and may not be the most appropriate for use in all meteorological situations. Thus there is interest in techniques that would allow compression of the spectra before transfer (to a more manageable data volume) and reconstruction of the full spectra by the user after transfer. This note outlines some very preliminary work that has been done (mostly by M. Goldberg at NOAA/NESDIS) using truncated principal components of the AIRS spectra as an efficient representation of the full channel set.

1A.2 Theory

Using a diverse training population of K full spectra, each represented by a vector $\mathbf{S}_k$ of length N (the number of channels) the elements of the observation covariance matrix $\mathbf{C}$ may be computed

$$C_{i,j} = \frac{1}{K}\sum_{k=1}^{K}\left[S_{i,k} - \bar{S}_i\right]\left[S_{j,k} - \bar{S}_j\right] \tag{1}$$

where $\bar{S}_i$ is the mean radiance in channel i . The covariance may then be diagonalized by the eigenvector transformation

$$\mathbf{C} = \mathrm{V}\,\Lambda\,\mathrm{V}^T \tag{2}$$

where $\mathbf{V}$ is a matrix containing the eigenvectors of $\mathbf{C}$ and $\mathbf{\Lambda}$ is a diagonal matrix of the corresponding eigenvalues. For any single observed spectrum $\mathbf{S}_k$ we can compute its projection (or rather the differences of it from the population mean) upon the l^{th} eigenvectors of $\mathbf{C}$

$$P_{k,l} = \sum_{i=1}^{N}\left[S_{i,k} - \bar{S}_i\right]V_{i,l} \tag{3}$$

the projection coefficients being a vector of length N (i.e. the same length of the spectrum vector equal to the number of channels). The radiance in each channel i of the original spectrum is reconstructed from the eigenvectors using

$$S_i^R = \bar{S}_i + \sum_{l=1}^{N} P_l V_{l,i} \tag{4}$$

If all of the eigenvectors are used in the reconstruction $\mathbf{S^R}$ will be an exact reproduction the original spectrum, but there is (obviously) no compression of the original information. However, we may choose to project the original spectrum $\mathbf{S}$ on only the first M ($<N$) eigenvectors (using equation 3) ordered by the magnitude of their eigenvalues. The reconstruction (using equation 4) will no longer be exact and introduce a reconstruction error vector $\mathbf{E^R}$. The smaller the value of M the more compression of the original information volume is achieved, but the reconstruction errors also grow.

1A.3 Practical implementation

A scenario for practical application of the above technique is as follows. The eigenvectors of the training sample covariance **C** are computed off-line by the data producer and transmitted just once to the data user and stored. As a new observed spectrum **S** is obtained, the coefficients **P** of its projection on the first *M* eigenvectors are computed by the data producer. The coefficient vector **P** (of length *M*) is transmitted to the data user as a compressed representation of the observed spectrum. The data user then reconstructs a full spectrum $\mathbf{S}^{\mathbf{R}}$ and has access to all *N* channels. The compression factor is clearly *N/M*.

Reconstruction errors

The rate at which the reconstruction error grows as the value of *M* decreases (i.e. with increasingly efficient compression) has been investigated in simulation by a number of studies (e.g. Huang and Antonelli 2001, Goldberg *pers.com*.). It has been found that using 200 leading eigenvectors allows each channel to be reproduced in the absence of clouds with a rms reconstruction error within the expected instrument noise limits for AIRS. To achieve the same reconstruction accuracy in cloudy-sky conditions it has been estimated that up to 500 eigenvectors would be required. However, some important points should be considered

1. The studies performed so far by Goldberg suggest the eigenvectors need to be updated regularly (i.e. recomputed every month or so) to maintain the same reconstruction accuracy. While the logistics of updating these and transmitting the results to the NWP centres is not difficult, the drift is obviously a cause for some concern (suggesting an air-mass or seasonal variation).

2. Reproducing the spectra to within the instrument noise (in an rms sense) may not be adequate for NWP. The choice of metric to measure reconstruction error is very important as some aspects of the spectra (relating to different atmospheric features, possibly with low variance) are clearly more important in NWP than others. Also, and as a general rule, we should avoid elements in the processing chain that introduce noise unless they are absolutely necessary.

With these points in mind the use of eigenvectors as a solution to the purely technical problem of excessive data transfer volumes may not be best (given the risk of degrading the data in a less than fully understood way) and a purely technical (non-loss) compression seems more appropriate.

Other scientific applications of the theory

In addition to efficient representation of the information in the radiance data, it is argued by Huang and Antonelli 2001 that the truncated eigenvector reconstruction can be also be tuned to simultaneously remove instrument noise from the data. This is the case if the contribution of instrument noise to the original measured data only projects on the higher order (low eigenvalue) eigenvectors (which are of course removed by the truncation process). Also, some NWP centers (e.g. the UKMO, Collard, *pers. com.*) are using the approach to detect and reject clouds in the radiance data. These are clearly very interesting NWP applications of the eigenvector theory and they should be studied further. However, to do this the complete spectrum should be communicated to the NWP centres as issues as important as noise filtering and cloud detection have to be tuned with the tolerances of the particular NWP system in mind and cannot be done by the data producer.

Appendix 1B: Details of the channel ordering procedure

Several 'measures' for ordering channels in the vertical were considered, the primary aim being to ensure that in a cloudy atmosphere of any kind, the effect of the cloud on the measurements is a monotonic increase with order number. In fact, this requirement can be relaxed somewhat since it is only in the region of the channels with small cloud impact (i.e. in the 0 - 1 or 2K effect) that monotonicity is required (channels with larger impacts can easily be eliminated). The latter consideration leads to ordering measures that are based on the low altitude / high pressure tail of the channel weighting function. The characteristic level for a channel is determined as the point at which a particular measure exceeds a threshold. Measures considered were a) the transmittance to top of atmosphere (TOA), threshold e.g. 0.05, b) ratio of radiance at TOA originating from below the level to the total, threshold e.g. 0.05, c) brightness temperature effect (δT_B) of an opaque black cloud, threshold e.g. 0.5K and d) ratio of radiance effect of an opaque black cloud to the total clear radiance $dR/R = (R_{clear}-R_{cloudy})/R_{clear}$, threshold 0.01. Measure a) has the slight drawback that both the temperature structure of the atmosphere and any non-linearity in the Planck function (e.g. in the SW bands) is not accounted for. The remaining measures are all more or less equivalent and differ mainly in the ease with which the RTM interface (RTTOV-6) can accommodate them. It is also more intuitive to use a measure which is directly related to the response to cloud, albeit a slightly unrealistic black cloud. In practice, measure d) has been adopted since RTTOV includes an opaque black cloud computation at all levels. Since cloud signals can sometimes be positive in sign (warm cloud over colder surfaces), the threshold is applied to the absolute value of the radiance ratio. This allows the ordering procedure to operate successfully through surface and other (e.g. tropopause) inversions.

A channel weighting function in general will have a dependency on the atmospheric state, obvious examples are channels sensitive to water vapour where the level of maximum response is considerably higher in the atmosphere for high water contents. All channels have some such dependency so that an ordering determined for a particular atmosphere may not be accurate for a dissimilar atmosphere. Consequently, we order the channels dynamically, i.e. for each sounding location a new order is calculated according to the RTM calculations for the model atmosphere.

Appendix 1C: The digital filter cloud detection method

The digital filter operates by detecting a physically intuitive cloud signature within the δT_B signal. It relies on a) a smoothing filter of some kind to remove high frequency (in channel space) noise from the $\mathbf{H.B.H^T+O}$ terms and b) a monotonically increasing or decreasing effect from the cloud. The process has been refined since the original implementation now takes the following steps:

1. Find the ordered channel, i_{low}, corresponding to the maximum assigned pressure; the filter will not search lower than this and channels below this level are assumed cloudy / unusable.

2. Calculate a smoothed δT_B signal, $S(\delta T_B)$, with a boxcar filter of width determined by the particular band.

3. Determine whether a detectable 'gross' cloud signal, $|S^{ilow}(\delta T_B)| > Thresh_{dT}$, is present at this lowest channel. If so, determine from the sign of $S^{ilow}(\delta T_B)$ whether the cloud effect is warm or cold.

4. Proceed in the higher pressure channel direction whilst the following conditions apply:

    a. $i < i_{high}$, where i_{high} is the index of the highest peaking channel deemed potentially cloud contaminated (i.e. not completely in the stratosphere), **AND**

    b. $|S^i(\delta T_B)| > Thresh_{dT}$. **OR**

    c. $S^{i-1}(\delta T_B) - S^{i+1}(\delta T_B) > Thresh_{grad}$ for 'cold' cloud; $< Thresh_{grad}$ for 'warm' cloud. **OR**

    d. $S^{i-5}(\delta T_B) - S^{i+1}(\delta T_B) > Thresh_{grad}$ for 'cold' cloud; $< Thresh_{grad}$ for 'warm' cloud.

5. When the filter stops a final check is made that $|S^i(\delta T_B)| < Thresh_{dT}$.

Some explanation for the various parameters of this filter is in order. A smoothing operation is required as the model and instrument noise in the raw signal rarely allows detection of a monotonic cloud effect. The premise is that model and instrument noise are relatively uncorrelated in the ordered channel space whereas the cloud signal is highly correlated and monotonically increasing. A lowest considered channel, i_{low}, is employed as it is found that including many surface sensing channels often leads to low gradients in $S(\delta T_B)$ and premature termination of the filter. Check b) that there is still a detectable gross cloud signal prevents this termination in most cases but not for signals that are less than the gross threshold. c) is the basic filter mechanism and checks that the supposed cloud signal continues to decrease monotonically and d) is a extension to this mechanism to allow the filter to step beyond false signal maxima that are due to model noise. Step 5) is only invoked if the channel i_{high} has been reached and the signal is still a detectable gross cloud effect. In practice, such a signal would have to originate from an unusually large model noise term. Figure App 1C- 1 shows an example of the filter in operation.

The variable parameters of the digital filter are the thresholds, the maximum assigned pressure and the smoothing width. Performance is least sensitive to the gradient threshold, $Thresh_{grad}$, which is set at 0.01 K. The gross threshold, $Thresh_{dT}$, is more important. Too large (loose constraint) a value and filter terminations (either through step 3) or check b.) lead to a few channels with damaging errors being classified as clear. Too

tight and the filter will classify channels with only model and measurement noise as cloudy; this is loss of good data and essentially loss of signal. An appropriate value for $Thresh_{dT}$ can be determined from statisitics of the *smoothed* model + measurement noise errors. Although these vary considerably in the high stratosphere and very near surface, a standard deviation of around 0.25 K is found in the tropospheric channels for the filter smoothing widths determined as optimum here. Using a value of 0.5 K for $Thresh_{dT}$ is therefore equivalent to a 2σ cutoff and should not lead to inappropriate data loss.

Filter smoothing width is also important. The width has to be sufficiently long to remove structure in the signal due to model and measurement noise that would otherwise lead to premature termination of the filter. However, the longer the filter window width the less precise the detection system can be about the first affected channel. Determination of the optimum width is largely a matter of experimentation and knowledge of the likely model noise structure. In the LW CO_2 band there are correlated model noise structures originating from groups of channels sensitive to ozone and water and the filter window width has to be relatively long; a value of 10 channels is used. The SW CO_2 band is 'cleaner', model noise originates only from temperature errors and the filter window width can be shorter; a value of 5 channels is used.

The last filter parameter is the maximum assigned pressure level. Its value appears to be less critical providing it serves to remove channels with high surface sensitivity from the system. An RTM level of 43 (pressure of 1013 mb) is used.

Figures

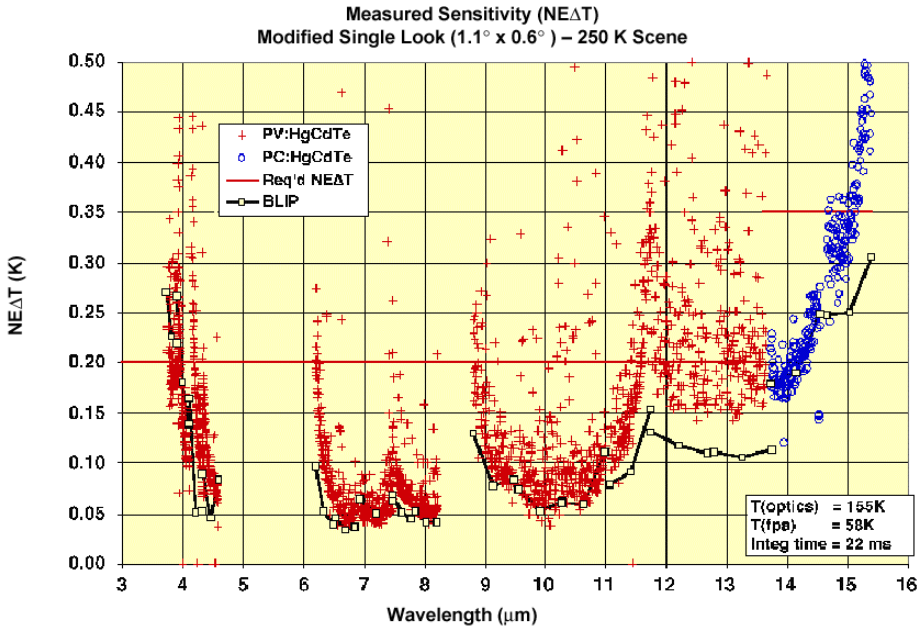

Figure 1 AIRS Flight Model measured NeΔT (from http://www-airs.jpl.nasa.gov/)

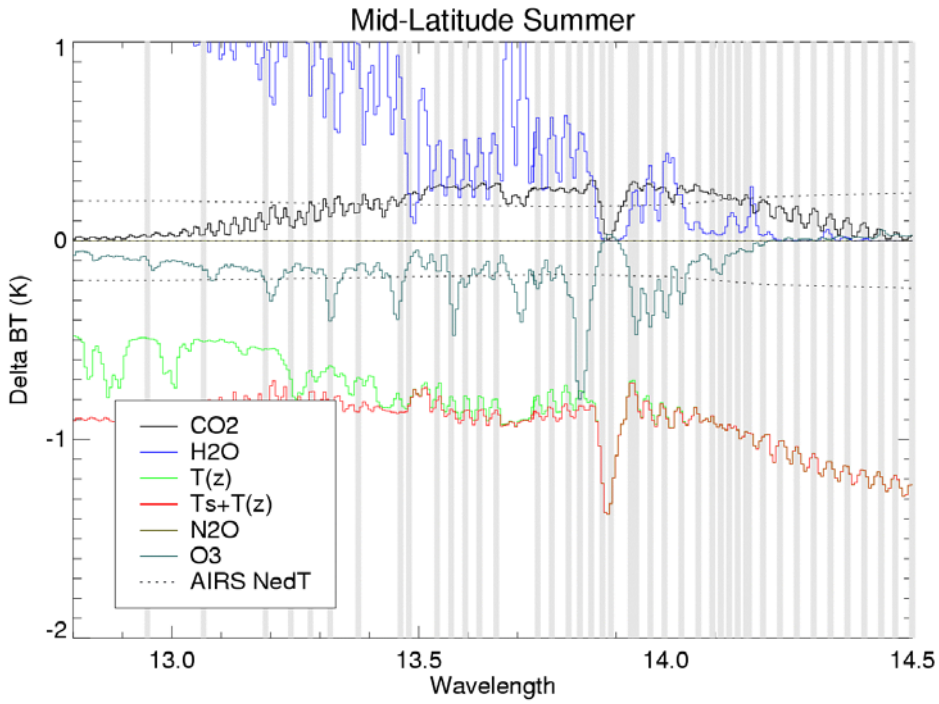

Figure 2 Response of LW band AIRS channels to standard perturbations in atmospheric and surface quantities. See text for details. Grey vertical bars indicate channels targeted by NESDIS for transmission immediately post-launch. Dotted line indicates the approximate Flight Model channel radiometric noise.

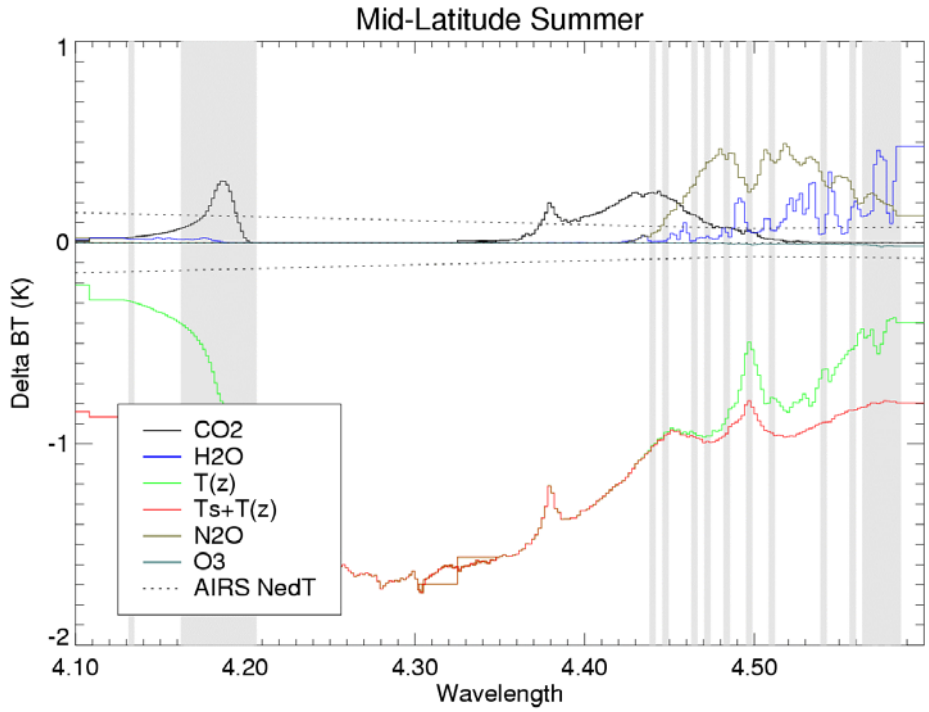

Figure 3 As Figure 2 but for the SW1 and 2 bands of AIRS

.

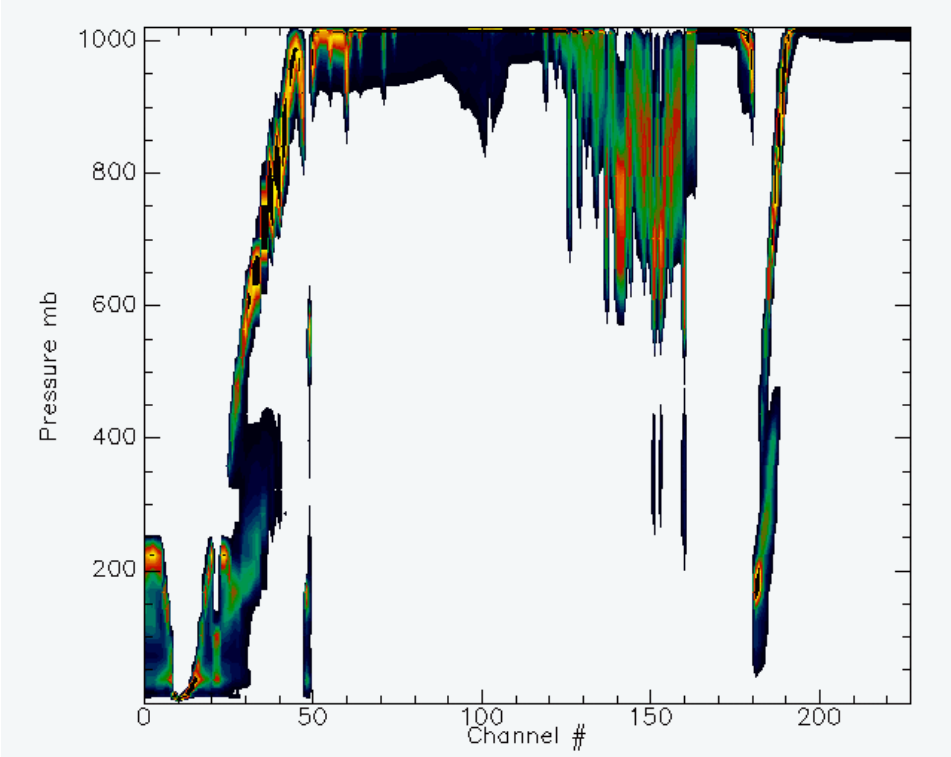

Figure 4 2D histogram of pressure level assignment by AIRS channel (numbering by position in NRT stream, 1-228.

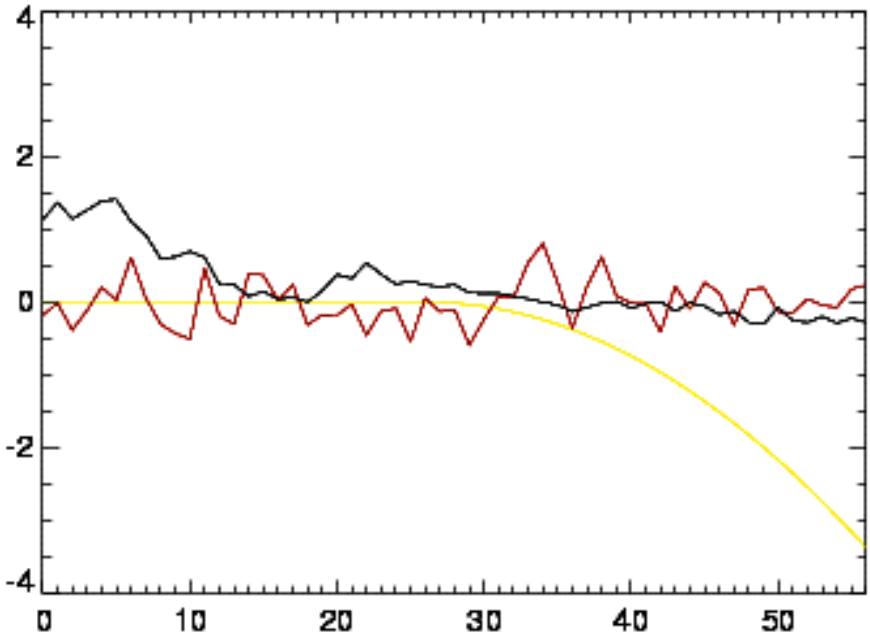

Figure 5. Cloud signal and noise, illustration only. Shows δT_B profiles (in ordered channel space); cloud signal (synthetic) in yellow, observation noise, O, in red and model noise, M, in black.

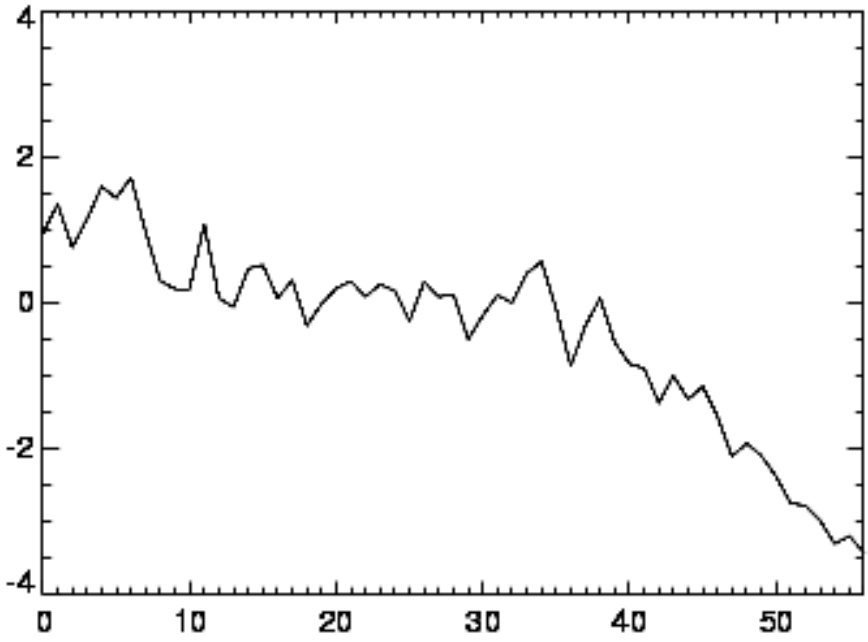

Figure 6 Cloud signal and noise, illustration only. Shows the combined signal from Figure 5 (the 'available' signal) from which the cloud signal must be deduced.

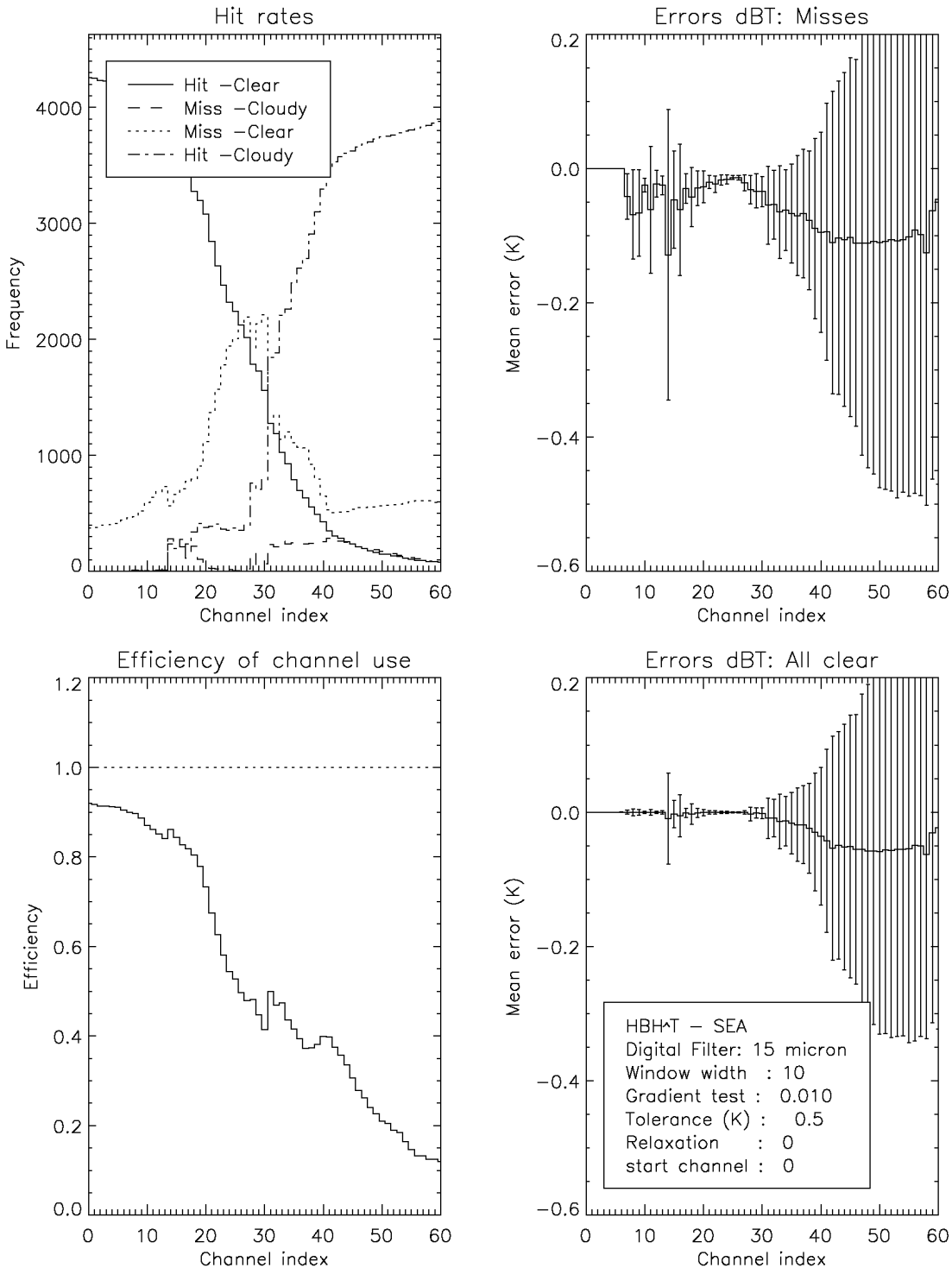

Figure 7 Detection statistics for the digital filter operating on the LW band measurements from the synthetic data set. Window width refers to the width (in channels) of the smoothing filter; the gradient test value is equivalent to $Thresh_{grad}$ *; the tolerance is equivalent to* $Thresh_{dT}$*; relaxation is not used and start channel is equivalent to* i_{high} *(see Appendix C: The digital filter cloud detection method for defimitions).*

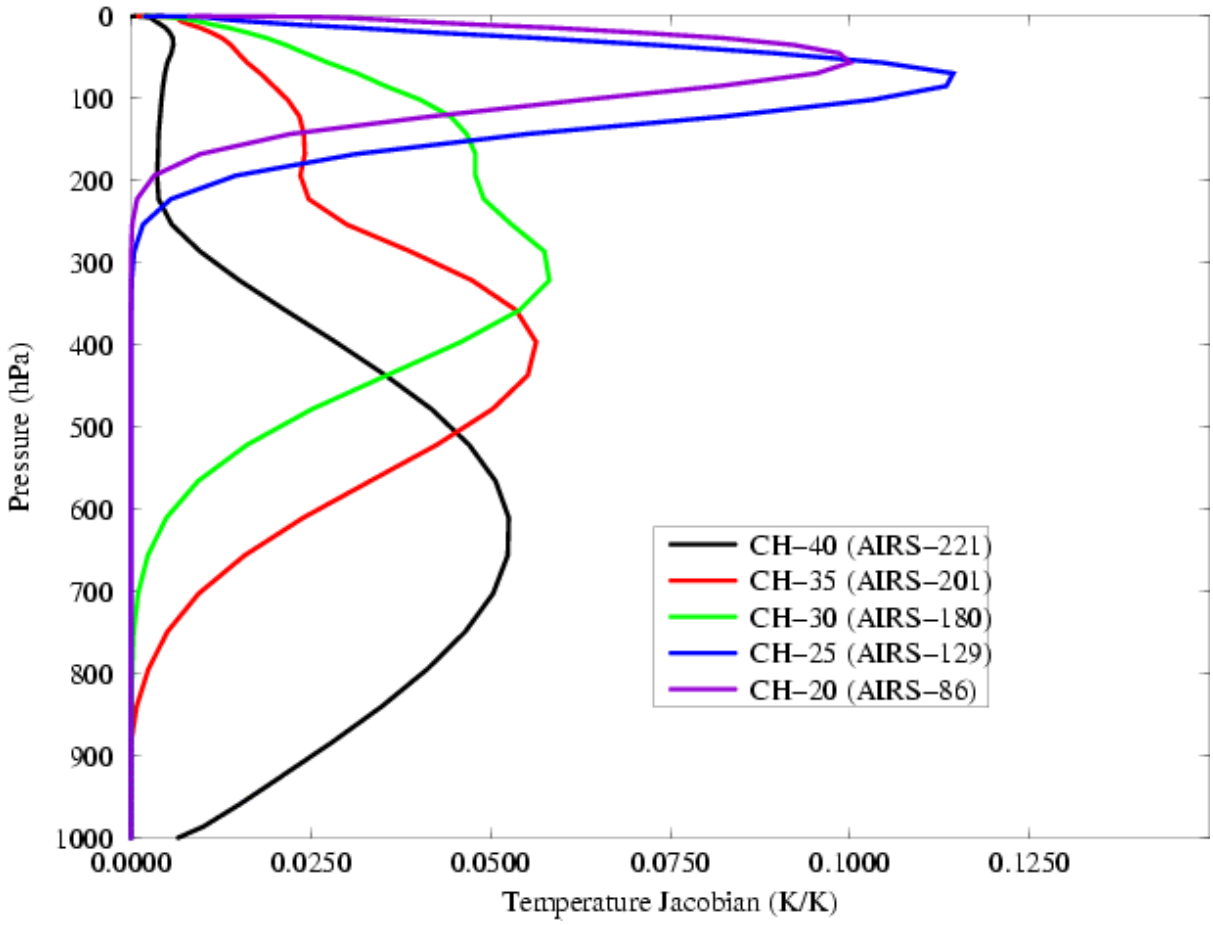

Figure 8 Temperature jacobians of a selection of LW channels from #20 to #40 calculated from a typical midlatitude profile.

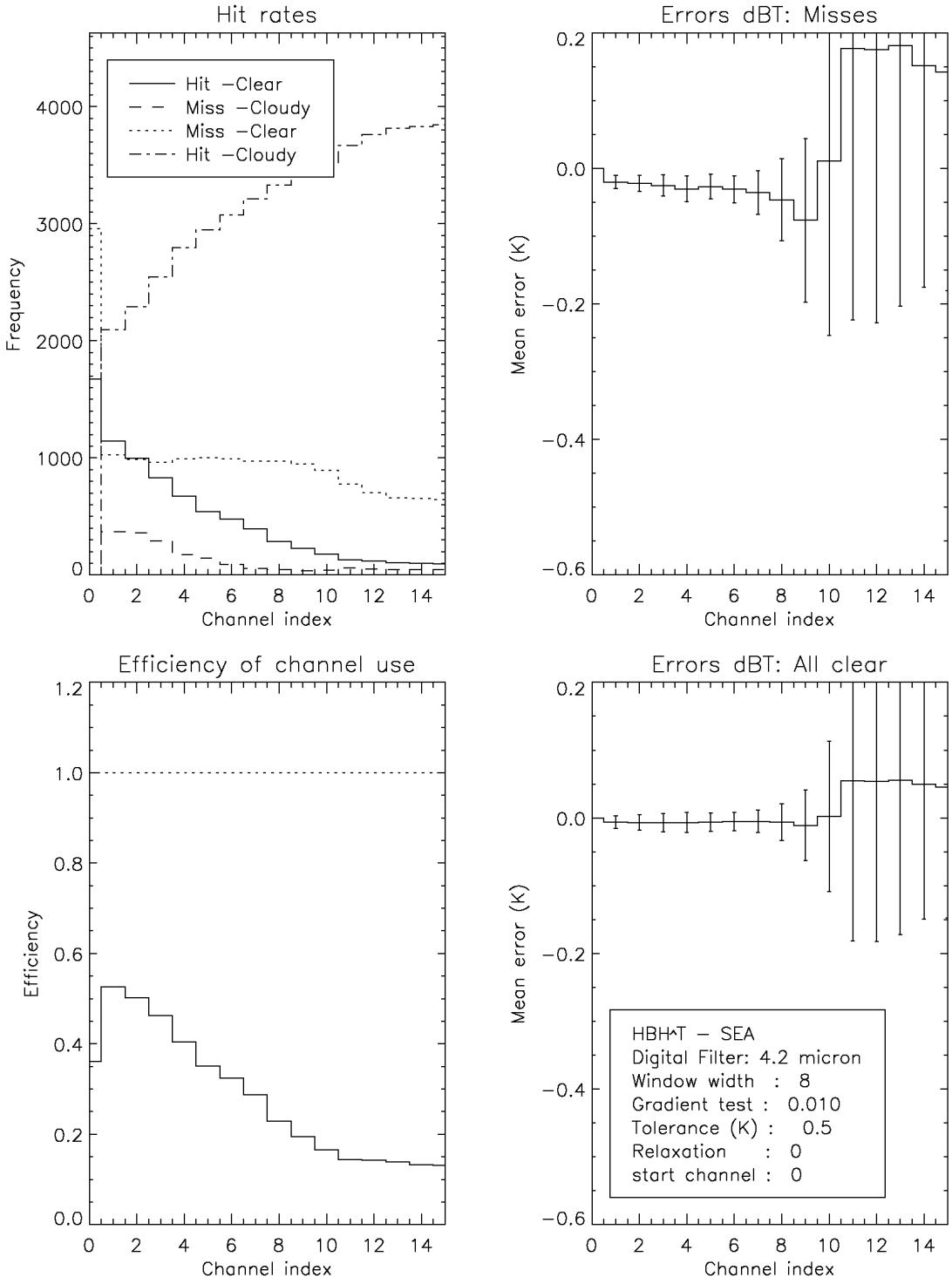

Figure 9 As Figure 7 but for the SW-2 band.

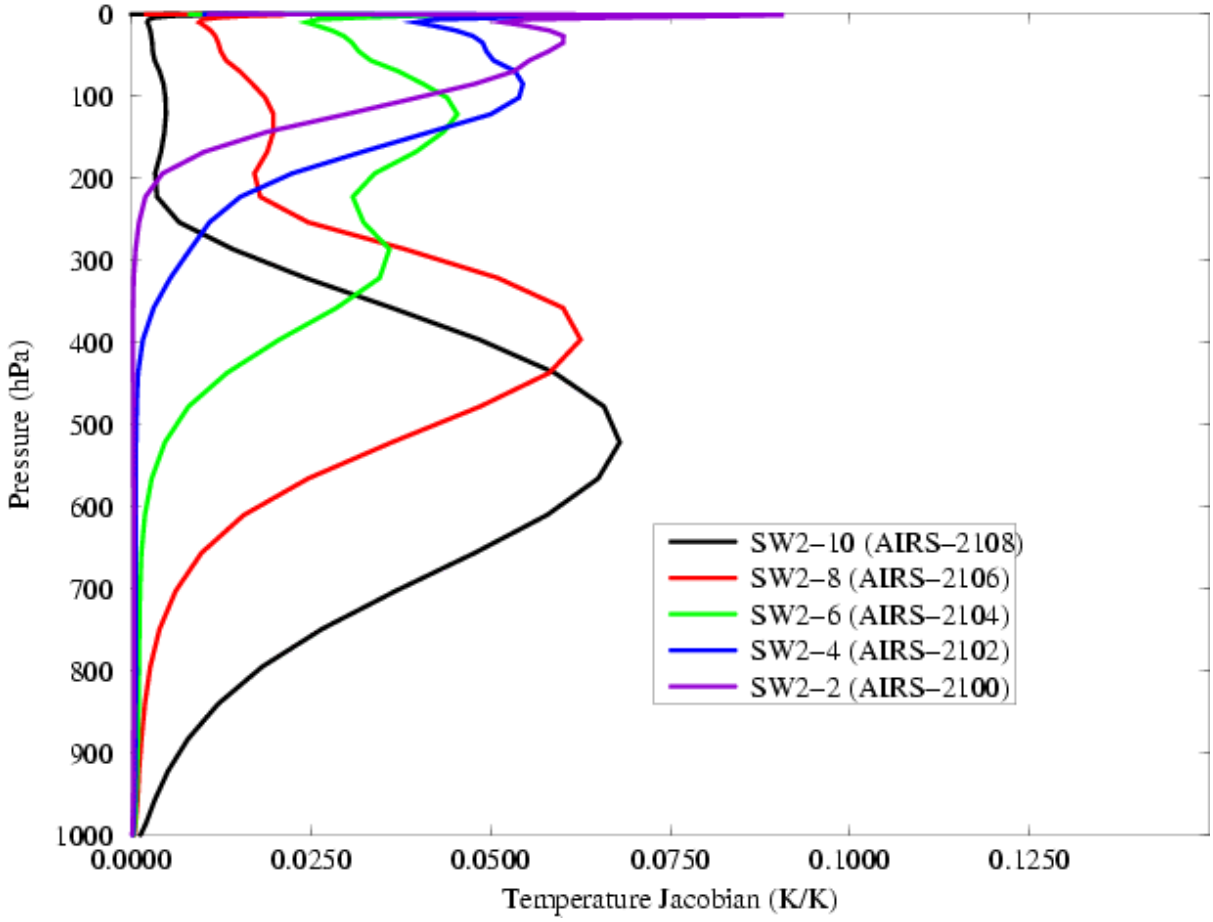

Figure 10 Temperature jacobians of a selection of SW-2 channels from #2 to #10 calculated from a typical midlatitude profile.

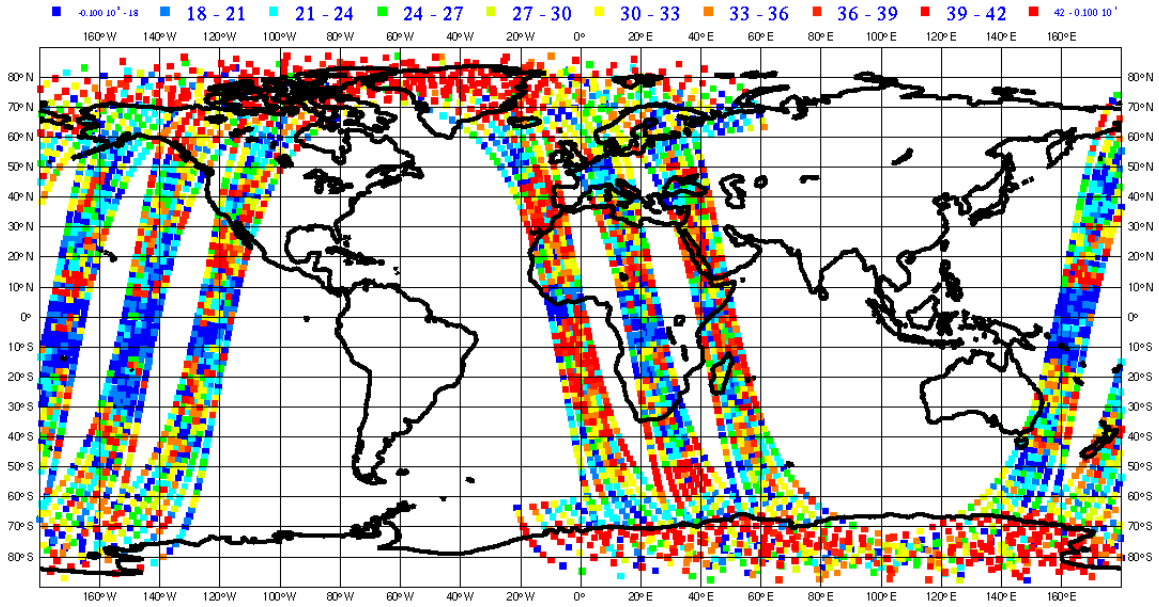

Figure 11 Map of the index of the lowest cloud-free LW channel as determined by the digital filter.

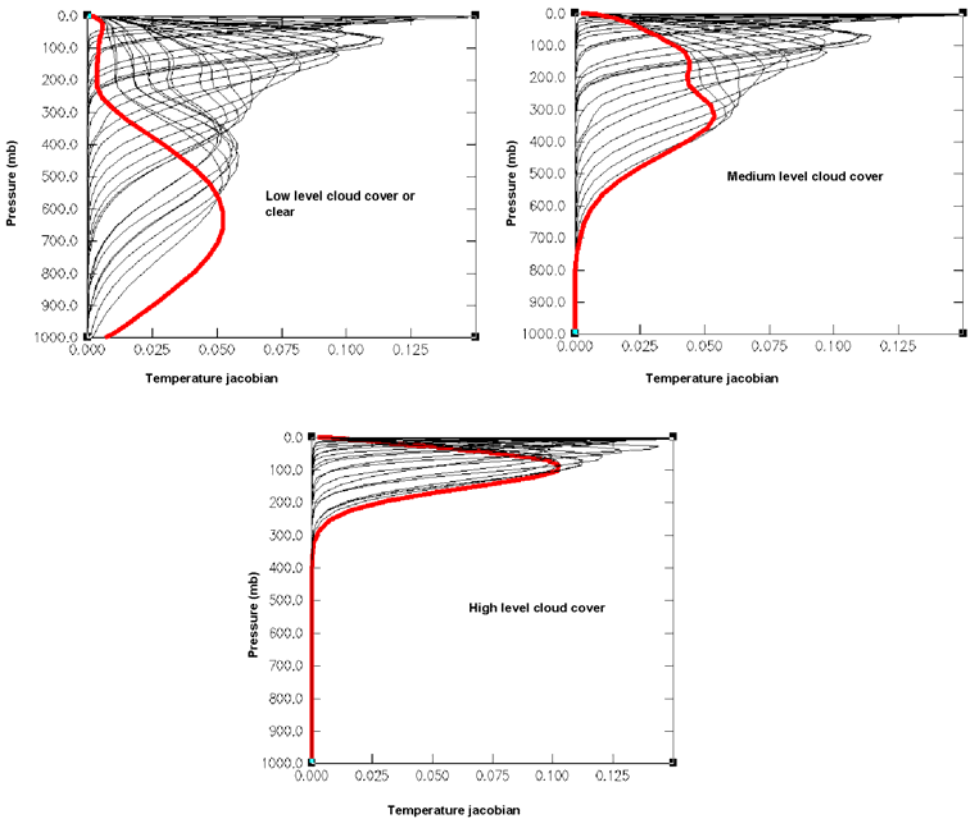

Figure 12 Temperature jacobians of channels available with cloud screening based on the lowest cloud-free channel.

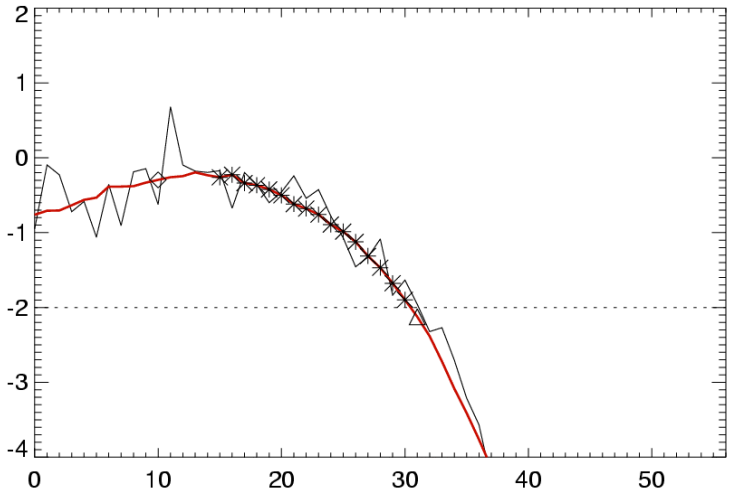

Figure App 1C- 1 Example of the digital filter operation. The δT_B signal is the black line, $S(\delta T_B)$ is shown red, i_{low} is channel 31 and the filter proceeds to channel 15. The true cloud on this occasion was, as marked by the diamond at channel 10 but negative model noise in the low channels masked the cloud effect.

Annex 2: Second Interim Report to the European Space Agency

Measurement of Seasonal CO_2 Fluctuations from Space

May 2002

Authors: P.D.Watts, A.P.McNally, J-N. Thépaut and M. Matricardi

ESA contract No. 14644/00/NL/JSC

European Centre for Medium-Range Weather Forecasts

Table of Contents

Annex 2 - Executive Summary

This is the second quarterly report (hereafter 2QR) for the contract study on measurement of seasonal CO_2 fluctuations from space. We report here only on progress made since the first quarterly report (1QR) except where repetition or a summary is required for clarity. The statement of work identifies four distinct workpackages (radiative transfer, data sampling, use of real AIRS data and system implementation) and schedules these to run in sequence. Whilst this structure is logical it has proved expedient to tackle areas in all of the workpackages during this second period.

In **WP1** (radiative transfer) an enhanced version of the fast radiative transfer model (RTTOV) that includes CO_2 as a variable quantity has been completed. Some issues pertaining to the CO_2 jacobians at 4.2 μm remain and the code needs incorporation into the ECMWF IFS.

In **WP2** (data sampling) the 'missing' channels from the important 4.5 μm band are now available within an extended (281 channel) Near Real Time (NRT) dissemination system. Work on channel optimisation for CO_2 channel by collaborators (LMD) broadly confirms the channel selection but suggests some additional channels that might be added in future definitions of the NRT set.

Within **WP3** (science study) the candidate cloud screening algorithm described in the first report and the channel ordering system has been incorporated into the IFS. An alternative algorithm based on Bayesian analysis of the measurements has been developed. The method is based on prior knowledge of the statistical character of cloud-free measurements. Results of preliminary testing using simulated data show that the new method has a detection efficiency and accuracy comparable to the digital filter (hereafter referred to as the Low Pass filter) method. Consequently, both methods will be retained for study until tests with real data establish a clear preference.

Progress on **WP4** (system implementation) has been made since the availability of the CO_2 enhanced RTM. Simulation studies have been performed that show the expected capability of the AIRS measurements for CO_2 estimation under certain assumptions about noise levels etc. Sensitivity to instrument and RTM errors is shown to be high emphasising the need for stringent cloud detection and RTM validation / tuning. A strong sensitivity to the prior knowledge of the CO_2 is also shown, particularly the effects of correlations between tropospheric and stratospheric amounts. The simulations also confirm that the AIRS sounder is significantly more useful for CO_2 estimation than is the currently operational infrared sounder HIRS. Neither instrument is capable however of estimating anything other than broad column average quantities.

A2-1. WP 1 Validation of a fast radiative transfer model (RTM) for AIRS

The fast radiative transfer model (RTTOV) has been extended to include variable CO_2 profile concentrations; both the forward (radiance calculation) and jacobian (radiance gradient calculation) models are complete. The validation of this model consists of two aspects: accuracy with respect to the LBL model and the underlying accuracy of the LBL model itself (see 1QR). The addition of the variable CO_2 profile to RTTOV (on the models 43 levels) was achieved with no discernable degradation of the accuracy with respect to the LBL. We have no further information concerning the underlying LBL accuracy compared to that presented in 1QR.

The jacobians of the new model with respect to the CO_2 profile, $\partial R/\partial CO_2$, are tested by comparison to values obtained by perturbation of the forward model and exact agreement is found. In general, the jacobian for a channel sensitive to CO_2 is negative where the local lapse rate is negative (decrease of temperature with height) and vice-versa. The physical reasoning for this is that increased CO_2 causes greater absorption and a therefore mean emission from higher in the atmosphere. For a small selection of channels in the 4.2 μm band, this predictable and understandable behaviour is not followed; positive jacobians are found for a region of the troposphere where there is a clear negative temperature gradient. Similar channels in the adjacent 4.5 μm band do not show the effect. Comparisons with jacobians from other models (LMD) are underway and the reasons for this possibly anomalous behaviour are being sought.

A2-2. WP 2 Science study to optimise AIRS data usage for NWP applications and for CO2 work

1QR described the reasons for, at least in the first instance, employing channel selection rather than eigenvector compression as a means of handling large data volumes. In 1QR it was highlighted that the current NESDIS Near Real Time (NRT) channel set (228 channels) did not include important CO2 sounding channels in the 4.5 μm band. This omission was communicated to NESDIS (Goldberg pers comm.). A new, (281 channel), NRT set has been defined by NESDIS which includes at least 9 channels from the 4.5 μm CO_2 band. Results by other researchers (Chédin, pers comm.) using formal methods of channel selection suggest further useful channels giving a total around 324, however, this selection is unlikely to be available from NESDIS on Day-1. Simulation studies (see WP4, this report) show that the 281 channels will provide CO_2 estimates of only marginally degraded accuracy compared to the 324 suggesting that the more limited set is adequate in the context of this study. It is understood that NESDIS will make available by ftp all-channel data from limited portions of the AIRS data stream. These data may be useful for testing more complete channel sets.

A2-3. WP 3 Science study with real AIRS data

A2-3.1 Cloud screening

In 1QR the method of cloud screening AIRS measurements by the method of δT_B 'digital filtering' (now referred to more accurately as 'low-pass filtering') of a forecast model minus measured brightness temperature vector was described. The vector is first re-ordered by the channel effective pressure and split according to wavelength (band separation). This technique has been coded and tested within the IFS using the simulated AIRS data described in 1QR.

A second technique, suggested by the work of English and Eyre 1999 is based on statistical rather than pure physical principles. It has been developed and tested outside of the IFS in a manner analogous to that used for the Low-pass filter method.

A2-3.1.1 Bayesian detection

The Bayesian method works by testing the probability that a measured δT_B vector has come from a clear sounding (English and Eyre 1999). Statistics of clear soundings are known since they are described by the forecast model and measurement error covariances (see 1QR). The method is extended to detect clear channels *within* a sounding by testing successive segments of the entire channel set from top of atmosphere

downwards. When a segment returns a sufficiently low probability of being clear, then all the channels within the segment and below are considered cloud affected. Appendix C gives a detailed description of the method.

The Bayesian method has potential advantages in that it:

- utilises reasonably well known statistics
- detects equally well cold cloud over warm surfaces (normal) and warm cloud over cold surfaces.
- is capable of treating all bands (4 -15 mm) together (this has not so far been investigated)
- is tuneable: window width trades off cloud-free channel resolution against sensitivity
- is not sensitive to the exact channel ordering.

Potential disadvantages are that

- It cannot use physical constraints (e.g. that the cloud signal is a monotonic function in an ordered channels space)
- It may be sensitive to incorrect specification of the 'reasonably well known' statistics.

A2-3.1.2 Quantitative evaluation of filter performance

The description of the evaluation follows that in 1QR but we repeat it here for clarity.

Using synthetic data the performance of the detection system can be evaluated quantitatively. It is known whether a channel for a given sounding is cloud-free as both cloudy and cloud-free model derived brightness temperatures are available . The error due to cloud of a channel incorrectly classified as clear can therefore be assessed. It would be simple of course to design a filter to be extremely stringent which obtained very few mis-classifications and accumulated very low errors; the cost would be severe loss of data. A measure of the detector efficiency is therefore included in our analysis. Channel / soundings are classified into one of four outcomes: Clear 'hit' (determined clear, actually clear), cloudy 'hit', cloudy 'miss' (determined clear, actually cloudy) and clear 'miss' (determined cloudy, actually clear). The 'hits' are obviously successful outcomes, a clear 'miss' does not introduce errors into the system but leads to loss of data and a cloudy 'miss' leads to errors.

The error analysis figures referred to in this section consist of four sections each. Figure 1 is an example for the Bayesian filter method on the LW band. Top left shows the counts of the four classifications. The abscissa (in all plots) is the ordered channel number from highest assigned pressure to lowest (since the channels are ordered dynamically a channel number cannot be assigned to a particular AIRS channel). The lower left plot shows the efficiency of channel use defined as the number of times an (ordered) channel was determined clear divided by the number of times it was actually clear. High efficiencies are desirable but of course must be traded with accuracy. The top right plot shows the mean (line) and standard deviations (bars) of the effect of cloud on the clear misses. Bottom right shows similar statistics but for all determined clear cases (the clear hits do not contribute any error). This latter plot and the efficiency are perhaps the most significant results although the statistics of the clear misses need to be monitored since even a low number of highly erroneous observations can have serious detrimental effect on the model analysis.

Bayesian filter results for the **LW band** are shown in Figure 1. Considering the difference in approach of this filter from the low-pass filter version (1QR figure 7), the results are remarkably similar and we highlight only the differences. Efficiencies are lower for the Bayesian filter by around 10% overall. For channels 0-25 (stratosphere and high troposphere) the Bayesian misses and all-clear mean and standard deviations are

lower than the low-pass filter, especially in the all-clear set because of a significantly lower number of cloudy misses. For the tropospheric channel numbers 25-40 biases are smaller in Bayesian especially towards channel 40, but standard deviations are similar. Below channel 40 (surface channels) biases in the low-pass filter level off whereas the Bayesian values continue to increase. Standard deviations in the Bayesian scheme are however, slightly lower.

SW-2 band Bayesian filter results are shown in Figure 2 and can be compared to low-pass filter results in 1QR figure 9. For channels from 0-8 there is very little difference in the schemes performance with the exception of significantly higher efficiency in the Bayesian scheme. In the lowest channels of this group there is a slightly lower standard deviation in the digital filter result. Below channel 8, the Bayesian filter is less efficient (around 10 rather than 20%) but returns significantly better error statistics.

A2-3.1.3 Summary

Two detection systems have been designed coded and tested on simulated clear and cloudy AIRS measurements. Both methods operate and rely on reordering of the AIRS channels within bands according to their sensitivity to cloud in order to screen for clear channels rather than clear fields of view. Efficiencies and error statistics of the schemes applied to the test data show remarkable similarities. Considering the uncertainties in the simulated data (especially the use of model cloud fields to produce 'measurements'), the results are too close to allow a firm recommendation at this stage except that we should retain the possibility to further develop either scheme when real AIRS data become available.

A2-4. WP 4 Design/ development/ initial testing of an assimilation strategy for NWP and a production strategy for CO_2

Progress in this work package has been made in understanding some of the characteristics of the inversion problem for AIRS CO_2 estimation. This has been achieved by utilising the estimated error in a one dimensional variational analysis the which assumes linearity about the solution and normally distributed errors, both of which conditions are likely to be held in this circumstance. Although this analysis differs from the likely implementation of a CO_2 estimation system (3 or 4 dimensional variational analysis) it nevertheless provides useful insight.

A2-4.1 Expected estimation error

Given prior information with error covariance B, measurements with error (observation and forward model) covariance (O+F) and measurement jacobian H (the gradient of the measurements with respect to the atmospheric state x), the expected error covariance of the maximum probability estimate of x is (e.g. Rodgers 1976):

$$\hat{S} = B - BH^T (HBH^T + O + F)^{-1} HB$$

where ^{T} denotes a matrix transpose.

A2-4.1.1 Background error covariance, B

The state vector x consists of profiles (on the 43 levels of the RTTOV RTM) of temperature, humidity, ozone and CO_2. B is then the error covariance of the prior estimate we have for x and here it is appropriate to

use values for B that represent the error in the 6 hour ECMWF forecast model. Although there is some uncertainty in the values for temperature, humidity and ozone and correlations between these variables are not modelled at all, a degree of confidence can be placed in them.

The B matrix for the CO_2 profile is harder to define because a) it has no direct representation in the forecast model so that climatological values are used for a priori and b) there are few in situ profile measurements of CO_2 so the covariance of the climatology is poorly defined. A preliminary CO_2 B matrix has been constructed under the following assumptions:

1. The atmosphere is considered to consist of three regions: boundary layer (BL), troposphere and stratosphere. These regions are more or less separated by the presence of stable layers which to a variable degree inhibit mixing of air and therefore the distribution of CO_2 for which the principle sources and sinks are at the surface.

2. Variances (diagonal elements of B) are set to characterize known seasonal variations in CO_2 concentration as measured by the global surface flask system. This is the appropriate error if a fixed single value climatology is used. Seasonal variations are well measured at the surface (and, we may therefore conclude, in the BL) and the relatively few aircraft sampling data (e.g. Nakzawa et al. 1991) suggest that the amplitude of variation is preserved in the troposphere. The same data suggest that the amplitude of seasonal variation in the stratosphere is diminished (and probably decreases with altitude) and has a phase lag compared to the troposphere and BL. Values used in this study are 6, 5 and 4 ppmv for the BL, tropospheric and stratospheric variances respectively.

3. Correlations of the CO_2 concentration within the three layers are almost impossible to define from in situ measurements available. Here we have followed Engelen 2000 and assumed a correlation scale-length consistent with CO_2 concentrations from the CSU GCM model. A value of 25 km has been suggested (Engelen pers comm.) which implies an expected high degree of correlation.

4. Correlations of the CO_2 concentration between the three layers are equally difficult to determine from in situ measurements. Flask measurements made at the U.S. Dept of Commerce NOAA Mauna Loa Observatory at 3397 m (i.e. in the troposphere) and the NOAA/CMDL Cape Kumukahi site at 3m (i.e. in the BL) are geographically within 75 km of each other. The monthly averaged CO_2 concentrations from the two stations are shown in ref1; the values show a high correlation (0.937). Such a high correlation probably reflects the oceanic environment (i.e. weak source / sinks and weak BL inversion) and the relatively long time scale average. This time scale is however consistent with expected averaging periods required for reliable estimation. For the stratospheric-tropospheric correlation we assume a small negative value following the evidence (albeit tenuous) from Nakzawa et al. 1991. It is possible that more realistic estimates of correlations could be derived from modelled CO_2 distributions and we will be pursuing this approach. For this study, we assume a broad BL-troposphere correlation of 0.9 and a stratosphere-troposphere correlation of –0.4.

A2-4.1.2 Measurement noise

The effective measurement noise consists of the observation noise, O, and the noise from errors in the forward modelling. O is reasonably well defined from the instrument flight model characterisation (see 1QR figure 1) with values between 0.05 and 0.4 K NeΔT depending on channel. For the 4 and 15 μm CO_2

sounding channels, Ne∆T values are generally close to 0.2 K and we assume this value for all channels for the measurement noise here. This noise source is assumed, and is likely to be, uncorrelated.

Forward model noise, F, can be separated into (see 1QR) fast model and line-by-line (or 'spectroscopic error') contributions. Fast model error can be quantified by comparison to LBL calculations. LBL errors require intensive field or laboratory measurements. Neither term is well characterised at this point in the study although it is known that the fast model errors are of order 0.05 K or less (see 1QR 1.1) and are therefore not a significant contribution compared to O. The LBL errors are likely to be larger (see 1QR 1.2) and correlated. Here we are forced to assume a simple characterisation of the fast model error; a value of 0.3 K is taken for all channels with no correlation. Because O and F are assumed uncorrelated, the total effective assumed noise is 0.36 K

A2-4.1.3 Channel selection

The baseline selection used in these results is the 281 channels currently selected for NRT transmission by NESDIS. For future testing, other channel sets will be used, notably those determined to be optimal for CO_2 estimation.

A2-4.1.4 Sensitivity of estimation error

This section applies the linear error estimator to the baseline values and perturbed values of B and O+F to measure the sensitivity of the CO_2 estimation. Figure 4 shows the results for the **baseline values**. Top left shows the clear potential for AIRS to provide information on temperature; errors are typically reduced from 1 to 0.5 K. Humidity errors are also reduced significantly except in the near surface layers. Lack of information near the surface for constituent retrieval from infrared measurements is a result of high (near unit) surface emissivity and low temperature contrast. Error reduction in the ozone is surprisingly modest. Significant error reduction is seen in the CO_2 error with the tropopause and BL boundaries marking changes in estimation skill. Unlike the humidity estimation and contrary to the theory, there appears to be information on CO_2 in the BL. In this case, the error reduction is due to the high correlation assumed in the CO_2 a priori error profile so that information from sensitivity high in the atmosphere influences the estimate in the BL. There is nothing wrong with this result, if the assumed correlations are correct (for example for the monthly timescale) then this estimation is possible. It merely suggests that BL perturbations due to strong CO_2 sources or sinks, although uncorrelated with the deep troposphere on a short timescale, filter through on the monthly scale. (For discussion resolution see **4.1.5 Vertical resolution**.)

The sensitivity of the CO_2 estimation error to the stratospheric-tropospheric correlation is shown in

Figure 5. It is clear that the broad nature of the sounding channel weighting functions mean that the high degree of overlap between the two regions leads to poor estimation when the correlation is low. Accuracy in the BL appears to have the opposite behaviour with higher accuracy for lower stratospheric-tropospheric correlation; a result which is difficult to understand at present but may be related to a physically unreasonable B_{co2}, see 4.1.5 Vertical resolution.

Figure 6 gives the sensitivity to the assumed measurement, O, and forward model, F, noise level; the lowest level, 0.2 K, effectively corresponds to zero F. Whilst F is uncertain at present, the figure shows clearly the stringent requirements on RTM errors if estimates of reasonable accuracy are to be obtained. F may well be

correlated between channels which will make the effect shown here (which assumes uncorrelated) somewhat optimistic. F is also likely to be correlated between soundings making the effect of averaging (measurements or estimates) less effective at noise reduction.

A2-4.1.5 Vertical resolution

Figure 7 shows the averaging kernels for the temperature and CO2 estimates calculated using the baseline parameters. The averaging kernel is the response, at each level, to a uniform perturbation in the true profile.

$$\frac{\partial \hat{x}_i}{\partial x} = BH^T \left(HBH^T + O + F \right)^{-1} H$$

The left-hand plots show the kernels and the right plots show the total of each kernel. The coloured vertical bar on the right-hand plot indicates the level to which the kernel is associated, e.g. kernels in dark blue are for levels at the top of the atmosphere. Associating the levels to kernels for the temperature estimate is straightforward as the kernels are narrow, indicating that the temperature estimate at a level responds to perturbations at the same and nearby levels, but not to distant levels, i.e. the temperature estimate has good vertical resolution. For CO_2 with the low information content and high assumed vertical correlation, the kernels are less intuitively placed. Clearly none of the kernels indicate any response to low-level CO_2; a result we expect. Kernels for the BL levels (orange coloured) respond to CO_2 perturbations from the mid-high troposphere and the lower stratosphere. Kernels for tropospheric levels (red) correspond to mid and high troposphere but with little or no resolution and kernels for the stratsphere (blue) respond to perturbations in the low stratosphere and negatively to perturbations in the high troposphere. There is obviously no significant vertical resolution in the estimates and the (artificial) correlations assumed give rise to rather distinct sensitivities. This is emphasised by the right-hand plots which show the area of each kernel. For the temperature sounding the areas are around unity in the troposphere indicating that most of the response to perturbation originates from the measurements and not the a priori (Rodgers 2000, p47). The kernel areas for the CO_2 estimation are generally significantly less than unity. The exception is for the BL where values > 1 are seen. This is the region where there is no direct measurement information and although (as stated above) information is communicated down from the troposphere, to have a sudden increase in measurement effect in the BL is certainly anomalous. We have ascertained that the explanation lies in the rather crude covariance, B_{co2}, which correlates all BL levels to all tropospheric levels with a value 0.9 and have since improved the representation of B_{co2}. However, the main results stand and we present the result as a reminder that great care must be taken over these issues.

The lack of vertical resolution in the CO_2 estimation means that care must be taken interpreting the error estimates for profile retrieval; it is a good approximation to say that only an unevenly weighted column average quantity is estimated with an error more or less as shown for the profile (given the high correlation). Future work will consider interpreting profile estimates in terms of column amounts and the more general question of whether the column average is a more appropriate variable for estimation than a profile.

References

English SJ, Eyre JR, Smith JA, A cloud-detection scheme for use with satellite sounding radiances in the context of data assimilation for numerical weather prediction, *Quart. J. Roy. Meteor. Socc*, **125** (559): 2359-2378, Part A Oct 1999

Engelen RJ, Denning AS, Gurney KR and Stephens GL, Global observations of the carbon budget: I. Expected satellite capabilities for emission spectroscopy in the EOS and NPOESS eras. *J. Geophys. Res*. **106**, 20,055-20,068.

Nakazawa T, Miyashita K, Aoki S, and Tanaka M, Temporal and spatial variations of upper tropospheric and lower stratospheric carbon dioxide, *Tellus*, **43B**: 106-117, 1991

Rodgers CD, Retrieval of atomspheric temperature and composition from remote measurements of thermal radiation, *Rev. Geophys and Space Phys*, **14** 609,1976.

Rodgers CD. Inverse methods for atmospheric sounding, theory and practice, World Scientific. 2000.

Appendix 2A: The Bayesian cloud detection method

This method utilises the fact that cloud contaminated signals, δT_B^c, will have statistical characteristics which are not well described by the statistics of the clear atmosphere δT_B. Cloud detection is achieved by calculating the probablility that a given δT_B vector belongs to a population described by the clear atmosphere covariance $\mathbf{H.B.H^T+O}$. The probability is defined by the Chi-squared quantity $\boldsymbol{\chi^2 = \delta T_B . (HBH^T+O)^{-1} \delta T_B^T}$ and a threshold (high) can be put on the value of χ^2 above which the observation can be considered likely to be cloud affected. χ^2 is not a normalised quantity, however, and it's magnitude will vary with the length of the vector δT_B. Therefore we use the associated probability implied by χ^2 for the vector length, $P(\chi^2)$, and define a threshold (low) below which the sounding is considered unlikely to have arisen from a cloud-free situation. (In a stable system with fixed number of channels it will be more efficient to use a threshold on χ^2 directly.)

If applied to the complete δT_B vector this method is quite powerful and in this case does not rely upon the channel ordering described in 1QR. Figure 2A 1 shows that, in a simple test scenario (simplified cloud and model/observation noise), almost complete discrimination is possible when cloud effects are up to 2 K maximum (in the lowest channel) and model noise is 0.5 K. However, as we are attempting to establish which channels in a particular sounding are cloud free as opposed to which entire soundings are cloud free, the method is adapted as follows. Having ordered the channels in the vertical we can assume that, in general, a subset of the N_c channels (from channel 1 to N, say) are cloud-free and the remainder (N+1 to N_c) are cloud affected. The $P(\chi^2)$ quantity can then be calculated for each position of a moving window of width $W < N_c$ and the channels in the window classified cloud-free or otherwise. An example of this process using the simplified definitions of cloud effect and model noise is shown in Figure 2A-2. The essential adjustable parameters of this filter are the window width and the threshold probability. It is not obvious a priori what the optimum window width will be as there are conflicting effects. A long window allows for better discrimination of the statistics (in the limit, a window width of 1 channel would be a weak discriminator because no correlation information would be available) but will generally contain cloud affected and cloud-free channels which weakens the signal. A long window also reduces the precision to which the first cloud affected channel can be located. The probability threshold can be used to tune the detection to the desired trade-off between conservative detection (i.e. low residual cloud contamination) and high data quantity. Some applications may be able to tolerate more noise in the measurements than others, however, for CO_2 estimation, it is likely that the trade-off would be towards high low contamination.

Figures

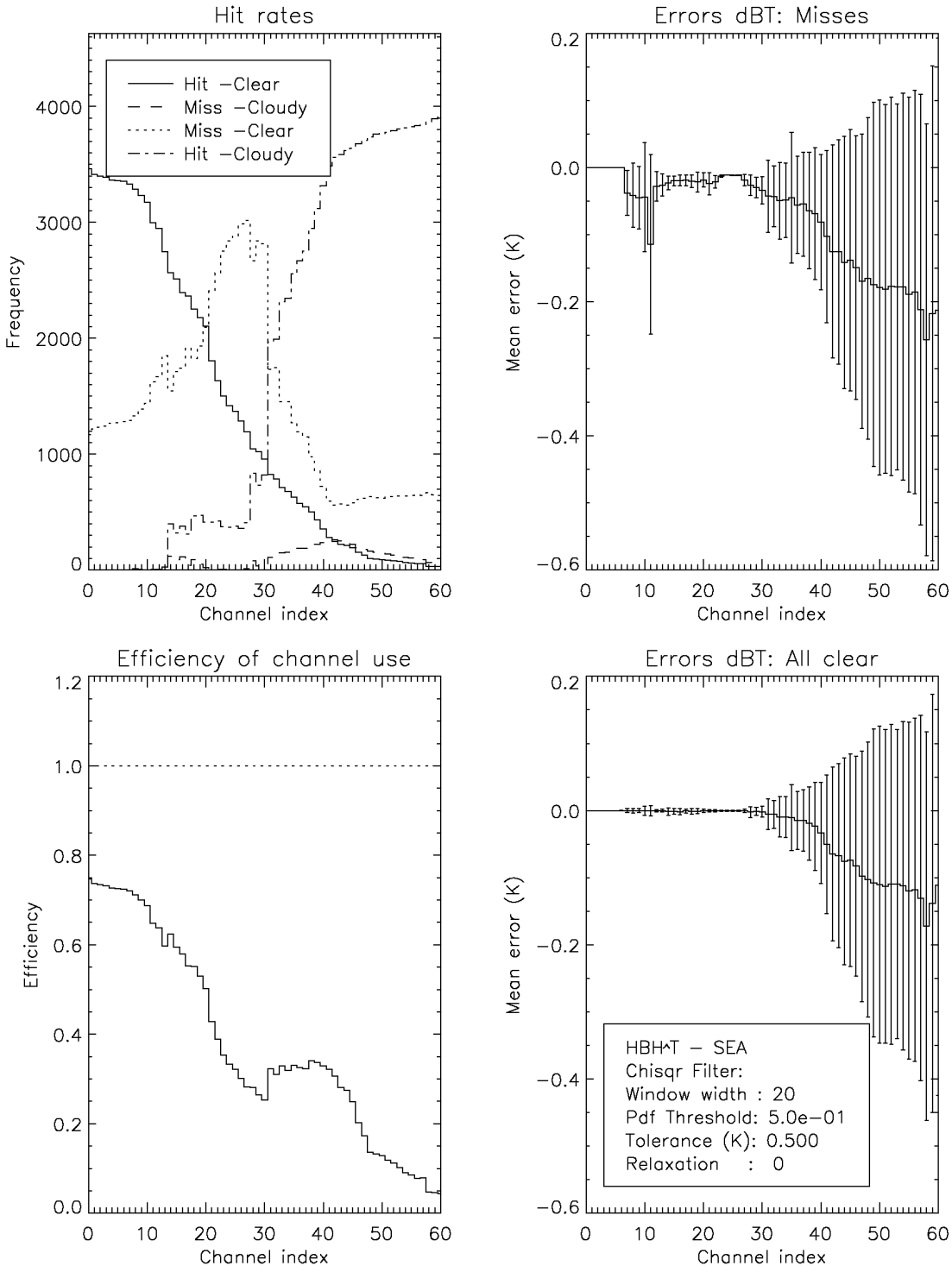

Figure 1 Detection statistics for the χ^2 filter operating on the LW band measurements from the synthetic data set. See text for details

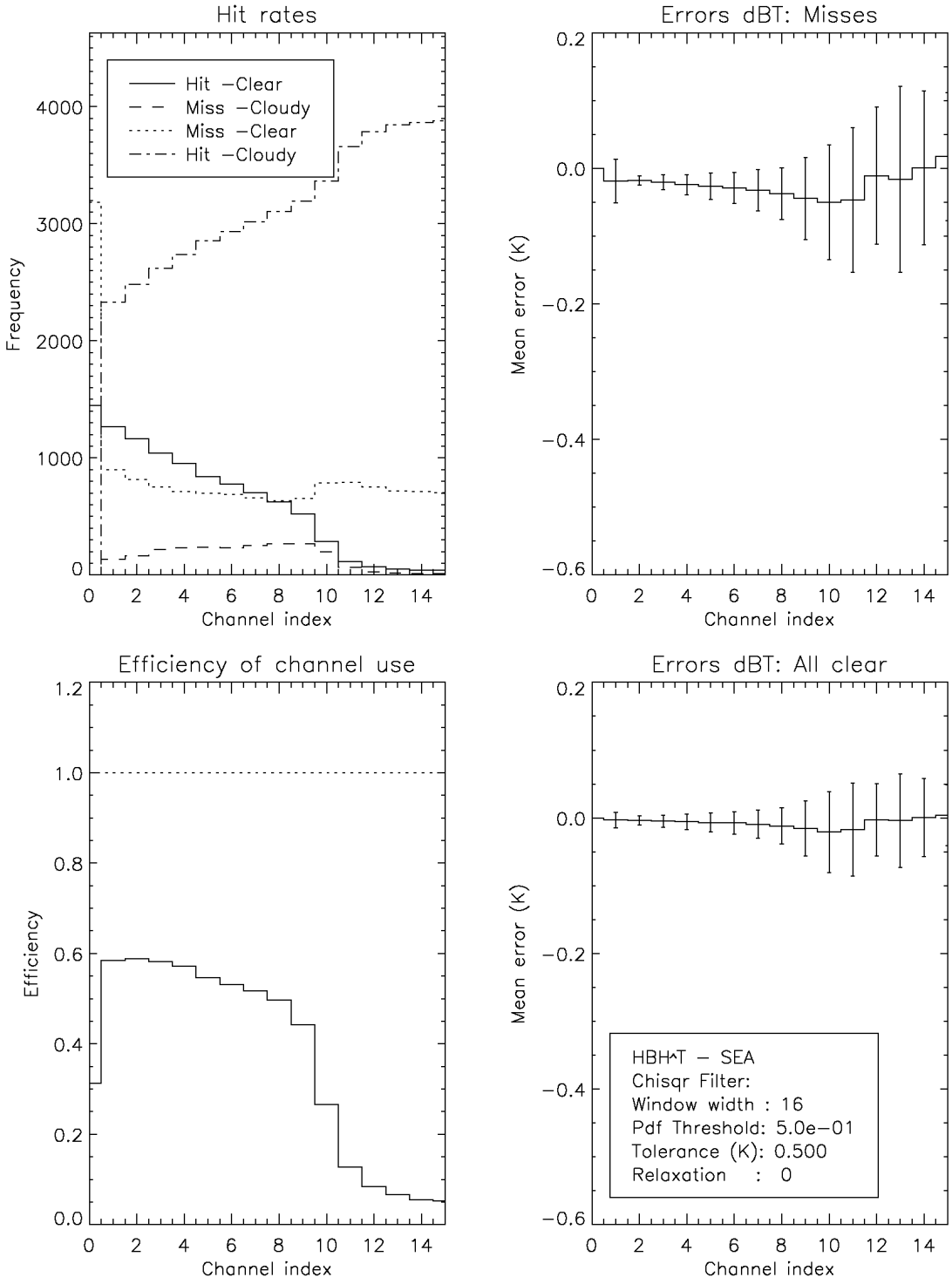

Figure 2 As Figure 1 but for the SW-2 band.

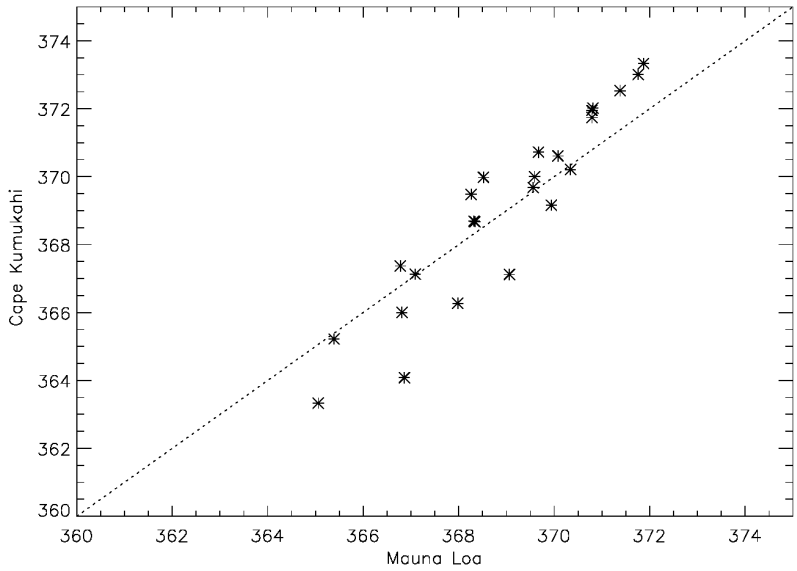

Figure 3 Monthly mean CO_2 flask estimates from two nearly adjacent sites: Mauna Loa at 3397m and Cape Kumukahi at 3m.

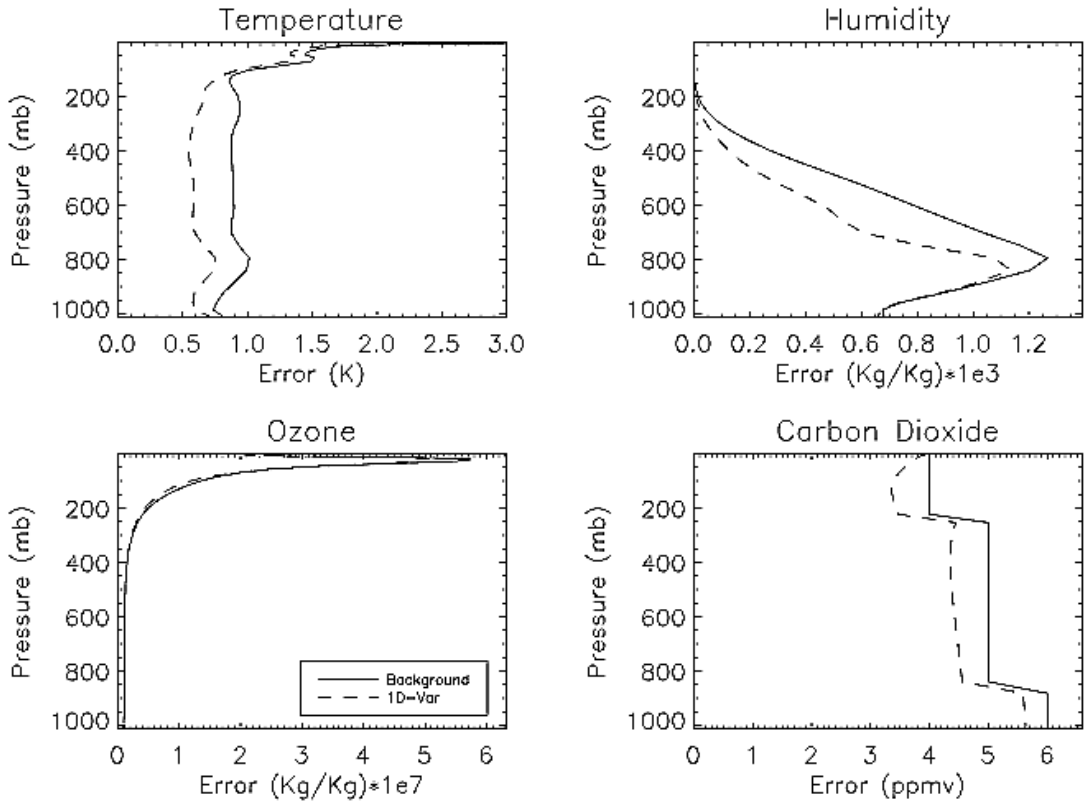

Figure 4 Linear error estimates for temperature, humidity, ozone and CO_2 for the baseline system (see text for details).

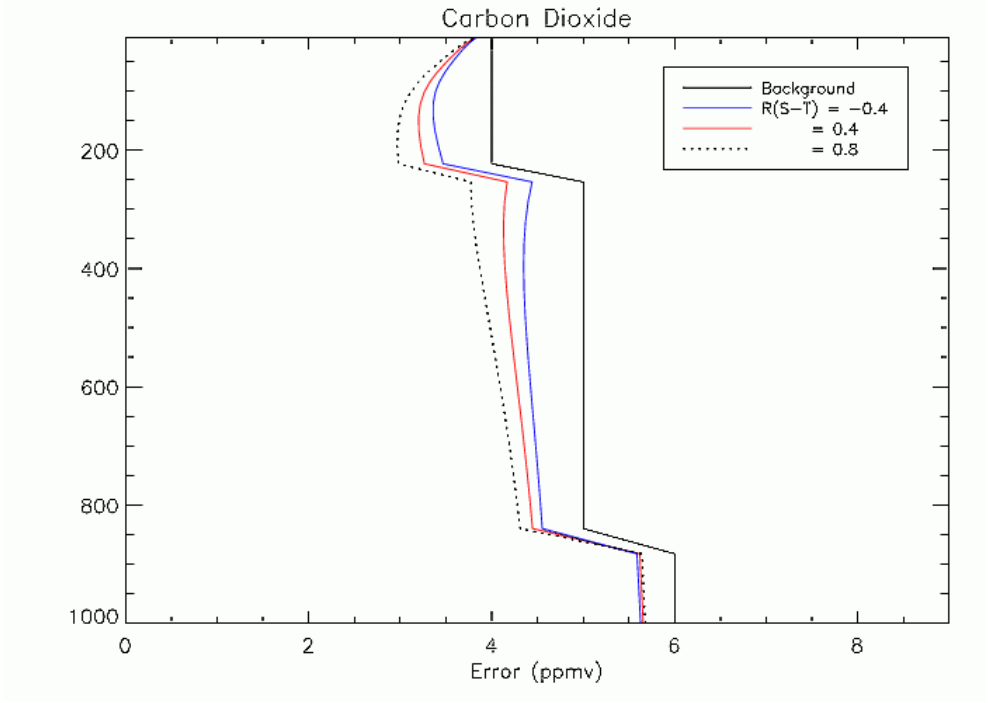

Figure 5 CO_2 error estimates for various assumed stratospheric-tropospheric correlations (R(S-T)). Other parameters take baseline values.

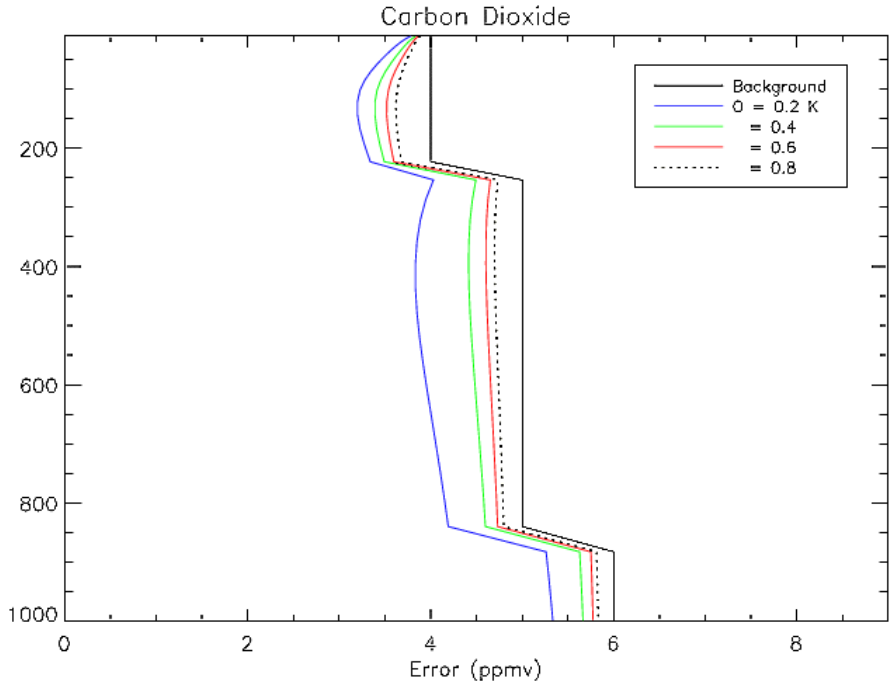

Figure 6 CO_2 error estimates for various assumed measurement and forward model noise levels. Other parameters take baseline values.

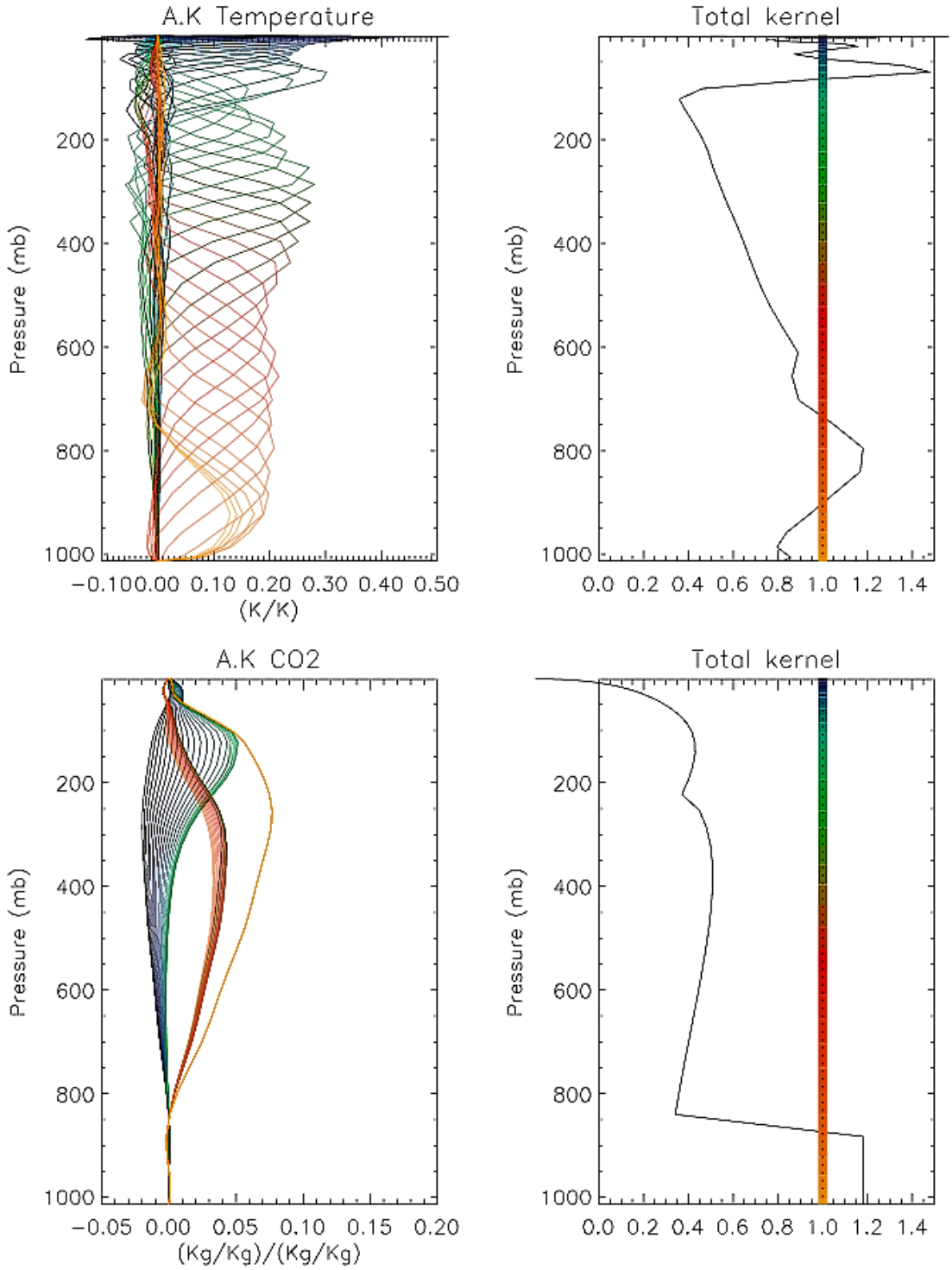

Figure 7 Averaging kernels (left plots) for temperature and CO_2 for the baseline conditions. Right-hand plots show the averaging kernel totals for each level indicating the degree of measurement and a priori information in the estimate.

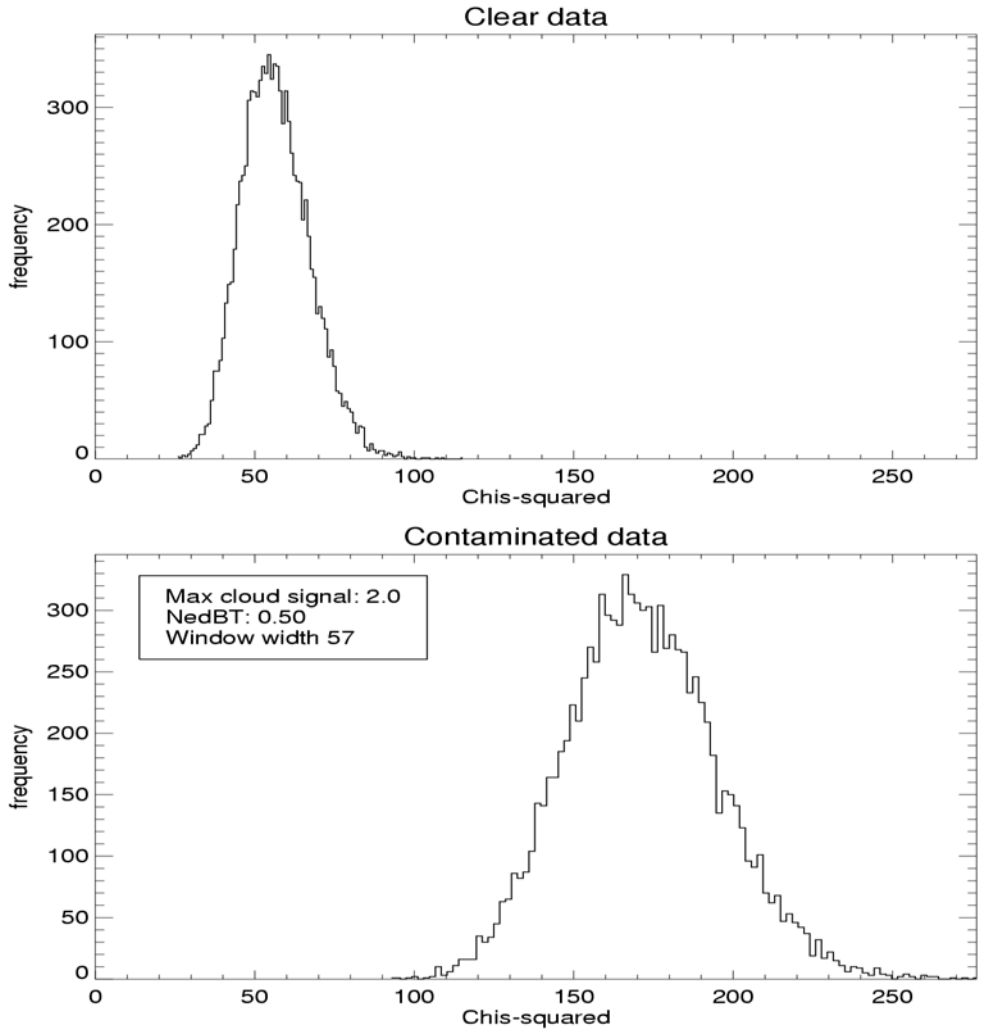

Figure 2A-1: χ^2 values calculated for a 57 channel window for a cloud-free δT_B profiles (top) and for cloud contaminated profiles (bottom). The cloud contaminations applied are realisations of the synthetic effect shown in figure 5 with a randomised 'starting channel' and maximum effect of up to 2.0 K. HBH^T+O noise is also given a simplified treatment and is assumed white with an amplitude of 0.5 K.

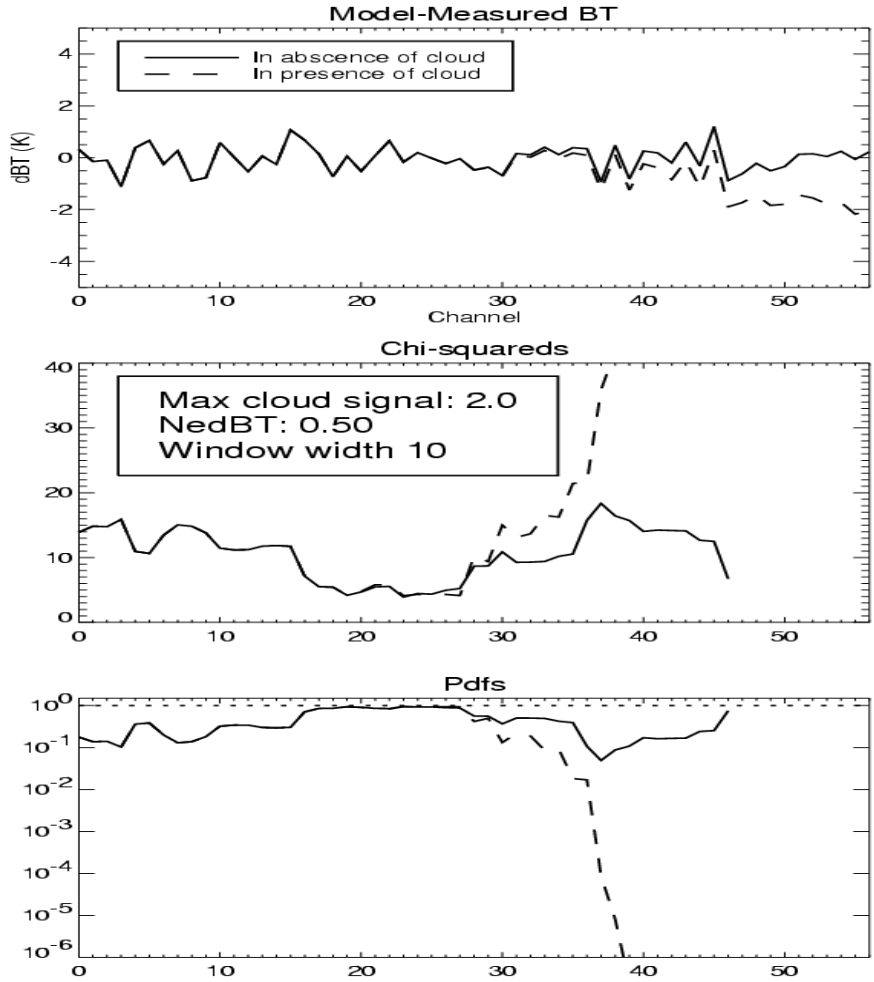

Figure 2A-2: Signal, χ^2 values and $P(\chi^2)$ for a single realisation the simple model and cloud effect simulation using a window of width 10 channels. The cloud signal can be seen (upper plot) as a gradually increasing deficit from around channel 32. The χ^2 and probability signals show strong deviation from the norm once the starting channel for the filter has reached 35-40.

Annex 3: Third Interim Report to the European Space Agency

Measurement of Seasonal CO_2 Fluctuations from Space

October 2003

Authors: P.D.Watts, A.P.McNally, J-N. Thépaut, M. Matricardi, R.J.Engelen and Niels Bormann

ESA contract No. 14644/00/NL/JSC

European Centre for Medium-Range Weather Forecasts

Table of Contents

Annex 3 - Executive Summary

This is the third quarterly report for the contract study on measurement of seasonal CO_2 fluctuations from space. We report here only on progress made since the first and second quarterly reports (1QR, 2QR) except where repetition or a summary is required for clarity. The statement of work identifies four distinct workpackages (radiative transfer, data sampling, use of real AIRS data and system implementation) and schedules these to run in sequence. Whilst this structure is logical it has proved expedient to tackle areas in all of the workpackages during this third period.

In this period AIRS reduced channel set (324) data has undergone extensive testing in the ECMWF experimental system and has recently (7/10/2003) become part of the operational system. Experiments with an enhanced assimilation system enabling CO_2 estimation have been made.

In **WP1** (radiative transfer) much experience has been gained from the operational monitoring of the AIRS data. Radiative transfer errors of the character expected (1QR) are found in the 15 micron region and similar errors are apparent in the water vapour region. Errors in the 4.5 micron band appear to be enhanced in part by poor specification of N_2O and in part by (during sunlight) non-Local Thermodynamic Equilibrium effects. Strategies to quantify and correct some of these errors are under development.

In **WP2** (data sampling) the high prevalence of cloud cover has led to improved techniques for pre-screening the data. First considerations have been made towards examination of EOF compressed full channel data streams.

In **WP3** (science study) several enhancements have been made to the low pass filter (LP) method of cloud detection, to avoid problems caused by erroneous NWP model surface temperatures and to allow for Polar Stratospheric Clouds. The detection results have been validated using AQUA MODIS imagery and AIRS visible channel information. A 'cross-band' method has also been developed to enable cloud detection results obtained in the straightforward 15 micron band to be applied to other less straightforward bands.

In **WP4** (system implementation) work has progressed, and is reported here, on two fronts. Use of AIRS in the *NWP system* continues to be studied, particularly the effects of large numbers of channels sensing the high stratosphere and the valuable information from monitoring on radiative transfer errors. A system for *CO_2 estimation* from AIRS has also been developed. From an initial study with 1D variational retrievals of CO_2 with a NWP atmosphere constraint (not reported in detail) we have progressed to the implementation of a single, then double, CO_2 'sink' variable in the full 4D variational assimilation system. Some preliminary global estimates of column CO_2 are presented.

A3-1. WP 1 Validation of a fast radiative transfer model (RTM) for AIRS

It was reported in 1QR that results of the CAMEX experiment (Rizzi et al 2001) showed spectroscopic uncertainties could lead to errors in RTM forward calculations for AIRS of up to 1 K. With over one year's AIRS data monitored against the ECMWF forecast model we are now in a position to comment on how these spectroscopic errors appear with real data. Such monitoring potentially leads to an ambiguity between NWP model error and spectroscopic error. However, the CAMEX experiment provides one important source of independent information and the high vertical resolution of the AIRS data itself can be exploited as another.

The AIRS instrument has proved to be extremely stable in radiance and spectral calibration. Bias estimates made six months apart are usually very similar except where an obvious forecast model seasonal bias is apparent. The biases (mean observation minus forecast model first guess) for our current best cloud detection methodology are shown in Figure 1 as red dots. The small black dots are the differences found between the High resolution Interferometer Sounder (HIS) instrument down looking from an aircraft at 20 Km, and calculations made using GENLN2 from the in situ atmospheric data (temperature, humidity, ozone etc). (GENLN2 is the base line by line model used to train the RTTOV fast model used at ECMWF.) Noise in the HIS instrument data makes the comparison somewhat meaningless in the regions <650cm^{-1}, 1050-1150 cm^{-1}, 1450-1800 cm^{-1} and 2200-2400 cm^{-1}. Elsewhere, it can be seen that AIRS biases are generally consistent in size with that expected from CAMEX. More specific details can be seen:

650-750 cm^{-1}; CO_2 sounding band. In the upper part of the band AIRS biases are systematically greater than zero and less scattered than the HIS. The positive bias is probably attributable to ECMWF forecast model bias in the stratosphere. The higher scatter in the HIS biases may be due to instrument noise, or perhaps because of its higher spectral resolution: some averaging of on/off line spectroscopic modelling error may be taking place in the AIRS measurements. In the lower part of the band the AIRS biases drop below zero and this may be due to neglect of P/R branch mixing in GENLN2 (Strow, 2003) although residual cloud errors may be contributing.

750-1000 cm^{-1}; Window region. Most AIRS channels in this region have biases that are very consistent with the HIS departures. The two AIRS channels that clearly stand out from the main cluster also stand out in the HIS, clearly demonstrating that these are spectroscopic in origin. (Improved water continuum modelling (Matricardi, 2003) in GENLN2 since has improved the fit of these channels and that of the other anomalous channels in this region).

Little can be made of the CAMEX results in the 1000-1100 cm-1 ozone region since ozone was poorly measured in the campaign. However, the ‘dipole’ error structure seen in the AIRS biases has the characteristics of poor modelling of the ozone absorption. It is also seen in the AIRS science team RTM kCARTA (Strow, 2003).

1200-1600 cm^{-1}; Water vapour band. The large scatter and overall shape of the biases here are consistent between HIS and AIRS suggesting these arise from spectroscopic errors. The sensitivity of the CAMEX results to specification of humidity, and uncertainty of the size of ECMWF forecast model biases both suggest that this conclusion should be speculative, but that CAMEX and ECMWF should have the same humidity bias structure would seem unlikely.

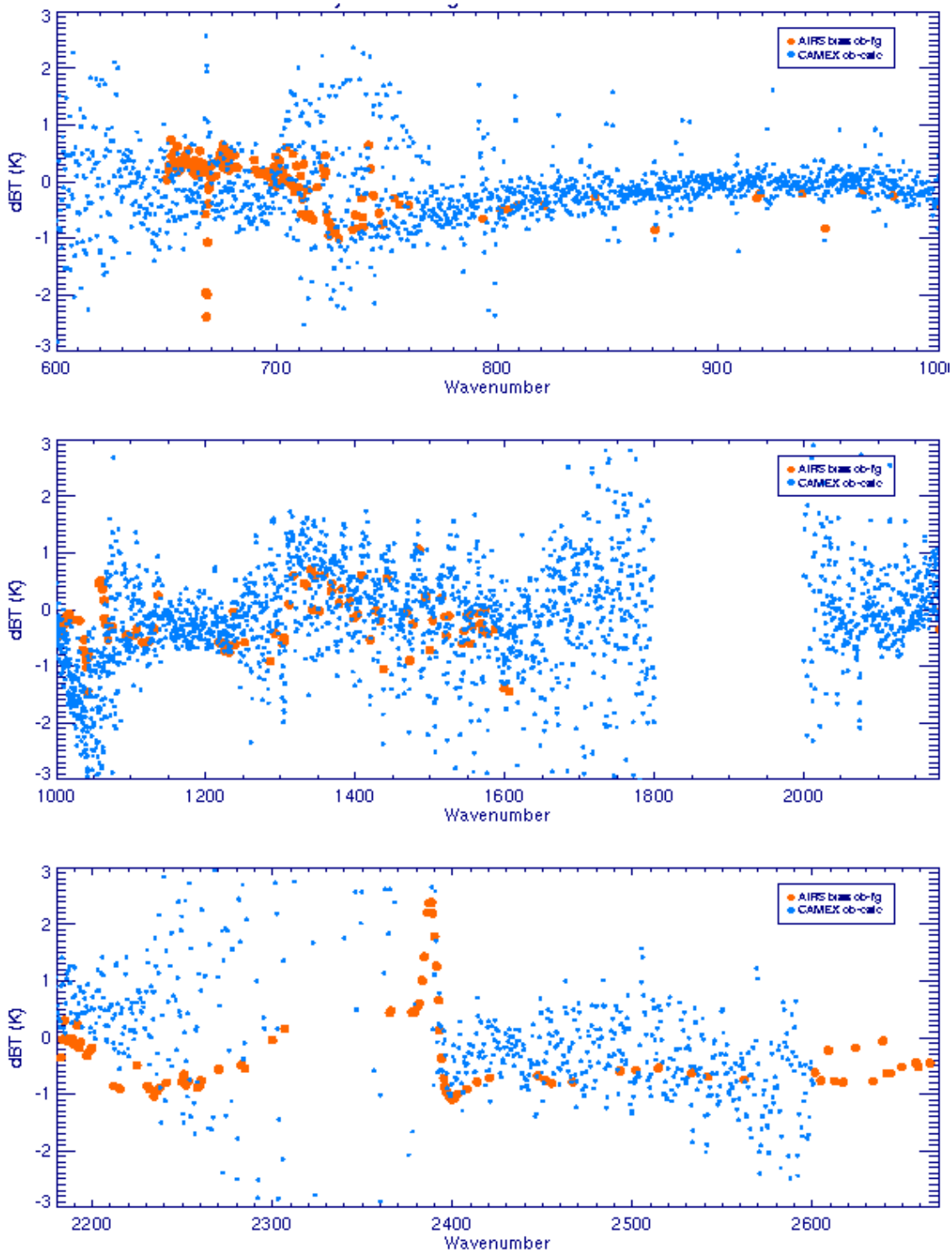

Figure 1 Figure 1 Bias vector found with current 'best current' algorithms (red) plotted with CAMEX GENLN2 / HIS interferometer differences. Data: June 1-5 2003.

2180-2300 cm^{-1}; (4.5 micron) CO_2 sounding band. This region is potentially an important sounding band for CO_2 (1QR), however the AIRS biases are currently rather large; up to 1K. It is probable that two effects are involved here. Figure 2 shows the AIRS biases in this region with the spectral signature in N_2O (scaled to be of the same magnitude).

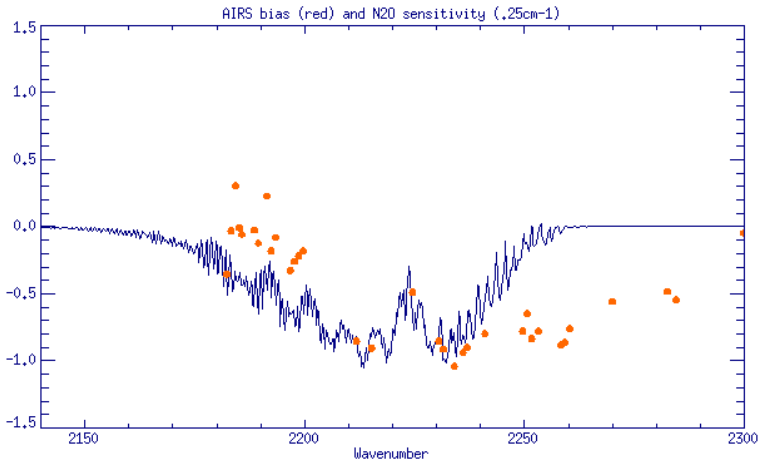

Figure 2 AIRS biases and scaled effect of incorrect N_2O concentration

In particular the signature around 2210-2240 cm^{-1} appears to be that of N_2O. Beyond 2240 cm^{-1} the CO_2 absorption becomes strong and biases here may become more a result of poor CO_2 line shape modelling (Strow). In addition to the spectral signature for N_2O, maps of bias in the 2230 cm^{-1} and at 1303 cm^{-1} (where there is almost pure N_2O absorption) contain very similar patterns (not shown).

This region also shows non LTE effects which are currently not modelled in the RTM. Figure 3 shows dramatically the difference in departures observed in daylight and night-time data at 4.381 micron (2282.6 cm^{-1}). The non-LTE contribution appears to have a strong limb effect but only a weak dependence on solar elevation (shown by little change along track).

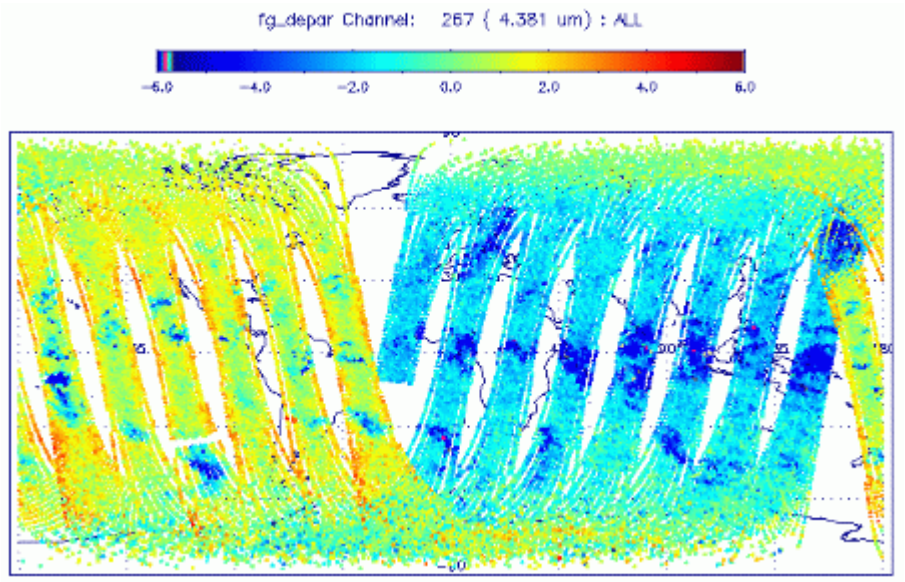

Figure 3 Departures in 4.381 micron channel showing daytime (left) and nigfht-time orbits.

Differences in monitored biases (mean observed minus model first guess departures) between daylight and night-time data show clearly the spectral region that is affected. Figure 4 shows the observed effect and the non-LTE effect estimated using the Oxford MIPAS LBL model (for three scenarios, all with solar elevation 60o, Dudhia et al. 2001). The agreement is good enough to firmly attribute the effect to non-LTE but not to

model it sufficiently accurately beyond about 2250 cm^{-1}). Note that the estimate non-LTE effect during night-time is negligible (not shown).

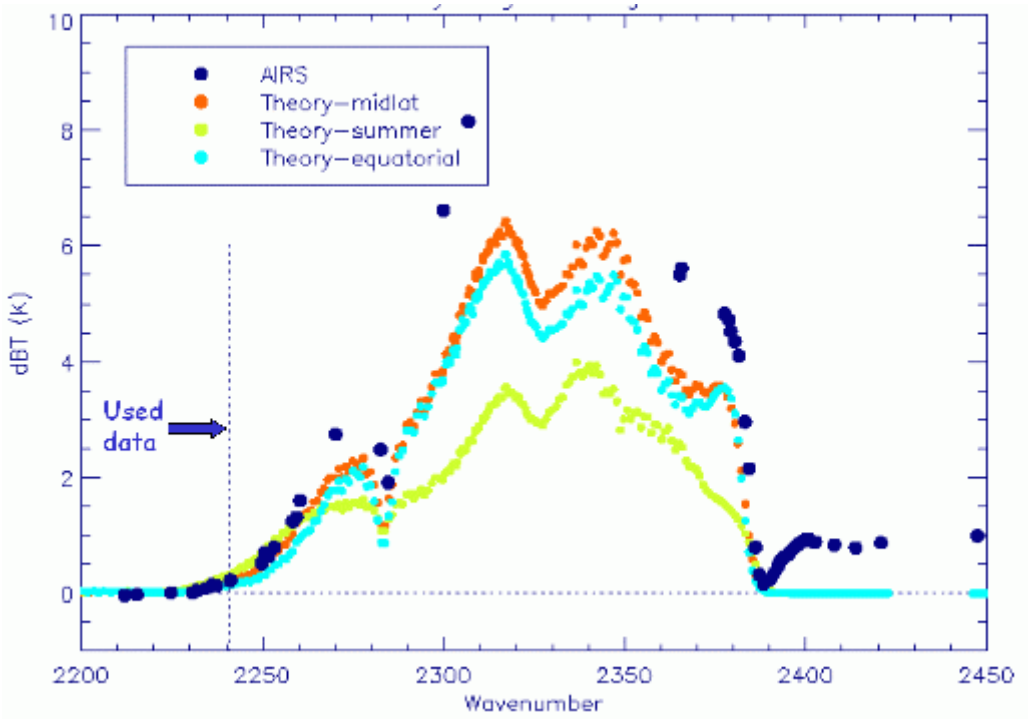

Figure 4 Daylight minus night-time AIRS biases (black dots) compared to non-LTE calculations in the 2200 - 2450 cm^{-1} region.

2380-2660 cm^{-1}; (4.2 micron) CO_2 sounding band. Another potentially important sounding band for CO_2 and again there are significant biases present. The HIS comparison also shows the strong positive bias through the sounding region (2385-2405 cm^{-1}) although the HIS noise is quite high here. The rest of the region, with relatively small and stable biases is a window region and of little interest to the CO_2 estimation.

The biases described above are typically of order 0.5 K, which, given the size of seasonal cycle CO_2 signals (~0.3-0.4 K, 1QR), is rather large. A global bias can be corrected however (and this is done in the current operational AIRS NWP assimilation, WP4). What is perhaps more important is the variation in the corrected bias. Figure 5 gives an indication of this by showing, for the 15 micron band, the 'airmass bias index' plotted against the bias itself. The 'airmass index' is simply the bias observed in high latitudes minus that observed in the tropics and Figure 5 shows that the bias variation, by this simple measure, is approximately a half the size of the bias. Thus, by applying a global bias correction to AIRS measurements, the residual error is typically 0.2-0.3 K, i.e. still of order the size of the CO_2 signal. The CO_2 signal is highly correlated (spectrally) whereas the biases are not; this may allow an assimilation system to extract CO_2 information. Nevertheless, it must be recommended that an attempt to correct the airmass variation in bias be made. There are several possible approaches to airmass bias correction which will be explored and discussed in the Final Report.

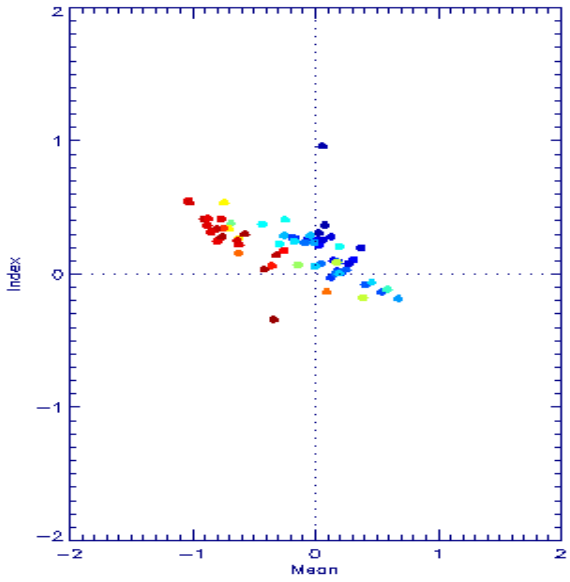

Figure 5 Airmass index as a function of bias for the tropospheric part of the 15 micron band

A3-2. WP 2 Science study to optimise AIRS data usage for NWP applications and for CO_2 work

At the time of 2QR this work package describing the sub-selection of AIRS data was more or less complete given the constraints of the trans-Atlantic data links and the capabilities of the ECMWF assimilation system. ECMWF receives 324 channels from the 2378 complete AIRS set of which 281 were chosen by NOAA/NESDIS and the extra 43 selected base on the work of Crevoisier et al. 2003.

Even with this relatively high data reduction the ECMWF NWP assimilation system requires further thinning of data so that the average 'distance' between observations is around 1.25° . Because of the low signal levels, the system implemented for CO_2 estimation has been forced to adopt a more discriminating data thinning so that a higher proportion of cloud-free information is retained. A simple cloud detection algorithm was implemented which acts a first filter to remove observations that are strongly affected by cloud. The detection does not have to be very precise as the full cloud detection system (1QR, 2QR) follows in the 4D-Var assimilation stage. The simple filter is based on methods used for HIRS (Li et al. 2000). All observations for which any of the following are true are *not* used:

1. BT(ch 787, 10.897 μm)	< 255 K	[night and day]
2. BT(ch 787, 10.897 μm) minus BT(ch 2209, 3.977 mm)	> 4 K	[night only]
3. BT(ch 2209, 3.977 μm) minus BT(ch 787, 10.897 mm)	> 2 K	[night only]

Test 1 is a simple cold threshold in the 11 μm window channel. Tests 2 and 3 are thresholds on the difference between the 3.9 and 11 μm window measurements. Test 2 is triggered by cloud emissivity (lower at 3.9 mm) and test 3 is triggered by the effect of partial cloud cover on the Planck function at the two wavelengths.

The effect of this filter is to remove most high and middle level cloud. It also removes much data over polar regions, but this is considered acceptable since the potential for CO_2 estimation in these regions is any case severely limited (by low level tropopause and small temperature lapse rates, see WP 4).

A3-3. WP 3 Science study with real AIRS data

In this period we have performed a validation of the LP filter cloud detection method that has been adopted for the operational processing of AIRS data. The validation is made using either the AIRS visible channel or collocated Aqua MODIS imagery. Notice that with both it is only possible to detect gross errors or corroborate hypothesized failures since both data are window channel imagery and cannot be reliably used to obtain cloud altitude.

The Aqua visible instrumentation consists of 4 channels in the visible and near-IR at 2.3 km resolution creating an 8 x 9 image in each AIRS field of view. The MODIS instrument provides many more wavelengths at higher spatial resolution but it technically harder to collocate with the AIRS footprint.

In summary, the validation led to several improvements in the algorithm design which are listed below. It has shown that the improved AIRS algorithm misses only a very few cases of cloud: contamination was rarely > 0.5 K compared to model brightness temperatures. The price paid for such stringency is the frequent assignment of cloud when the cause is model error.

The scheme improvements (referring to the original scheme in 1QR Appendix C in *italics*):

- ***Original scheme**: Check the lowest channel departure for |departure| > 0.5 K*
    - **New**: Search all channels with tropospheric trip levels for the minimum departure. The rationale here is to avoid cases where the lowest channel departure has compensating model error and cloud effects. By searching all channels, a non-compensating regime will generally be found.
- ***Original scheme**: If lowest channel departure is within tolerance (+/-0.5 K), declare whole profile cloud free.*
    - **New**: If minimum departure is within tolerance (+/-0.5 K), declare whole profile cloud free unless :-
    - check lowest channel for warm departure > 0.5 K, if so, start warm cloud algorithm from surface.
- ***Original scheme**: Operate departure gradient and threshold checks up the profile until first 'stratospheric' (always cloud-free) channel.*
    - **New**: Operate departure gradient and threshold checks up the entire profile. This avoids serious contamination by very high tropical convection and Polar Stratospheric Clouds.

It is not appropriate to present evidence to support all these algorithm changes but we illustrate the tools used for validation. Figure 6 shows a composite MODIS image of the Western Mediterranean with a band of low cloud in the Gulf du Lion and Figure 7 shows a composite of the AIRS visible channels with the AIRS sounder location indicated by boxes.

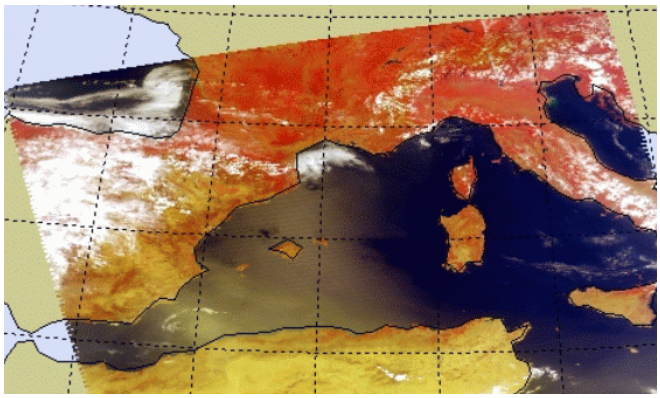

Figure 6 Composite MODIS imagery of western Mediterranean

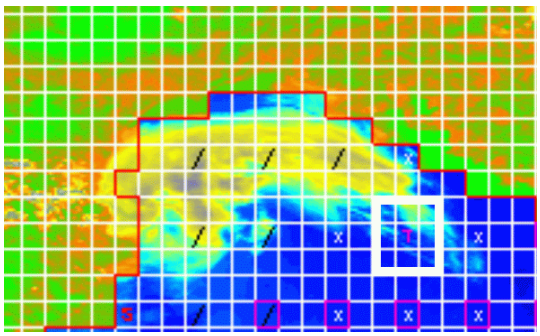

Figure 7 AIRS visible channel composite for same scene as Figure 6

The original cloud detection scheme reported cloud-free 15 micron window channels in the AIRS sounding highlighted (with a "T"). This is a complex case however, and although cloud is obvious in the visible imagery, it is in fact cloud with almost no temperature contrast with the surface temperature. This is demonstrated by the MODIS 3.7 and 12 micron images of the cloud area shown in Figure 8.

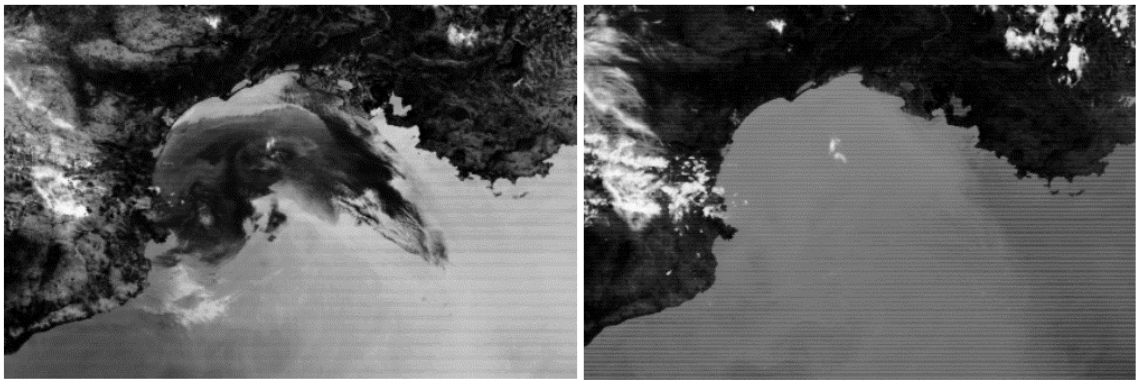

Figure 8 MODIS 3.7 (left) and 12 micron images of the cloud in the Gulf du Lion.

The cloud is very apparent and warmer than the sea in the 3.7 micron image because of solar reflection and more or less indistinguishable (if anything slightly cooler than the sea) in the 12 micron image. The LP filter detector (see 1QR Appendix C for details) for the 15 micron band on this sounding gives the result shown in

Figure 9. Lower level warm cloud is indicated by the increasing positive departures in channels 100-128 (ranked space).

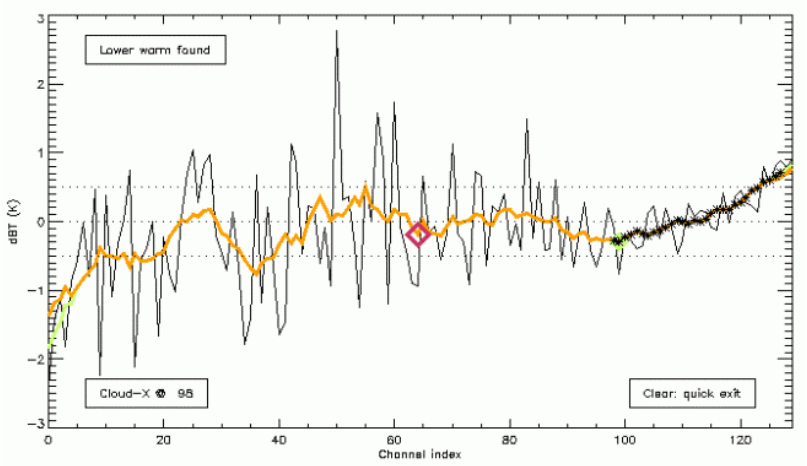

Figure 9 LP filter detection on 15 micron band for 'missed cloud' case.

However, we know from the 12 micron MODIS image that the warm temperature is not due to cloud, so can attribute it to a cold NWP model surface temperature. Although inappropriate in this case (i.e. the signal is probably a model error), the figure does demonstrate the warm cloud check improvement made to the cloud detection.

A3-4. Future improvements to the cloud detection.

The water band (around 7 microns) is particularly sensitive to the issue raised above: that of model error being misinterpreted as cloud. This is because the NWP model humidity error typically translates into 2-3 K of brightness temperature increment. The 0.5 K tolerance value (see 1QR) is therefore not appropriate to this band and could be widened, but at the expense of allowing many genuinely cloud-contaminated radiances into the system.

An alternative method under investigation involved utilizing the 15 micron band detection results to determine which 7 micron channels are cloud-free; so called 'cross-band' method. The method is straightforward:

- Take trip level of lowest clear 15 micron band channel, T_L
- Add (or subtract) a relaxation factor (i.e. move down (or up) in the atmosphere), T_L+R
- Declare 7 micron band channels with trip levels < T_L+R cloud-free.
- Declare 7 micron band channels with trip levels > T_L+R cloudy.

The relaxation factor is empirically determined and allows for two factors when interpreting the trip level across spectral bands. Firstly, the trip level definition (level at which opaque black cloud causes a 1% radiance effect) implies different brightness temperature effects at different wavelengths. Secondly, cloud effects are variable across the different bands. Relaxation factors are typically 1-3 model levels.

Results of this technique for a mid tropospheric water vapour channel are demonstrated in Figure 10 and Figure 11. Figure 10 shows the geographical and histogrammed distribution (inset) of clear departures (observation minus first guess) obtained with the LP filter scheme and Figure 11 shows the same when the cross band method is applied. The coverage is much improved in the cross band result with around three times the number of clears found. The histogram also appears more normally distributed; the LP filter histogram appears skewed towards positive departures, probably a result of the 0.5 K departure constraints in this algorithm.

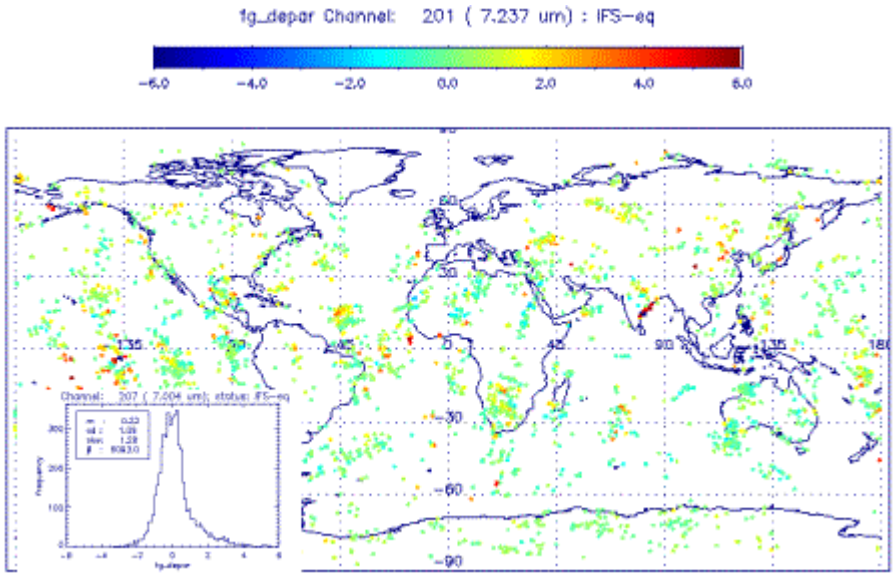

Figure 10 Humidity channel departure map and histogram using LP filter algorithm

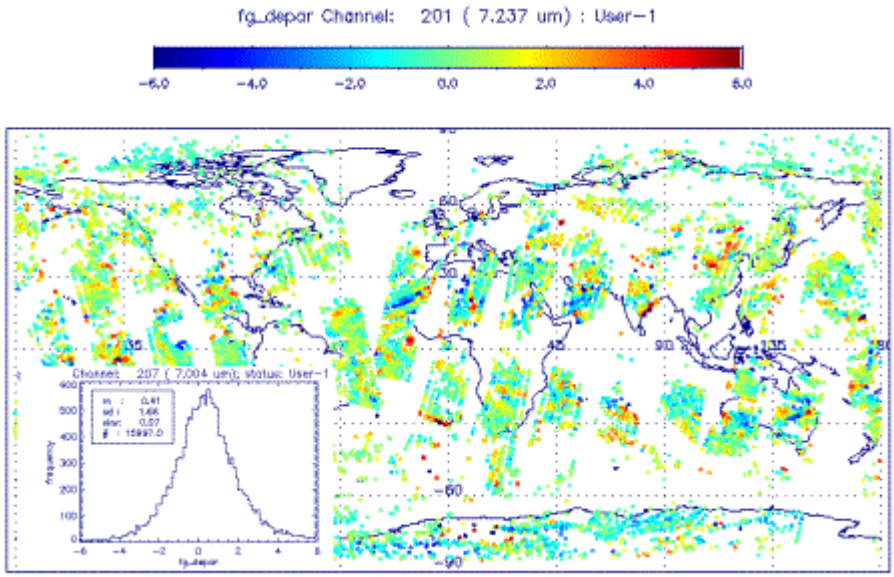

Figure 11 Humidity channel departure map and histogram using Cross-band algorithm

The cross band technique appears promising for the humidity band but may also be of use elsewhere. For example, during daytime the LP filter technique in the 4.2 micron band is compromised by solar reflection

from clouds. Certainly we find that whilst large biases are still uncorrected in the shortwave sounding bands the cross band method gives more reliable detection than the LP filter.

A3-5. WP 4 Design/ development/ initial testing of an assimilation strategy for NWP and a production strategy for CO_2

It is appropriate to split this WP into separate sections; AIRS in NWP assimilation and AIRS for CO_2 estimation.

A3-5.1 Assimilation for NWP

Since 2QR AIRS data has been assimilated in the experimental ECMWF 4D-Var system and from 7 October 2003 has been operationally assimilated. The implementation of the assimilation is set up as follows:

- Near real time data stream: 324 channels and 1 in 18 fovs
- Internal thinning to ~250 Km
- LP filter cloud detection
- All channels assimilated apart from the blacklisting:
    - Ozone band (difficulties with surface contributions)
    - 4.5 micron band beyond 2241 cm-1 (daytime non-LTE)
    - 4.2 micron band (Large biases and solar effects)
    - Low peaking channels over land (difficulties with surface contributions)
- Noise assumed according to channel:
    - 0.6 K in dry tropospheric channels with low surface and stratopause contributions
    - 1.0 K in stratospheric channels
    - 2.0 K in window and water vapour channels

The blacklisting and noise levels indicate that this is a conservatively tuned system. Since this implementation the characterization of effects due to N_2O (~20 channels), CO (1 channel) and several other poorly understood bias structures, has led us to experiment with these channels additionally blacklisted.

The baseline AIRS configuration described above has been tested at full resolution in 12hr 4DVAR using cycle 25R4 of the IFS between 10 Dec 2002 and 19 March 2003 (a total of 100 cases) and is subsequently referred to as “AIRS”. The control against which the AIRS impact is compared (subsequently referred to as “CTRL”) is generally the operational system. In summary, results with the ‘AIRS’ system show a small but consistent positive improvement over the ‘CTRL’ system. We show a couple of diagnostics to demonstrate this.

Changes to the analysis. Figure 12 shows a difference map (AIRS minus CTRL) of RMS analysis temperature increments at 500hPa (averaged over a ten day period in December 2002). While the contour interval is extremely fine (shading starting at 0.1K) the map shows that there are slightly larger increments over the oceans (where most of the AIRS radiances are used) and a small (but fairly consistent) decrease in

increments at radiosonde stations when the AIRS radiances are assimilated (the large increase over central Africa originates from the use of AIRS data over lake Chad that is treated as "sea" in the assimilation). The reduced increments at radiosonde stations is an encouraging diagnostic and shows that the extra work being done by the AIRS data in the analysis improves the agreement with radiosonde data through the assimilation cycle.

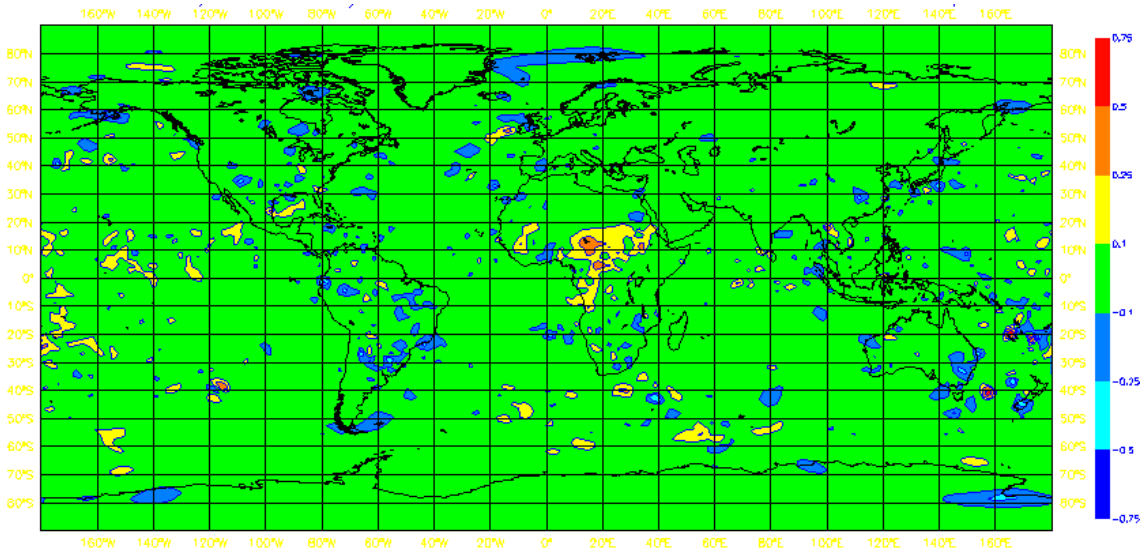

Figure 12 Difference map showing RMS analysis increments of the AIRS system minus those of the CTRL for temperature at 500hPa (averaged over 10 days). Shading starts at 0.1K.

Impact on forecast. Figure 13 and Figure 14 show a sample of forecast comparisons (100 cases) displayed as four area-averaged mean forecast scores for 500hPa geopotential height. However, it should be noted that these have been computed using the CTRL analyses for verification, a choice that may slightly penalize the AIRS system. It can be seen that averaged over 100 cases there is a very small, but very consistent improvement at all ranges in the Northern Hemisphere (the results of significance testing are contained in Table 1 and Table 2 show that the improvement is statistically significant at the 1% level for day-5). For the European area (embedded in the Northern Hemisphere statistics) the positive impact is marginally clearer, but less significant. In the Southern Hemisphere, only a slight improvement is seen at day-3 (significant at the 5% level) and beyond this no improvement is seen over the CTRL (the negative impact at day-10 was not found to be significant < 10%). The verification of temperature forecasts from the 2 systems is generally consistent with the height results in the mid-latitudes, but they additionally show a positive impact of the AIRS in the tropical temperatures at 200hPa. The same statistic for the southern hemisphere shows larger RMS errors when AIRS data are used, but a closer investigation indicates a large systematic difference between the AIRS and CTRL analyses, localized to the edge of the Antarctic continent and not evident at any other level than 200hPa.

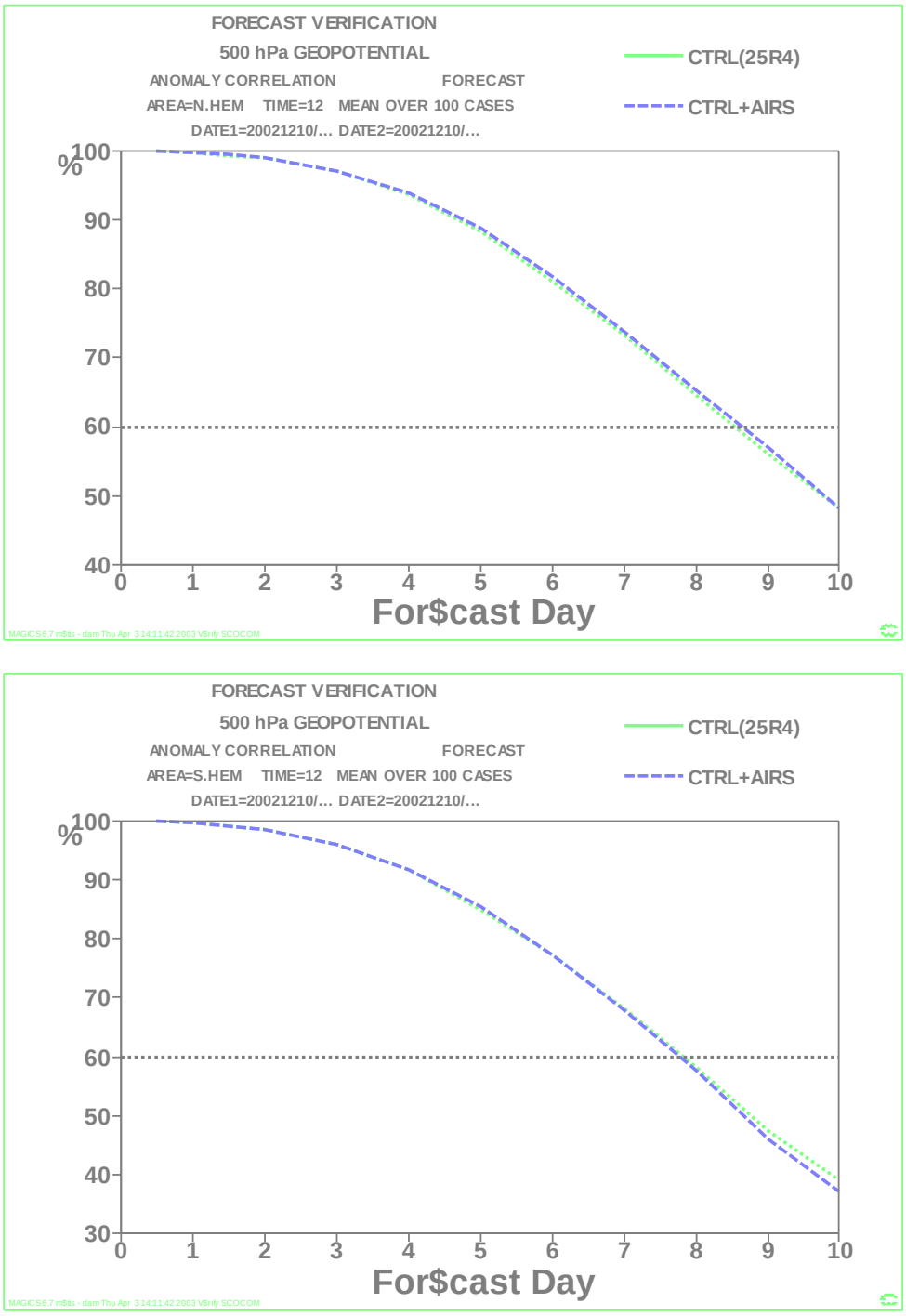

Figure 13 Mean anomaly correlation of 500hPa height for the Northern and Southern hemispheres averaged over 100 cases (10 Dec 2002 to 19 March 2003)

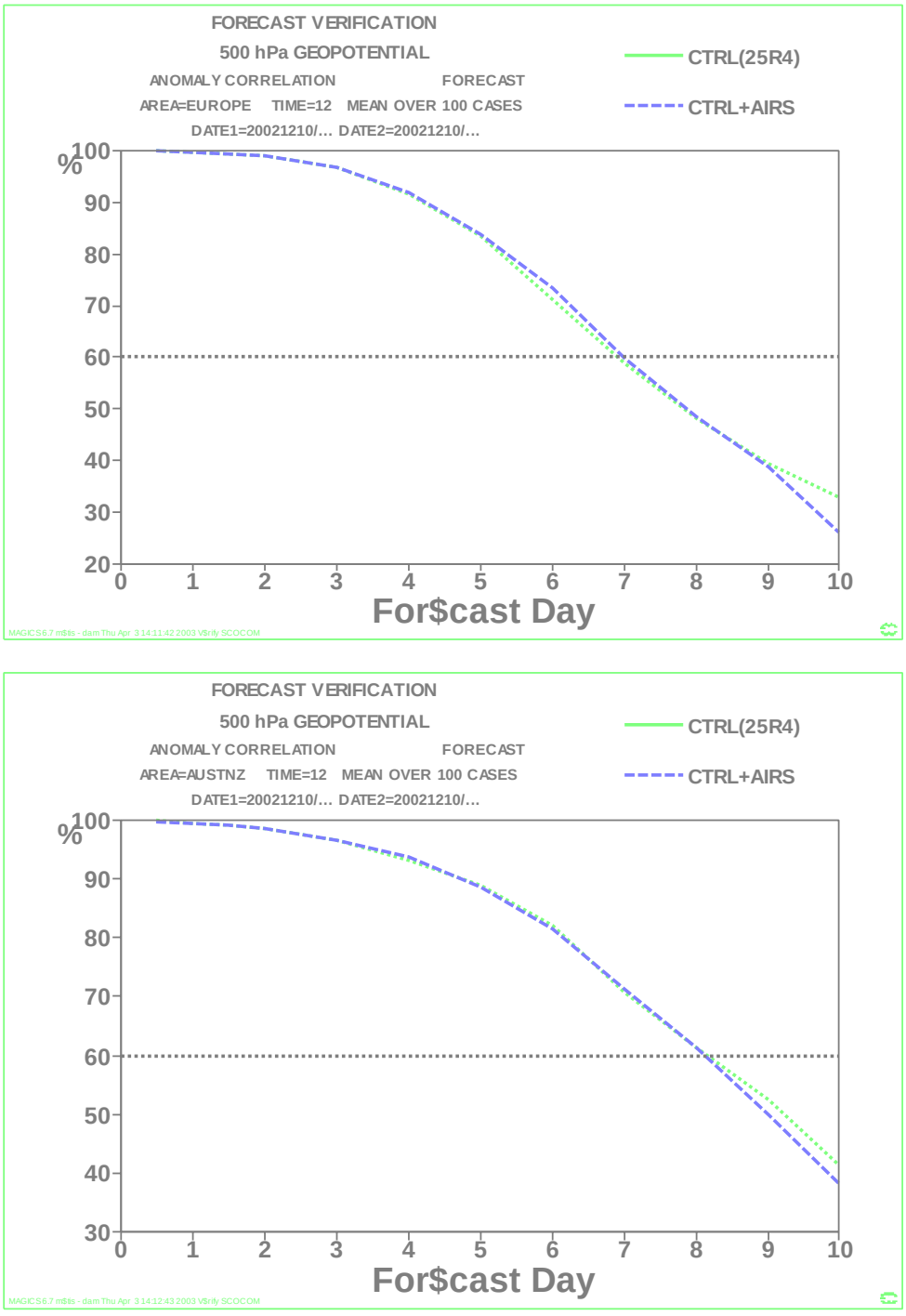

Figure 14 Mean anomaly correlation of 500hPa height for Europe and Australia / New Zealand averaged over 100 cases (10 Dec 2002 to 19 March 2003).

In the statistical significance testing of the forecast impact (shown in Table 1 and Table 2) red indicates a positive impact due to AIRS and blue a negative impact. The percentage figure indicates the level at which a t-test found the results statistically significant. If no significance better than 10% is found the result is marked with an X.

The assimilation of AIRS radiances with the baseline system described here shows no adverse effects in the analysis (in terms of the fit to other observations) and slightly reduced analysis increments at radiosonde locations. Overall the forecast performance of the baseline AIRS assimilation scheme is encouraging, essentially showing a consistent positive impact in most areas and parameters. However, averaged over the 100 cases the impact is small and warrants some discussion. The assimilation configuration is clearly conservative and a variety of further enhancements has been discussed above. However, large improvements over the CTRL may also be limited by the quality of the CTRL system itself. The average level of forecast skill for the CTRL (that currently uses radiances from 3 AMSUA, 2 HIRS, 3 GEOS and 3 SSM/I instruments) is very high and over the period tested was significantly better than forecasts from any other NWP centre. Furthermore, a time series analysis of forecast skill shows that the CTRL system produces very few poor forecasts or "busts". During the 100 day trial no day-5 forecasts of 500hPa height scored less that 60% anomaly correlation averaged over either of the hemispheres. Verified over the much smaller European area, still only 6 day-5 forecasts from the CTRL scored worse than 60%. In 4 of these cases the AIRS system improved the forecast by 10% or more (4 AIRS forecasts scored worse than 60% over the period, but the CTRL was never 10% better). Most of the cases where AIRS improves the poor forecasts correlate with when adjoint sensitivity perturbations to the initial conditions (rather than "forced" perturbations) were found to have a large effect. However, the improvements are far less dramatic than those achieved (retrospectively) by the sensitivity perturbations. Usually cloud was found to obscure many of the sensitive locations (resulting in very few tropospheric AIRS radiances being used). In the one case that was relatively clear (24 Feb 2003) it appeared that the some of the analysis increments due to AIRS did correlate with the sensitivity perturbations, but many did not. Overall it is difficult to argue that the assimilation of AIRS is dramatically fixing bad forecasts on any regular basis. It appears more that the assimilation of AIRS (with the current configuration) is having a small, but relatively consistent positive impact upon the forecast skill.

Table 1 Significance testing of 1000 hPa (first figure) and 500 hPa (second figure) height forecast verification

Forecast Range	Northern Hemisphere	Southern Hemisphere	Europe
day-3	5% / 1%	5% / 10%	X / 2%
day-5	0.1% / 1%	10% / X	10% / 5%
day-7	X / X	X / X	X / X

Table 2Significance testing of 1000 hPa (first figure) and 500 hPa (second figure) wind forecast verifications

Forecast Range	Northern Hemisphere	Southern Hemisphere	Europe
day-3	X / 5%	0.1% / 0.1%	10% / 0.5%
day-5	0.1% / 0.1%	2% / 5%	5% / X
day-7	0.1 / 2%	X / X	X / 10%

A3-5.2 Assimilation for CO_2

Since 2QR we have made preliminary steps towards assimilation of AIRS radiances in a version of the ECMWF assimilation system that includes variable CO_2. It is currently implemented as an independent column variable meaning that CO_2 is not a tracer variable in the transport model and is only estimated at the observation locations. No background error correlations exist between CO_2 and all the other assimilation variables. In practice this means that, while the forecast model variables like temperature and water vapour appear in the control vector as 3-dimensional fields at initial time t0, CO_2 appears in this control vector as a vector of column variables at all observation locations. The link between the initial state and the states at observation locations and times does not exist for CO_2.

This procedure allowed for a relatively quick implementation of CO_2 in the data assimilation system without having to change the forecast model itself. Although this implementation makes full use of the accurate temperature and water vapour analysis fields constrained by all available observations, it also has some limitations. By assimilating column CO_2 values instead of full profiles a hard constraint is applied to the analysis in the form of a fixed profile shape. This removes some of the flexibility in the adjustments and can lead to large errors if the used profile shape is far from the truth. This hard constraint also means that all vertical levels are basically fully correlated and for instance any adjustments in the stratosphere will therefore also adjust the troposphere. In case of many stratospheric radiance channels and only few tropospheric radiance channels this leads to a dominant stratospheric signal in the assimilated CO_2 column value.

Based on first results (not shown here) that indicated that the column variable was indeed dominated by the large amount of stratospheric AIRS channels, the column variable was split into a tropospheric column and a stratospheric column. These two columns act as completely independent variables without any error correlation between them in the analysis (see Figure 15). The tropopause height that separates the two columns, is estimated from the background temperature profile based on a lapse rate definition, and varies with location.

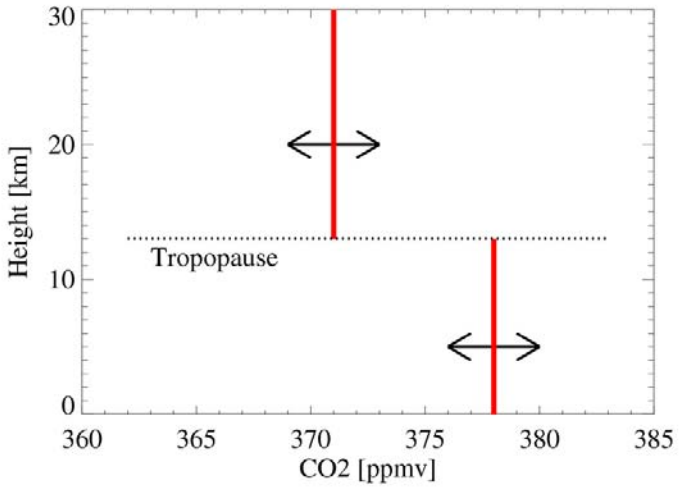

Figure 15 Diagram of the 2-column setup of the CO_2 data assimilation. The two column estimates can vary independently and are separated by a variable tropopause.

This ensured that information from the stratosphere did not dominate the tropospheric analysis results. However, any potential useful correlations (see 2R section 4.1.4) between stratospheric CO_2 and tropospheric CO_2 are disregarded. Another drawback is that the tropospheric column is quite variable. Depending on the tropopause height and the cloud top height, the column varies from shallow to deep allowing respectively less or more channels to be used in the tropospheric analysis. As shown in the next section the number of channels used in the analysis is an important determining factor of the analysis error.

A3-5.3 Analysis error estimation

In order to do a proper spatial and temporal averaging of the analysis results, it is crucial to have an estimate of the individual analysis errors. A proper average will give more weight to high quality analysis values and less weight to low quality analysis values. By using the individual analysis errors as weights ($w_i = 1/\sigma_i^2$), we get the following expression:

$$\bar{x} = \frac{\sum_i w_i x_i}{\sum_i w_i}$$

This way, we also minimize the background bias in the averaged results. The analysis value is in principal a weighted average of the background and the observations. If the analysis error is high, the background value was the main contributor to the analysis value, while, if the analysis error is small, the observations mainly determine the analysis value. Therefore, by de-weighting the analysis values with large analysis errors in the spatial-temporal averages, the effect of the assumed background values is minimized. The analysis error itself is estimated from the background error and the observation error as follows:

$$\sigma_a^2 = \left(\sigma_b^{-2} + \mathbf{H}^{\mathrm{T}}\mathbf{R}^{-1}\mathbf{H}\right)^{-1}$$

where σ_a is the analysis error, σ_b is the background error, **H** is the Jacobian matrix coming from the radiative transfer model, and **R** is the observation error covariance matrix. The analysis error is determined largely by the size of the Jacobian matrix (defined by the number of channels used in the analysis) and the amplitude of the individual Jacobians (determined largely by the temperature lapse rate).

A3-6. Results

Some first results of the CO_2 data assimilation scheme are presented here to illustrate the capabilities of the system. The background values used in the assimilation, shown in Figure 16, were zonal mean mixing ratios based on surface flask observations (GlobalView, 2003) with a background error of 30 ppmv.

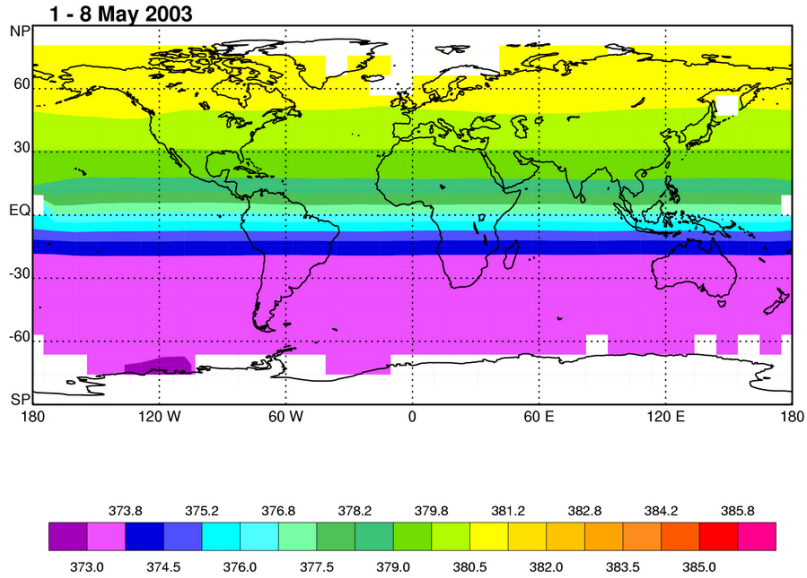

Figure 16 Background CO2: zonal mean monthly averaged GlobalView values for May 2003

The background error was set to be large deliberately to minimise the contribution of the background to the analysis in these preliminary experiments. Individual analysis values at the observation locations were gridded onto a 10º x 10º latitude-longitude grid over a period of 8 days in May 2003. Within a grid box the data were averaged using a weighted average with the analysis errors as weights. Furthermore, only analysis values with an analysis error smaller than 20 ppmv were used in the averaging. This filters out all observations with very little CO_2 information content, which would bias the resulting average to the background. Figure 17 shows the resulting CO_2 distribution with clear patterns of synoptic meteorological patterns. Also, the CO_2 mixing ratios are still high in the northern latitudes, but areas of decrease can be seen as well. This decrease in atmospheric CO_2 is caused by the onset of vegetation photosynthesis in the northern hemisphere spring.

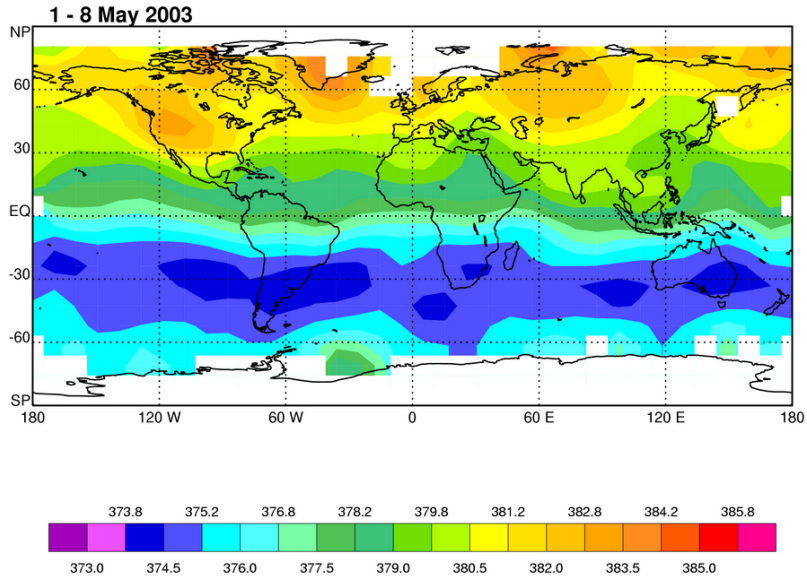

Figure 17 Analysed tropospheric CO_2 values averaged for the period 1- 8 May 2003.

Finally, Figure 18 and Figure 19 show the upper and lower estimates of the analysis error, respectively. The upper bound was calculated by assuming that all observations within a grid box are fully correlated, which means that the average analysis error is just a simple average of all individual analysis errors. The lower estimate was calculated by assuming that all observations within a grid box are fully uncorrelated, which means that the average analysis error is the root-mean-square of all individual analysis errors. The main conclusion from these error distributions is that the CO_2 analysis works best in the tropics (roughly between 30° S and 30°N). A significant reduction in the error (from 30 ppmv to 7 ppmv) can be achieved. At higher latitudes the errors increase significantly.

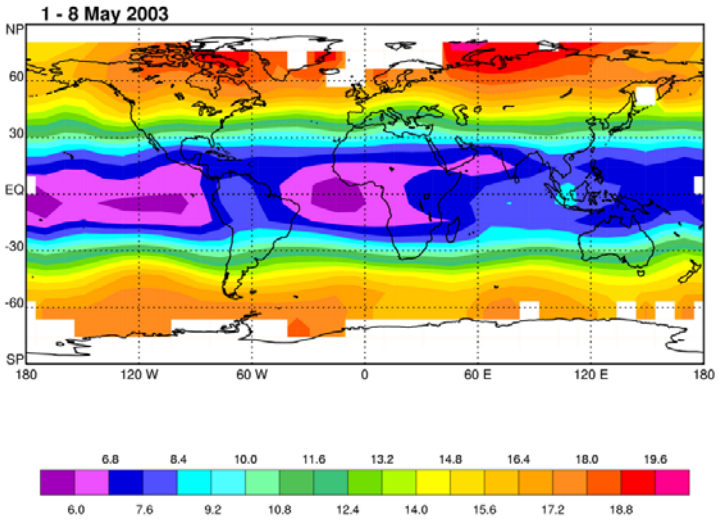

Figure 18 Upper bound of the averaged analysis error for tropospheric CO_2 (see text for explanation).

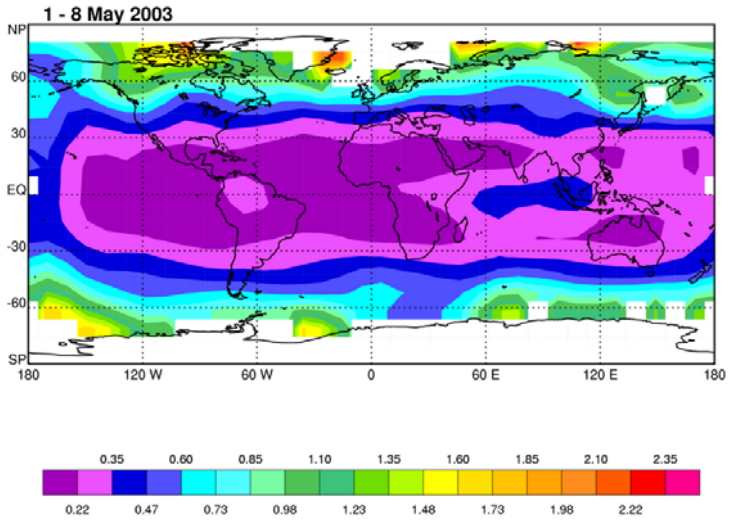

Figure 19 Lower bound of the averaged analysis error for tropospheric CO_2 (see text for explanation).

This is mainly because of the decreasing number of channels due to a lower tropopause, and the decreased temperature lapse rate. In conclusion, these first results show significant skill in tropical regions in retrieving tropospheric CO_2 from AIRS observations and possibly some skill at higher latitudes after spatial and temporal averaging.

References

Crevoisier C., Chedin A. and Scott N., AIRS channel selection for CO_2 and other trace-gas retrievals. *Quart. J. Roy. Meteor. Soc*., **129**: 2719-2740, 2003

Dudhia A., Morris P.E., Wells R.J. Fast monochromatic radiative transfer calculations for limb sounding. *J. Quant. Spectroscopy,* **74** pp745-756.

GLOBALVIEW-CO_2, Cooperative Atmospheric Data Integration Project - Carbon Dioxide, CD-ROM, NOAA CMDL, Boulder, Colorado [Also available on Internet via anonymous FTP to ftp.cmdl.noaa.gov, Path: ccg/co2/GLOBALVIEW], 2003.

Li J. Wolf W.W., Menzel W.P. Zhang W. Huang H.-L. and Achtor T.H. Global soundings of the atmosphere from ATOVS measurements: the algorithm and validation. *J. Appl. Meteorol.* **39**, 1248-1268, 2000.

Matricardi, M.: RTIASI-4, a new version of the ECMWF fast radiative transfer model for the infrared atmospheric sounding interferometer. *ECMWF Tech Memo 425*, 2003.

Strow L. Pers Comm, 2003.

Rizzi R, Matricardi M, and Miskolczi F, On the simulation of up-looking and down-looking high-resolution radiance spectra using two different radiative transfer models. *ECMWF Tech Memo 343*. 2001.